

# **A Microscopic Study of the DNA Damage Response**

Een microscopische studie van de DNA schade respons

Christoffel Dinant



# **A Microscopic Study of the DNA Damage Response**

Een microscopische studie van de DNA schade respons

Proefschrift ter verkrijging van de graad van doctor aan de  
Erasmus Universiteit Rotterdam op gezag van de rector magnificus  
Prof.dr. S.W.J. Lamberts en volgens besluit van het College voor  
Promoties.

De openbare verdediging zal plaatsvinden op  
woensdag 22 oktober 2008 om 15:45 uur door

**Christoffel Dinant**  
geboren te Amsterdam



## Promotiecommissie

Promotor: Prof.dr. J.H.J. Hoeijmakers

Overige leden: Prof.dr. A. Grootegoed  
Prof.dr. T. W. J. Gadella  
Dr. N. Galjart

Copromotor: Dr. W. Vermeulen

Copromoter: Dr. A. B. Houtsmuller

Dit proefschrift kwam tot stand binnen de vakgroep Celbiologie en Genetica en de vakgroep Pathologie van de faculteit der Geneeskunde en Gezondheidswetenschappen van de Erasmus Universiteit Rotterdam. De vakgroep Celbiologie en Genetica maakt deel uit van het Medisch Genetisch Centrum Zuid-West Nederland. De vakgroep Pathologie maakt deel uit van de Molecular Medicine Post-Graduate School. Het onderzoek is financieel ondersteund door de Nederlandse Organisatie voor Wetenschappelijk Onderzoek. Dit proefschrift is mede gefinancierd door de Nederlandse Vereniging voor Microscopie.

## CONTENTS

<b>CHAPTER 1: chromatin structure and dna damage repair .....</b>	<b>7</b>
<b>CHAPTER 2: fluorescence microscopy and live-cell imaging .....</b>	<b>29</b>
<b>CHAPTER 3: fluorescence resonance energy transfer of gfp and yfp by spectral imaging and quantitative acceptor photobleaching .....</b>	<b>43</b>
<b>CHAPTER 4: activation of multiple dna repair pathways by sub-nuclear damage induction methods .....</b>	<b>57</b>
<b>CHAPTER 5: accelerated exchange of h2a and h2b at sites of dna damage depends on histone chaperone fact .....</b>	<b>81</b>
<b>CHAPTER 6: heterochromatin protein 1 is involved in the dna damage response .....</b>	<b>93</b>
<b>CHAPTER 7: minireview: assembly of multi-protein complexes that control genome function .....</b>	<b>115</b>
<b>summary .....</b>	<b>131</b>
<b>samenvatting .....</b>	<b>135</b>
<b>curriculum vitae .....</b>	<b>138</b>
<b>list of publications .....</b>	<b>139</b>
<b>dankwoord .....</b>	<b>141</b>



## Chapter 1

# Chromatin Structure and DNA Damage Repair

Christoffel Dinant, Adriaan B. Houtsmuller and Wim  
Vermeulen

*Submitted*

## **ABSTRACT**

The integrity of the genome is continuously challenged by both endogenous and exogenous DNA damaging agents. These damaging agents can induce a wide variety of lesions in the DNA, such as double strand breaks (DSB), single strand breaks (SSB), oxidative lesions and pyrimidine dimers. The cell has evolved intricate DNA damage response (DDR) mechanisms to counteract the genotoxic effects of these lesions. The two main features of the DDR are cell-cycle checkpoint activation and, at the heart of the response, DNA repair. For both damage signalling and repair, chromatin remodelling is most likely a prerequisite. Here, we discuss current knowledge on chromatin remodelling with respect to the cellular response to DNA damage, with emphasis on the response to single strand damage resolved by nucleotide excision repair (NER). We will discuss the role of histone modifications as well as their displacement or exchange in NER and make a comparison with their requirement in transcription and DSB repair.

## **INTRODUCTION**

Proper functioning of all living organisms depends on faithful maintenance of genomic information. Although it is generally believed that information stored is relatively safe and stable, the integrity of DNA is continuously challenged by numerous genotoxic agents and environmental stress. Essential cellular functions such as oxidative respiration and lipid peroxidation create reactive oxygen species that can damage DNA. In addition, spontaneous hydrolysis of nucleotides induces non-instructive abasic sites. Finally, environmental physical and chemical agents, such as UV and ionising radiation, as well as numerous genotoxic chemicals present in food or combustion products in the air, induce a wide variety of DNA lesions. It has been estimated that in an average mammalian cell ten to a hundred thousand DNA lesions are introduced each day [1].

The consequences of DNA damage are diverse and adverse. Acute cellular effects arise from impeded gene transcription and DNA replication, causing cellular malfunctioning, irreversible cell cycle arrest (senescence) or cell death (apoptosis) which are important factors in (premature) aging [2, 3]. DNA lesions interfere with proper chromosome segregation during cell division resulting in chromosome aberrations. In addition, replication errors due to DNA damage may introduce irreversible mutations. Chromosomal aberrations as well as mutations in coding genes may lead to carcinogenesis [3].

To counteract the severe biological consequences of DNA lesions an intricate network of genome surveillance mechanisms or DNA damage response (DDR) processes has evolved. The heart of this defence system is formed by complementary DNA repair systems that cover most of the genetic insults. In addition to the direct removal of lesions, DNA injuries trigger a signalling cascade that results in a slowdown of cell cycle progression providing cells more time to repair DNA damage prior to replication or cell division.

---



The template for DDR, damaged DNA, is packed into chromatin and it is expected that, analogous to other chromatin-associated processes such as replication and transcription [4, 5], chromatin structure influences the DDR and *vice versa*. Recently, an array of different types of chromatin structural modulations has been reported in relation to DDR. In this review we summarize and discuss current knowledge on chromatin remodelling, with emphasis on one specific DNA repair process, nucleotide excision repair. For recent reviews on the connection between chromatin remodelling and other repair pathways than NER, see [6-13].

### *DNA repair*

The many different types of DNA lesions cannot be repaired by a single repair system. Instead, a number of specific repair processes have evolved that each remove a subset of lesions [14, 15]. At least four major damage repair pathways operate in mammals: nucleotide excision repair (NER), base excision repair (BER), homologous recombination (HR) and end joining (EJ). NER deals with the wide class of single strand lesions that destabilize the double helix, potentially obstructing transcription and replication. Small types of chemical alterations in the bases and single-strand DNA breaks are targeted by BER. Lesions for NER and BER affect only one of the strands of the double helix. In both processes the injury is excised and the resulting gap is filled by DNA synthesis using the intact complementary strand as a template, enabling error-free DNA repair. To properly heal the more problematic double strand breaks (DSB) two major pathways have developed. In mammals homologous recombination appears to be the predominant mode of DSB repair in S and G2, when an intact second copy of the sequence (sister chromatid) is available. The more error-prone non-homologous end joining operates mainly in G1 phase, but can also work on DSBs in S-phase.

Nucleotide excision repair is a versatile repair pathway able to remove many different types of single strand lesions including the major UV-induced DNA photoproducts: cyclobutane pyrimidine dimers (CPD) and 6-4 photoproducts (6-4PP), as well as large or bulky chemical adducts [16]. In actively transcribed genes, such lesions cause stalling of RNA polymerase II, which in turn recruits downstream NER proteins, a pathway termed transcription coupled NER (TC-NER). In regions of the genome that are not actively transcribed, helix-distorting lesions are detected by the collective action of the UV-DDB complex and the XPC-containing complex (RAD4 in yeast), initiating the global genome NER (GG-NER) sub-pathway [16]. Both UV-DDB and XPC complexes are able to bind to a surprisingly broad range of lesions that create short stretches of unpaired bases. The substrate versatility of XPC is achieved by binding to the unpaired bases in the non-damaged strand opposite the lesion [17, 18]. After recognition of the damage by either stalled RNA pol II or XPC, repair complexes are assembled from freely diffusing NER factors: two helicases (XPB and XPD as part of the multi-functional, multi-subunit repair/transcription factor TFIIH), two single

---

strand DNA binding proteins (XPA and RPA), two structure-specific endonucleases (XPF-ERCC1 and XPG), the DNA replication machinery and two DNA ligases (Ligase1 and XRCC1-Lig3) [15, 19-22].

### *Cell-cycle checkpoint activation*

To allow a cell to repair DNA lesions before it passes through mitosis and potentially harmful mutations are propagated to the daughter cells, DNA damage checkpoints block the cell cycle in G1, S or G2 phases in response to genotoxic stress. The three mammalian phosphoinositide 3-kinase like kinases (PIKKs) ATM, ATR and DNA-PKcs have a central role in the activation of DNA damage checkpoints. These kinases induce a cascade of phosphorylations on a large number of different substrates, via mediators and transducers to effector-molecules, such as the checkpoint kinases Chk1 and Chk2 [23-26]. Other targets include the histone variant H2AX, checkpoint mediator protein 53BP1, DSB recognition factor Nbs1 and many others [27, 28]. ATM, ATR and DNA-PKcs are not only required for activating cell-cycle checkpoints but they also phosphorylate many substrates involved in other aspects of the DDR.

Although most types of DNA lesions have the ability to trigger cell-cycle checkpoint activation, damage signalling has been mainly studied in relation to DSBs. DNA double strand breaks induced by ionizing radiation generally cause large-scale chromatin rearrangements, initiated by phosphorylation of the histone H2A variant H2AX (see below) [29]. Phosphorylated H2AX ( $\gamma$ H2AX) triggers the accumulation of a multitude of different DSB repair and DNA damage signalling molecules, thereby concentrating repair proteins in small discrete nuclear foci termed ionizing radiation induced foci (IRIF). Although their nature and function has been a topic of debate, it is believed that they at least play a role in the signalling pathway. Furthermore, it has been proposed that a function of increased local concentrations of proteins involved in the DDR will both stimulate repair and serve as an amplification of checkpoint signals [30, 31]. Because even a single endonuclease-induced DSB can induce chromosomal instabilities [32], amplification of checkpoint signals most likely is required to block the cell-cycle until the DSB is repaired.

Proteins involved in NER typically bind to areas of DNA damage resulting in temporary immobilization of the proteins, but rather than accumulating in foci, they retain a homogenous distribution in G1 and G2 [33, 34]. This suggests that signal amplification by increased protein concentrations through foci formation, whether for activation of a cell-cycle checkpoint or for more efficient repair, is not required in NER. In addition, there is no evidence that NER-inducing lesions activate ATM or DNA-PKcs. However, during S-phase NER-related foci are formed when NER lesions generate stalled DNA replication forks, which create single stranded stretches that are quickly covered by RPA/ATRIP and finally ATR, triggering replication-stress signalling [35, 36]. Recently, evidence has been provided that also NER-intermediates (short single-strand strand gaps, resulting from

---

excised lesions) activate ATR [35-38]. It is currently unknown whether NER-induced ATR-signalling requires amplification in another way than by formation of foci as seen in DSB repair.

### *Chromatin remodelling*

In transcription and replication, changes in the chromatin structure are required in order to allow binding of the factors involved [4, 5]. There is increasing evidence that this is also the case for DNA repair. Chromatin remodelling to alter the accessibility of proteins to DNA occurs by two mechanisms: covalent histone modifications by means of post-translational modifications (PTMs) and displacement of histones or entire nucleosomes, either by sliding along the DNA or by removal. In this review we will discuss recent literature addressing questions like if and how the DDR and more particularly, NER requires modifications of chromatin structure and whether sequence specific epigenetic marks are restored after repair. Table 1 and 2 give an overview of chromatin remodelling events that take place during NER as compared with these events during transcription.

## **HISTONE MODIFICATIONS**

Covalent histone modifications or epigenetic changes are important regulatory elements for many biological processes. They function by influencing chromatin contacts or by recruiting non-histone proteins to chromatin [39]. Some covalent histone modifications that are involved in transcription are also associated with repair. On the other hand, modifications like phosphorylation of H2AX appear to be unique for DDR. In the next paragraphs we will focus on the four epigenetic marks that are implicated in DDR: phosphorylation, acetylation, methylation and ubiquitination.

### *Phosphorylation*

Phosphorylation of H2AX probably is the most important hallmark of DDR-related epigenetic change. Upon DSB induction by ionizing radiation, histone H2AX in the vicinity of DSBs is phosphorylated by ATM and DNA-PKcs at Serine 139. H2AX is phosphorylated over surprisingly long stretches of DNA of up to  $2 \times 10^6$  bp around the break [8, 29, 40, 41], creating a robust chromatin mark. In DSB repair, phosphorylated H2AX ( $\gamma$ H2AX) is important for the formation of IRIF. In the absence of  $\gamma$ H2AX, repair factors as NBS1 (part of a for homologous recombination essential complex MRN) and Brca1 as well as checkpoint proteins MDC1 and 53BP1 fail to accumulate in IRIF, although they are still recruited to DNA damage [31]. Despite the dramatic chromatin changes and highly concentrated repair factors induced by  $\gamma$ H2AX, its absence only mildly affects DSB repair [42]. This indicates that  $\gamma$ H2AX-induced concentration of repair factors at sites of DNA damage does not play a crucial role in DNA repair. However, the formation of these IRIF through phosphorylation of H2AX are important for the activation of cell-cycle

---

checkpoints in response to low doses of ionizing radiation [30], whereas yH2AX is dispensable for checkpoint activation at higher doses [42].

H2AX is also phosphorylated at residue S139 in response to UV-irradiation [37, 43-45], as well as its equivalent serine (S129 of H2A) in *S. cerevisiae* [46]. However, a S129A mutant strain was only slightly UV-sensitive. Rather, it appeared that three different serine residues, S2, S18 and S122 play important roles in UV-survival. The serine 122 residue is involved in a general response to DNA damage, as it is required for HR, NHEJ and NER. Surprisingly, this residue becomes dephosphorylated rather than phosphorylated upon UV-irradiation, whereas other damage inducing agents cause an increase of phosphorylation of S122 [46]. Whereas the DDR involves differential phosphorylation of multiple residues on both termini of H2A in yeast, no evidence currently is available that other residues than S139 of mammalian H2AX and H2A are implicated in DDR as well.

Also two histone residues of H3, serine 10 and threonine 11, appeared to be a target of differential phosphorylation during NER [47, 48].

**Table 1. Histone modifications associated with transcription and NER.**

ph = phosphorylation; ac = acetylation; me = methylation; ub = ubiquitination, '+' = upregulation or positive effect of the PTM, '-' = downregulation or negative effect of the PTM and '?' = unknown function.

PTM	Transcription	NER
H2AXS139ph/yH2AS129ph	?	+
yH2AS122ph	?	-
H2Aub	-	+
H3K9/K14ac	+	+
H3K79me	+	+
H3S10ph	+	-
H3T11ph	+	-
H4K20me	-	+
H3/H4ub	?	+

Phosphorylation of both these residues is associated with transcription activation [49, 50]. Like H2AS122 in yeast, H3S10 and H3T11 in mouse are dephosphorylated by UV irradiation and rephosphorylated after repair of the damage [47, 48]. The function of this H3 modification by DDR is not known yet. It is however tempting to speculate that the non-histone chromosomal protein HMGN1 plays a role, since HMGN1 inhibits the phosphorylation of H3S10 [51, 52], enhances repair of UV-lesions [51, 52] and was shown to be recruited to TC-NER complexes [53]. A possible scenario for the role of HMGN1 in differential H3 phosphorylation within DDR could be that HMGN1 is responsible for the dephosphorylation of H3S10. Hypophosphorylation of H3 at S10 and T11 is associated with transcription repression, and this might

---

be one of the mechanisms cells employ to inhibit transcription at UV-damaged areas.

### *Acetylation*

Another abundant histone PTM is differential acetylation, mainly associated with transcription activation. Different lysines in both histones H3 and H4 are targets for this modification that neutralizes the basic charge of the lysine, thereby potentially altering the interaction between adjacent histones and between histones and DNA [39]. It was shown already 20 years ago that histones become hyperacetylated in response to UV-irradiation and that DNA repair is more efficient in hyperacetylated nucleosomes [54, 55]. This suggests that changes in chromatin structure induced by acetylation make DNA more accessible to both transcription factors and repair factors.

Two histone acetyl transferases (HATs), Gcn5 and p300, responsible for the acetylation of multiple lysine residues within all 4 core-histones, are implicated in UV-induced DDR. In yeast, Gcn5 hyperacetylates H3 (at K9 and K14) at the repressed *MFA2* promoter upon UV-irradiation [56]. This acetylation is accompanied by increased accessibility of the DNA template (as tested by activity of restriction enzymes at the promoter), suggesting that the function for this modification is to allow access of proteins to the damaged DNA. Histone H3 acetylation by Gcn5 governs the transcription of ~5 % of the yeast genome, including at *MFA2*. Another promoter, *RPB2*, which does not require Gcn5 for histone acetylation, also does not require Gcn5 for damage removal [57].

Also in mammalian cells, there is evidence for the involvement of Gcn5 and the acetylation of H3 and H4 in DDR. Gcn5, is recruited to DNA damage as part of a large complex, TFTC, which also includes SAP130, a splicing factor with sequence homology to DDB1, which is one of the subunits of UV-DNA damage binding (UV-DDB) complex. Gcn5 is also part of another complex, STAGA, which interacts with both SAP130 and DDB1 in HeLa [58]. In yeast, also the Rad16/Rad7 complex is implicated in UV-induced histone acetylation [59]. This protein complex is essential for yeast GG-NER [60, 61]. Although GG-NER is conserved to mammals, surprisingly no sequence homologues for Rad16 or Rad7 have been found in mammalian cells. However, it has been suggested that the UV-DDB complex (containing DDB1 and the GG-NER-specific DDB2) might be a functional homologue of Rad16/Rad7 [62]. Besides the involvement of both these complexes in histone acetylation upon UV irradiation, there is more evidence pointing towards an at least partial functional homology between these complexes. For example, both are also involved in early steps of GG-NER and the ubiquitination of the NER recognition factor XPC/Rad4 [63, 64].

Gcn5 regulates a subset of genes, whereas p300 HAT is a more global regulator of transcription [65]. Multiple proteins have been implicated in targeting p300 to UV damage including Ing1B [66], DDB1 [67], PCNA [68], CSB [53] and p53 [69]. This suggests that besides Gcn5, p300 also has a function in acetylating histones before, during or after NER, although no

---

direct evidence has so far been presented that p300 activity is required for efficient NER.

### *Methylation*

A third abundant epigenetic histone mark is the differential methylation of lysine and arginine residues. Histones can be either mono-, di- or trimethylated and either be a marker for transcriptionally active or inactive chromatin, depending on the type of methylation and the residue involved. Arginine methylation is less well studied than lysine methylation and no connection of this modification with a DNA damage response has been found so far. Methylation of lysines H3K4, H3K36 and H3K79 is associated with transcription activation while methylation of H3K9 and H3K27 and H4K20 is connected to transcription repression [39]. In response to UV-irradiation, H3K79me and H4K20me have been identified as important players.

Studies in *S. cerevisiae* have shown that H3K79 methylation by Dot1p is required for efficient UV damage response. Disruption of H3K79 methylation, by *dot1* or *K79E* mutations, results in hypersensitivity to UV and intra-S phase checkpoint deficiency [70, 71]. In a similar study, H4K20 and its methyltransferase Set9 were mutated resulting in UV sensitivity and checkpoint deficiency in fission yeast [72]. Both H3K79 and H4K20 methylation are involved in checkpoint signalling after DSB induction by recruiting 53BP1/CRB2 to IRIF [72-76]. In addition to DSB, there are indications that 53BP1 is also activated by UV-irradiation [27, 77-79]. This indicates that histone methylation might have the same checkpoint activation function after UV-damage induction as it has in response to DSBs.

### *Ubiquitination*

One of the largest PTMs of histones is by conjugation of ubiquitin or ubiquitin-like moieties to lysine residues. Ubiquitin is a small 8.5 kD peptide that can either target the conjugated protein to proteasomal degradation or serve as a modifier for protein function [80, 81]. Modification of proteins by ubiquitin usually occurs via a three-step enzymatic reaction, involving a ubiquitin-activating, -conjugating and -ligating (respectively E1, E2 and E3) activity and conjugates either one (monoubiquitination) or multiple (polyubiquitination) ubiquitin moieties, depending on the substrate-specific combination of used E2 and E3. All four core-histones are targets for ubiquitination but the precise function for most histone ubiquitination activities remains obscure. During transcription, ubiquitination of H2A is generally associated with gene silencing whereas ubiquitination of H2B has been related with both gene activation and silencing [82-85]. Ubiquitination of H3 and H4 is less abundant and as of yet, no functional consequence has been assigned to this modification.

In yeast, histone H2B ubiquitination at lysine 123 by the Rad6/Bre1 E2/E3 complex is required in the response to several DNA damage sources, including UV [71, 86]. Absence of this modification (either by mutating Rad6

---

or H2B (K123R)), affects activation of the checkpoint kinase Rad53 and appeared connected with exposure of lysine 79-methylated H3 and its subsequent activation of another checkpoint protein Rad9 [70, 71]. No evidence has yet been presented that ubiquitination of H2B is increased after DNA damage induction. In mammalian cells, H2A rather than H2B appeared to be the main target of ubiquitination in response to UV-irradiation [87]. Remarkably, this modification was not required for NER, but rather occurs as a consequence of functional NER, as several defined NER-mutants did not result in UV-induced H2A-ubiquitination. Damage-induced H2A ubiquitination was further shown to depend on ATR, which suggests that it has a function in cell cycle signalling.

Besides H2A, both H3 and H4 are also ubiquitinated in response to UV damage induction [88]. A complex containing UV-DDB and CUL4A was required for this ubiquitination. H3 and H4 ubiquitination occurs early in DDR, in contrast to H2A ubiquitination, and together with the notion that ubiquitinated H3 and H4 reduce nucleosomal stability, it was suggested that this ubiquitination increases accessibility of repair factors. Therefore it has been suggested that the UV-DDB complex creates a chromatin environment that facilitates the assembly of the NER complex on damaged DNA [89].

Besides UV-induced H2A ubiquitination, recently also ubiquitination of H2A and H2AX in response to DSB induction was observed [90-92]. This epigenetic change is dependent on the ubiquitin-conjugating (E2) enzyme Ubc13 and the E3-ligase RING finger containing protein RNF8 [90-92]. The ubiquitination was shown to depend on H2AX phosphorylation and the subsequent recruitment and activation of MDC1, to which RNF8 binds. Ubiquitinated targets (H2A and H2AX) are crucial for the formation of IRIF and assembly of downstream repair and checkpoint factors (RAP80, BRCA1 and 53BP1). The dynamic equilibrium of differential H2A ubiquitination was shown to be important for genome stability as a mutant form of the H2A-specific deubiquitination (or DUB) enzyme USP3 causes delay of S-phase progression and activation of checkpoints [93].

## **HISTONE DISPLACEMENT AND EXCHANGE**

### *ATP-dependent chromatin remodelling*

Besides covalent histone modifications, another important mechanism that changes chromatin structure is accomplished by a series of ATP-dependent chromatin remodelling complexes. ATP-dependent chromatin remodelling involves displacement of histones, either by completely removing or replacing them, or by sliding whole nucleosomes along the DNA strand. Like covalent histone modifications, this activity can control the recruitment of DNA-interacting proteins to chromatin and it is a versatile control mechanism in all nuclear processes [94].

---

Next to a clear function in transcription regulation, a number of ATP-dependent remodelers were shown to play a role during DSB repair, including SWR1, RSC, INO80, Rad54 and SWI/SNF [95-98]. Only SWI/SNF has also been associated with NER in *in vitro* experiments [99]. All ATP-dependent chromatin remodelling complexes contain a motor subunit belonging to Snf2-like family of ATPases [100]. This Snf2-like family includes

**Table 2. Chromatin remodelers associated with transcription and NER.**

'+' = remodeler enhances transcription or NER, '-' = remodeler is involved in transcription repression and '?' = unknown function.

Remodeler	Transcription	NER
ACF	-	+
SWI/SNF	+	+
CAF-1	-	+
NAP1L1	+	?
FACT	+	?

a few known DNA repair proteins such as Rad16 and Rad5 in yeast (no mammalian orthologues have been identified) and Rad54 and Rad26 (RAD54 and CSB in mammals, respectively). The yeast Rad16, which harbours a Snf2-like domain, is exclusively involved in GG-NER [60], although no evidence exists for a role in chromatin remodelling. Rather, it acts in complex with Rad7 and Abf1 to generate superhelical torsion in DNA and its activity appears to be hindered by intact nucleosomes [61, 101]. On the other hand, in an *in vitro* accessibility assay the TC-NER-specific CSB disarranged regularly spaced nucleosomes in an ATP dependent manner [102]. Furthermore CSB directly interacted with doublestranded DNA and histone tails, which were required for this activity, suggesting that CSB may act as a UV-induced chromatin remodeler.

Two ATP-dependent chromatin remodelers that have been shown to stimulate NER by their remodelling activity are ACF and SWI/SNF [99, 103]. ACF is known to have a function in replication, especially of heterochromatin regions [104]. It also enhances binding of heterochromatin protein 1 (HP1) to transcriptionally inactive chromatin and it does not colocalize with RNA Polymerase II at salivary gland polytene chromosomes in *Drosophila*. This suggests that ACF is associated with transcription repression rather than activation [105, 106]. In contrast, SWI/SNF is mainly associated with transcription activation [107, 108].

ACF consists of two subunits, Acf1 and ISWI, which move nucleosomes along the DNA, generating internucleosomal spaces of 50 to 60 basepairs, without removing histones [109]. This nucleosomal sliding enhances NER activity, mainly in the linker regions between nucleosomes [103]. In contrast, the yeast SWI/SNF complex rather enhances NER of lesions located in nucleosome core regions [99]. This *in vitro* remodelling activity by SWI/SNF was dependent on the presence of NER factors XPC, XPA and RPA. In



addition, two subunits of the yeast SWI/SNF complex, Snf5 and Snf6, copurified with the NER factors Rad4 (the yeast homologue of XPC) and Rad23 [110]. Furthermore, Snf5 and Snf6 were shown to enhance NER and rearrange chromatin at the silent *HML* locus after UV irradiation. Most likely, yeast SWI/SNF is recruited to DNA lesions by binding to the Rad4-Rad23 complex, which is an early event in NER. It will be interesting to investigate whether the mammalian orthologue of ACF is also implicated in DDR.

### *Histone chaperones*

Genome function depends for a large part on the accessibility of the DNA template. Above, several mechanisms are summarized that provide more plasticity to the dense chromatin structure. However long-range transactions on the DNA helix, require more than simply increasing accessibility. During transcription elongation and replication, polymerases progress over long distances on DNA and extended nucleoprotein-filaments (involving RPA and RAD51) are formed in homologous recombination, which involve large-scale nucleosomal rearrangements. Although, it is likely that the discussed chromatin remodelers provide sufficient space to allow these elongations, displaced nucleosomes need to be repositioned after termination of these reactions. While some ATP-dependent chromatin remodelers are able to (re)deposit histones onto DNA, it is likely that for these more robust chromatin changes specialized activities exist to restore the chromatin structure. This group of specialized enzymes is referred to as histone chaperones. Histone chaperones deposit core histones onto DNA in an ATP-independent manner [111].

Asf1 is a histone chaperone that works together with either CAF-1 or HIRA to deposit H3/H4 dimers or tetramers. Throughout the cell cycle, Asf1-HIRA is responsible for the incorporation of H3 and H4, whereas Asf1-CAF-1 is involved in replication-dependent histone deposition [112-114]. Upon UV-damage induction, Asf1 promotes nucleosome assembly together with CAF-1 in a NER-dependent manner [115-117]. CAF-1 knockdown does not inhibit NER in mammalian cells, suggesting that this H3.1 deposition is part of a chromatin restoration step after damage has been repaired which likely has no or limited influence on the repair rate itself.

In yeast, Asf1 and CAF-1 are also involved in the response to UV irradiation. Both *cac1* (the yeast CAF-1 gene) and *asf1* mutants are sensitive to UV, but a *cac1 asf1* double mutant is more sensitive than either single mutant [118, 119]. This suggests that Asf1 can perform its function in the absence of CAF-1 and vice versa, albeit at a lower efficiency.

So far, no evidence has been found for the involvement of an H2A/H2B histone chaperone in NER. Possible candidates for this function are NAP1L1 or FACT, responsible for H2A/H2B deposition during replication and transcription [120-122]. In fact, FACT was recently shown to co-purify in complex with H2AX, DNA-PK and PARP1 and to promote the integration and dissociation of H2AX in a reconstituted nucleosomes experiment [122].

---

Phosphorylation of H2AX by DNA-PK increased the exchange of H2AX, indicating that FACT might function in histone exchange during DNA repair.

## **DISCUSSION**

Because factors involved in both DNA repair and transcription require access to DNA, it is not surprising that a number of remodelling proteins and histone modifications that are associated with active transcription are shared with NER (e.g. SWI/SNF and H3 acetylation) (see Table 1 and 2). However, in transcriptionally active chromatin, transcription over a damaged template should be prevented while repair factors should still be allowed to bind the damaged DNA. Upon UV-damage induction, RNA synthesis is inhibited by several mechanisms to protect the cell against the production of potentially dangerous proteins or RNAs [123-125]. One of these mechanisms involves phosphorylation, ubiquitination and proteolytic breakdown of RNA polymerase II [126, 127]. Physical removal of RNA polymerase II ensures that transcription does not take place at UV-damaged areas. In a more speculative scenario, a similar chromatin-mediated signal transduction pathway as for cell cycle control, through e.g. covalent histone modifications and histone displacement can be envisaged to inhibit transcription in a compromised genome. Although this mode of damage-induced transcriptional control after genomic insult has been proposed for many years, currently evidence is lacking whether this actually occurs.

It is unlikely that histone modifications and remodelling proteins with functions in preventing access to DNA during transcription inhibition have the opposite function during repair. Therefore, it is surprising that a number of involved in controlling NER-efficiency are associated with transcription inhibition rather than activation (H3 dephosphorylation, H4K20me, H2Aub, CAF-1). This may be explained by auxiliary functions of remodelling proteins and histone modifications in transcription inhibition at damaged areas besides RNA pol II degradation. Alternatively they may play a role in restoration of chromatin status after repair has taken place. Indeed CAF-1 activity at NER sites has been suggested to restore chromatin status after repair is finished rather than enhance repair by its remodelling activity [115].

We have discussed some of the chromatin remodelling activities that take place in association with NER in light of what is known for repair of DSBs. Besides requiring access of repair proteins to damaged DNA, different repair pathways also have in common that they should enable activation of cell-cycle checkpoints in order to remove lesions before they can turn into mutations. During the repair of DSBs, remodelled chromatin, especially by ATM-induced phosphorylation and subsequent ubiquitination of H2AX, has been shown to be a major signal in checkpoint activation and amplification [30, 90-92]. UV irradiation also induced phosphorylation of H2AX and ubiquitination of H2A both in an ATR-dependent fashion, most likely resulting in amplification of checkpoint signalling. Surprisingly and in contrast with DSBs, UV-lesions require NER activity prior to activation of ATR-signalling [38, 43], histone ubiquitination [87] and finally phosphorylation

---

---

of key checkpoint proteins Chk1 and p53 [128]. This absence of a chromatin-associated damage signalling might in part explain the extreme cancer-predisposition in naturally occurring NER mutants (i.e. NER-deficient xeroderma pigmentosum patients) on top of severely attenuated damage removal in these patient cells [3]. There are more interesting differences between chromatin remodelling responses upon DSB induction and NER activation. For example, in yeast, serine 122 of H2A becomes dephosphorylated upon UV irradiation, while after induction of other types of damage this residue is phosphorylated [46]. Interestingly, also the checkpoint activator protein p53 shows differential phosphorylation at a different residue in response to UV than  $\gamma$ -irradiation [129, 130]. One of the main challenges in the field of DNA damage response research will be to identify more such differences and similarities between responses to different types of lesions and determine their functions.

Finally, current knowledge on DDR and chromatin remodelling is based on studies each focusing on a separate DDR factor or different aspect of chromatin remodelling. More insight into the complex network of chromatin-associated DDR could be provided by systematic approaches combining genetic screening, transcriptional profiling, proteomic analysis and imaging approaches to study the spatio-temporal organisation of the entire DDR.

## REFERENCES

1. Lindahl T: **Instability and decay of the primary structure of DNA.** *Nature* 1993, **362**:709-715.
2. Hasty P, Campisi J, Hoeijmakers J, van Steeg H, Vijn J: **Aging and genome maintenance: lessons from the mouse?** *Science* 2003, **299**:1355-1359.
3. Mitchell JR, Hoeijmakers JH, Niedernhofer LJ: **Divide and conquer: nucleotide excision repair battles cancer and ageing.** *Curr Opin Cell Biol* 2003, **15**:232-240.
4. Li B, Carey M, Workman JL: **The role of chromatin during transcription.** *Cell* 2007, **128**:707-719.
5. Groth A, Rocha W, Verreault A, Almouzni G: **Chromatin challenges during DNA replication and repair.** *Cell* 2007, **128**:721-733.
6. Osley MA, Tsukuda T, Nickoloff JA: **ATP-dependent chromatin remodeling factors and DNA damage repair.** *Mutat Res* 2007, **618**:65-80.
7. Ataian Y, Krebs JE: **Five repair pathways in one context: chromatin modification during DNA repair.** *Biochem Cell Biol* 2006, **84**:490-504.
8. Costelloe T, Fitzgerald J, Murphy NJ, Flaus A, Lowndes NF: **Chromatin modulation and the DNA damage response.** *Exp Cell Res* 2006, **312**:2677-2686.
9. Altaf M, Saksouk N, Cote J: **Histone modifications in response to DNA damage.** *Mutat Res* 2007, **618**:81-90.
10. van Attikum H, Gasser SM: **The histone code at DNA breaks: a guide to repair?** *Nat Rev Mol Cell Biol* 2005, **6**:757-765.
11. Wong LY, Recht J, Laurent BC: **Chromatin remodeling and repair of DNA double-strand breaks.** *J Mol Histol* 2006, **37**:261-269.

12. Wurtele H, Verreault A: **Histone post-translational modifications and the response to DNA double-strand breaks.** *Curr Opin Cell Biol* 2006, **18**:137-144.
  13. Caldecott KW: **Mammalian single-strand break repair: mechanisms and links with chromatin.** *DNA Repair (Amst)* 2007, **6**:443-453.
  14. Essers J, Vermeulen W, Houtsmuller AB: **DNA damage repair: anytime, anywhere?** *Curr Opin Cell Biol* 2006, **18**:240-246.
  15. Hoeijmakers JH: **Genome maintenance mechanisms for preventing cancer.** *Nature* 2001, **411**:366-374.
  16. Gillet LC, Scharer OD: **Molecular mechanisms of mammalian global genome nucleotide excision repair.** *Chem Rev* 2006, **106**:253-276.
  17. Maillard O, Solyom S, Naegeli H: **An aromatic sensor with aversion to damaged strands confers versatility to DNA repair.** *PLoS Biol* 2007, **5**:e79.
  18. Min JH, Pavletich NP: **Recognition of DNA damage by the Rad4 nucleotide excision repair protein.** *Nature* 2007, **449**:570-575.
  19. Evans E, Moggs JG, Hwang JR, Egly JM, Wood RD: **Mechanism of open complex and dual incision formation by human nucleotide excision repair factors.** *EMBO J* 1997, **16**:6559-6573.
  20. Moser J, Kool H, Giakzidis I, Caldecott K, Mullenders LH, Foustieri MI: **Sealing of chromosomal DNA nicks during nucleotide excision repair requires XRCC1 and DNA ligase III alpha in a cell-cycle-specific manner.** *Mol Cell* 2007, **27**:311-323.
  21. de Laat WL, Jaspers NG, Hoeijmakers JH: **Molecular mechanism of nucleotide excision repair.** *Genes Dev* 1999, **13**:768-785.
  22. Volker M, Moné MJ, Karmakar P, Hoffen A, Schul W, Vermeulen W, Hoeijmakers JHJ, van Driel R, Zeeland AA, Mullenders LHF: **Sequential Assembly of the Nucleotide Excision Repair Factors In Vivo.** *Molecular Cell* 2001, **8**:213-224.
  23. Falck J, Coates J, Jackson SP: **Conserved modes of recruitment of ATM, ATR and DNA-PKcs to sites of DNA damage.** *Nature* 2005, **434**:605-611.
  24. Bartek J, Lukas J: **DNA damage checkpoints: from initiation to recovery or adaptation.** *Curr Opin Cell Biol* 2007, **19**:238-245.
  25. Liu Q, Guntuku S, Cui XS, Matsuoka S, Cortez D, Tamai K, Luo G, Carattini-Rivera S, DeMayo F, Bradley A, et al: **Chk1 is an essential kinase that is regulated by Atr and required for the G(2)/M DNA damage checkpoint.** *Genes Dev* 2000, **14**:1448-1459.
  26. Shiloh Y: **ATM and related protein kinases: safeguarding genome integrity.** *Nat Rev Cancer* 2003, **3**:155-168.
  27. Jowsey P, Morrice NA, Hastie CJ, McLauchlan H, Toth R, Rouse J: **Characterisation of the sites of DNA damage-induced 53BP1 phosphorylation catalysed by ATM and ATR.** *DNA Repair (Amst)* 2007, **6**:1536-1544.
  28. Bakkenist CJ, Kastan MB: **Initiating cellular stress responses.** *Cell* 2004, **118**:9-17.
  29. Rogakou EP, Pilch DR, Orr AH, Ivanova VS, Bonner WM: **DNA double-stranded breaks induce histone H2AX phosphorylation on serine 139.** *J Biol Chem* 1998, **273**:5858-5868.
  30. Fernandez-Capetillo O, Chen HT, Celeste A, Ward I, Romanienko PJ, Morales JC, Naka K, Xia Z, Camerini-Otero RD, Motoyama N, et al: **DNA damage-induced G2-M checkpoint activation by histone H2AX and 53BP1.** *Nat Cell Biol* 2002, **4**:993-997.
-

- 
31. Celeste A, Fernandez-Capetillo O, Kruhlak MJ, Pilch DR, Staudt DW, Lee A, Bonner RF, Bonner WM, Nussenzweig A: **Histone H2AX phosphorylation is dispensable for the initial recognition of DNA breaks.** *Nat Cell Biol* 2003, **5**:675-679.
  32. Bennett CB, Lewis AL, Baldwin KK, Resnick MA: **Lethality induced by a single site-specific double-strand break in a dispensable yeast plasmid.** *Proc Natl Acad Sci U S A* 1993, **90**:5613-5617.
  33. Zotter A, Luijsterburg MS, Warmerdam DO, Ibrahim S, Nigg A, van Cappellen WA, Hoeijmakers JH, van Driel R, Vermeulen W, Houtsmuller AB: **Recruitment of the nucleotide excision repair endonuclease XPG to sites of UV-induced dna damage depends on functional TFIIH.** *Mol Cell Biol* 2006, **26**:8868-8879.
  34. Houtsmuller AB, Rademakers S, Nigg AL, Hoogstraten D, Hoeijmakers JH, Vermeulen W: **Action of DNA repair endonuclease ERCC1/XPF in living cells.** *Science* 1999, **284**:958-961.
  35. Ward IM, Chen J: **Histone H2AX is phosphorylated in an ATR-dependent manner in response to replicational stress.** *J Biol Chem* 2001, **276**:47759-47762.
  36. Jeggo P, Lohrich M: **Radiation-induced DNA damage responses.** *Radiat Prot Dosimetry* 2006, **122**:124-127.
  37. Hanasoge S, Ljungman M: **H2AX phosphorylation after UV-irradiation is triggered by DNA repair intermediates and is mediated by the ATR kinase.** *Carcinogenesis* 2007.
  38. Matsumoto M, Yaginuma K, Igarashi A, Imura M, Hasegawa M, Iwabuchi K, Date T, Mori T, Ishizaki K, Yamashita K, et al: **Perturbed gap-filling synthesis in nucleotide excision repair causes histone H2AX phosphorylation in human quiescent cells.** *J Cell Sci* 2007, **120**:1104-1112.
  39. Kouzarides T: **Chromatin modifications and their function.** *Cell* 2007, **128**:693-705.
  40. Rogakou EP, Boon C, Redon C, Bonner WM: **Megabase chromatin domains involved in DNA double-strand breaks in vivo.** *J Cell Biol* 1999, **146**:905-916.
  41. Lowndes NF, Toh GW: **DNA repair: the importance of phosphorylating histone H2AX.** *Curr Biol* 2005, **15**:R99-R102.
  42. Celeste A, Petersen S, Romanienko PJ, Fernandez-Capetillo O, Chen HT, Sedelnikova OA, Reina-San-Martin B, Coppola V, Meffre E, Difilippantonio MJ, et al: **Genomic instability in mice lacking histone H2AX.** *Science* 2002, **296**:922-927.
  43. O'Driscoll M, Ruiz-Perez VL, Woods CG, Jeggo PA, Goodship JA: **A splicing mutation affecting expression of ataxia-telangiectasia and Rad3-related protein (ATR) results in Seckel syndrome.** *Nat Genet* 2003, **33**:497-501.
  44. Stiff T, Walker SA, Cerosaletti K, Goodarzi AA, Petermann E, Concannon P, O'Driscoll M, Jeggo PA: **ATR-dependent phosphorylation and activation of ATM in response to UV treatment or replication fork stalling.** *Embo J* 2006, **25**:5775-5782.
  45. Marti TM, Hefner E, Feeney L, Natale V, Cleaver JE: **H2AX phosphorylation within the G1 phase after UV irradiation depends on nucleotide excision repair and not DNA double-strand breaks.** *Proc Natl Acad Sci U S A* 2006, **103**:9891-9896.
-

46. Moore JD, Yazgan O, Ataian Y, Krebs JE: **Diverse roles for histone H2A modifications in DNA damage response pathways in yeast.** *Genetics* 2006.
47. Sen SP, De Benedetti A: **TLK1B promotes repair of UV-damaged DNA through chromatin remodeling by Asf1.** *BMC Mol Biol* 2006, **7**:37.
48. Shimada M, Niida H, Zineldeen DH, Tagami H, Tanaka M, Saito H, Nakanishi M: **Chk1 is a histone H3 threonine 11 kinase that regulates DNA damage-induced transcriptional repression.** *Cell* 2008, **132**:221-232.
49. Clements A, Poux AN, Lo WS, Pillus L, Berger SL, Marmorstein R: **Structural basis for histone and phosphohistone binding by the GCN5 histone acetyltransferase.** *Mol Cell* 2003, **12**:461-473.
50. Ivaldi MS, Karam CS, Corces VG: **Phosphorylation of histone H3 at Ser10 facilitates RNA polymerase II release from promoter-proximal pausing in Drosophila.** *Genes Dev* 2007, **21**:2818-2831.
51. Lim JH, Catez F, Birger Y, West KL, Prymakowska-Bosak M, Postnikov YV, Bustin M: **Chromosomal protein HMGN1 modulates histone H3 phosphorylation.** *Mol Cell* 2004, **15**:573-584.
52. Birger Y, West KL, Postnikov YV, Lim JH, Furusawa T, Wagner JP, Laufer CS, Kraemer KH, Bustin M: **Chromosomal protein HMGN1 enhances the rate of DNA repair in chromatin.** *Embo J* 2003, **22**:1665-1675.
53. Fousteri M, Vermeulen W, van Zeeland AA, Mullenders LH: **Cockayne syndrome A and B proteins differentially regulate recruitment of chromatin remodeling and repair factors to stalled RNA polymerase II in vivo.** *Mol Cell* 2006, **23**:471-482.
54. Ramanathan B, Smerdon MJ: **Changes in nuclear protein acetylation in u.v.-damaged human cells.** *Carcinogenesis* 1986, **7**:1087-1094.
55. Ramanathan B, Smerdon MJ: **Enhanced DNA repair synthesis in hyperacetylated nucleosomes.** *J Biol Chem* 1989, **264**:11026-11034.
56. Yu Y, Teng Y, Liu H, Reed SH, Waters R: **UV irradiation stimulates histone acetylation and chromatin remodeling at a repressed yeast locus.** *Proc Natl Acad Sci U S A* 2005, **102**:8650-8655.
57. Teng Y, Yu Y, Waters R: **The Saccharomyces cerevisiae histone acetyltransferase Gcn5 has a role in the photoreactivation and nucleotide excision repair of UV-induced cyclobutane pyrimidine dimers in the MFA2 gene.** *J Mol Biol* 2002, **316**:489-499.
58. Martinez E, Palhan VB, Tjernberg A, Lyman ES, Gamper AM, Kundu TK, Chait BT, Roeder RG: **Human STAGA complex is a chromatin-acetylation transcription coactivator that interacts with pre-mRNA splicing and DNA damage-binding factors in vivo.** *Mol Cell Biol* 2001, **21**:6782-6795.
59. Teng Y, Liu H, Gill HW, Yu Y, Waters R, Reed SH: **Saccharomyces cerevisiae Rad16 mediates ultraviolet-dependent histone H3 acetylation required for efficient global genome nucleotide-excision repair.** *EMBO Rep* 2007.
60. Verhage R, Zeeman AM, de Groot N, Gleig F, Bang DD, van de Putte P, Brouwer J: **The RAD7 and RAD16 genes, which are essential for pyrimidine dimer removal from the silent mating type loci, are also required for repair of the nontranscribed strand of an active gene in Saccharomyces cerevisiae.** *Mol Cell Biol* 1994, **14**:6135-6142.
61. Yu S, Owen-Hughes T, Friedberg EC, Waters R, Reed SH: **The yeast Rad7/Rad16/Abf1 complex generates superhelical torsion in DNA that**

- 
- is required for nucleotide excision repair. *DNA Repair (Amst)* 2004, **3**:277-287.
62. Lombaerts M, Peltola PH, Visse R, den Dulk H, Brandsma JA, Brouwer J: **Characterization of the rhp7(+) and rhp16(+) genes in Schizosaccharomyces pombe.** *Nucleic Acids Res* 1999, **27**:3410-3416.
63. Sugawara K, Okuda Y, Saijo M, Nishi R, Matsuda N, Chu G, Mori T, Iwai S, Tanaka K, Tanaka K, Hanaoka F: **UV-induced ubiquitylation of XPC protein mediated by UV-DDB-ubiquitin ligase complex.** *Cell* 2005, **121**:387-400.
64. Gillette TG, Yu S, Zhou Z, Waters R, Johnston SA, Reed SH: **Distinct functions of the ubiquitin-proteasome pathway influence nucleotide excision repair.** *Embo J* 2006, **25**:2529-2538.
65. Sterner DE, Berger SL: **Acetylation of histones and transcription-related factors.** *Microbiol Mol Biol Rev* 2000, **64**:435-459.
66. Kuo WH, Wang Y, Wong RP, Campos EI, Li G: **The ING1b tumor suppressor facilitates nucleotide excision repair by promoting chromatin accessibility to XPA.** *Exp Cell Res* 2007, **313**:1628-1638.
67. Ropic-Otrin V, McLenigan MP, Bisi DC, Gonzalez M, Levine AS: **Sequential binding of UV DNA damage binding factor and degradation of the p48 subunit as early events after UV irradiation.** *Nucleic Acids Res* 2002, **30**:2588-2598.
68. Hasan S, Hassa PO, Imhof R, Hottiger MO: **Transcription coactivator p300 binds PCNA and may have a role in DNA repair synthesis.** *Nature* 2001, **410**:387-391.
69. Rubbi CP, Milner J: **p53 is a chromatin accessibility factor for nucleotide excision repair of DNA damage.** *Embo J* 2003, **22**:975-986.
70. Bostelman LJ, Keller AM, Albrecht AM, Arat A, Thompson JS: **Methylation of histone H3 lysine-79 by Dot1p plays multiple roles in the response to UV damage in Saccharomyces cerevisiae.** *DNA Repair (Amst)* 2007, **6**:383-395.
71. Giannattasio M, Lazzaro F, Plevani P, Muzi-Falconi M: **The DNA damage checkpoint response requires histone H2B ubiquitination by Rad6-Bre1 and H3 methylation by Dot1.** *J Biol Chem* 2005, **280**:9879-9886.
72. Sanders SL, Portoso M, Mata J, Bahler J, Allshire RC, Kouzarides T: **Methylation of histone H4 lysine 20 controls recruitment of Crb2 to sites of DNA damage.** *Cell* 2004, **119**:603-614.
73. Botuyan MV, Lee J, Ward IM, Kim JE, Thompson JR, Chen J, Mer G: **Structural basis for the methylation state-specific recognition of histone H4-K20 by 53BP1 and Crb2 in DNA repair.** *Cell* 2006, **127**:1361-1373.
74. Kim J, Daniel J, Espejo A, Lake A, Krishna M, Xia L, Zhang Y, Bedford MT: **Tudor, MBT and chromo domains gauge the degree of lysine methylation.** *EMBO Rep* 2006, **7**:397-403.
75. Du LL, Nakamura TM, Russell P: **Histone modification-dependent and -independent pathways for recruitment of checkpoint protein Crb2 to double-strand breaks.** *Genes Dev* 2006, **20**:1583-1596.
76. Huyen Y, Zgheib O, Ditullio RA, Jr., Gorgoulis VG, Zacharatos P, Petty TJ, Sheston EA, Mellert HS, Stavridi ES, Halazonetis TD: **Methylated lysine 79 of histone H3 targets 53BP1 to DNA double-strand breaks.** *Nature* 2004, **432**:406-411.
77. Silverman J, Takai H, Buonomo SB, Eisenhaber F, de Lange T: **Human Rif1, ortholog of a yeast telomeric protein, is regulated by ATM and**
-

- 53BP1 and functions in the S-phase checkpoint.** *Genes Dev* 2004, **18**:2108-2119.
78. Rappold I, Iwabuchi K, Date T, Chen J: **Tumor suppressor p53 binding protein 1 (53BP1) is involved in DNA damage-signaling pathways.** *J Cell Biol* 2001, **153**:613-620.
79. Anderson L, Henderson C, Adachi Y: **Phosphorylation and rapid relocalization of 53BP1 to nuclear foci upon DNA damage.** *Mol Cell Biol* 2001, **21**:1719-1729.
80. Herrmann J, Lerman LO, Lerman A: **Ubiquitin and ubiquitin-like proteins in protein regulation.** *Circ Res* 2007, **100**:1276-1291.
81. Glickman MH, Ciechanover A: **The ubiquitin-proteasome proteolytic pathway: destruction for the sake of construction.** *Physiol Rev* 2002, **82**:373-428.
82. Kao CF, Hillyer C, Tsukuda T, Henry K, Berger S, Osley MA: **Rad6 plays a role in transcriptional activation through ubiquitylation of histone H2B.** *Genes Dev* 2004, **18**:184-195.
83. Osley MA: **Regulation of histone H2A and H2B ubiquitylation.** *Brief Funct Genomic Proteomic* 2006, **5**:179-189.
84. de Napoles M, Mermoud JE, Wakao R, Tang YA, Endoh M, Appanah R, Nesterova TB, Silva J, Otte AP, Vidal M, et al: **Polycomb group proteins Ring1A/B link ubiquitylation of histone H2A to heritable gene silencing and X inactivation.** *Dev Cell* 2004, **7**:663-676.
85. Turner SD, Ricci AR, Petropoulos H, Genereaux J, Skerjanc IS, Brandl CJ: **The E2 ubiquitin conjugase Rad6 is required for the ArgR/Mcm1 repression of ARG1 transcription.** *Mol Cell Biol* 2002, **22**:4011-4019.
86. Robzyk K, Recht J, Osley MA: **Rad6-dependent ubiquitination of histone H2B in yeast.** *Science* 2000, **287**:501-504.
87. Bergink S, Salomons FA, Hoogstraten D, Groothuis TA, de Waard H, Wu J, Yuan L, Citterio E, Houtsmuller AB, Neefjes J, et al: **DNA damage triggers nucleotide excision repair-dependent monoubiquitylation of histone H2A.** *Genes Dev* 2006, **20**:1343-1352.
88. Wang H, Zhai L, Xu J, Joo HY, Jackson S, Erdjument-Bromage H, Tempst P, Xiong Y, Zhang Y: **Histone H3 and H4 ubiquitylation by the CUL4-DDB-ROC1 ubiquitin ligase facilitates cellular response to DNA damage.** *Mol Cell* 2006, **22**:383-394.
89. Luijsterburg MS, Goedhart J, Moser J, Kool H, Geverts B, Houtsmuller AB, Mullenders LH, Vermeulen W, van Driel R: **Dynamic in vivo interaction of DDB2 E3 ubiquitin ligase with UV-damaged DNA is independent of damage-recognition protein XPC.** *J Cell Sci* 2007, **120**:2706-2716.
90. Mailand N, Bekker-Jensen S, Faustrup H, Melander F, Bartek J, Lukas C, Lukas J: **RNF8 Ubiquitylates Histones at DNA Double-Strand Breaks and Promotes Assembly of Repair Proteins.** *Cell* 2007.
91. Huen MS, Grant R, Manke I, Minn K, Yu X, Yaffe MB, Chen J: **RNF8 Transduces the DNA-Damage Signal via Histone Ubiquitylation and Checkpoint Protein Assembly.** *Cell* 2007.
92. Kolas NK, Chapman JR, Nakada S, Ylanko J, Chahwan R, Sweeney FD, Panier S, Mendez M, Wildenhain J, Thomson TM, et al: **Orchestration of the DNA-Damage Response by the RNF8 Ubiquitin Ligase.** *Science* 2007.
93. Nicassio F, Corrado N, Vissers JH, Areces LB, Bergink S, Marteijn JA, Geverts B, Houtsmuller AB, Vermeulen W, Di Fiore PP, Citterio E: **Human**
-



- 
- USP3 is a chromatin modifier required for S phase progression and genome stability.** *Curr Biol* 2007, **17**:1972-1977.
94. Gangaraju VK, Bartholomew B: **Mechanisms of ATP dependent chromatin remodeling.** *Mutat Res* 2007, **618**:3-17.
95. Osley MA, Shen X: **Altering nucleosomes during DNA double-strand break repair in yeast.** *Trends Genet* 2006, **22**:671-677.
96. van Attikum H, Fritsch O, Hohn B, Gasser SM: **Recruitment of the INO80 complex by H2A phosphorylation links ATP-dependent chromatin remodeling with DNA double-strand break repair.** *Cell* 2004, **119**:777-788.
97. Morrison AJ, Highland J, Krogan NJ, Arbel-Eden A, Greenblatt JF, Haber JE, Shen X: **INO80 and gamma-H2AX interaction links ATP-dependent chromatin remodeling to DNA damage repair.** *Cell* 2004, **119**:767-775.
98. van Attikum H, Fritsch O, Gasser SM: **Distinct roles for SWR1 and INO80 chromatin remodeling complexes at chromosomal double-strand breaks.** *Embo J* 2007, **26**:4113-4125.
99. Hara R, Sancar A: **The SWI/SNF chromatin-remodeling factor stimulates repair by human excision nuclease in the mononucleosome core particle.** *Mol Cell Biol* 2002, **22**:6779-6787.
100. Lusser A, Kadonaga JT: **Chromatin remodeling by ATP-dependent molecular machines.** *Bioessays* 2003, **25**:1192-1200.
101. Li S, Ding B, Lejeune D, Ruggiero C, Chen X, Smerdon MJ: **The roles of Rad16 and Rad26 in repairing repressed and actively transcribed genes in yeast.** *DNA Repair (Amst)* 2007.
102. Citterio E, Van Den Boom V, Schnitzler G, Kanaar R, Bonte E, Kingston RE, Hoeijmakers JH, Vermeulen W: **ATP-Dependent Chromatin Remodeling by the Cockayne Syndrome B DNA Repair-Transcription-Coupling Factor.** *Mol Cell Biol* 2000, **20**:7643-7653.
103. Ura K, Araki M, Saeki H, Masutani C, Ito T, Iwai S, Mizukoshi T, Kaneda Y, Hanaoka F: **ATP-dependent chromatin remodeling facilitates nucleotide excision repair of UV-induced DNA lesions in synthetic dinucleosomes.** *Embo J* 2001, **20**:2004-2014.
104. Collins N, Poot RA, Kukimoto I, Garcia-Jimenez C, Dellaire G, Varga-Weisz PD: **An ACF1-ISWI chromatin-remodeling complex is required for DNA replication through heterochromatin.** *Nat Genet* 2002, **32**:627-632.
105. Deuring R, Fanti L, Armstrong JA, Sarte M, Papoulas O, Prestel M, Daubresse G, Verardo M, Moseley SL, Berloco M, et al: **The ISWI chromatin-remodeling protein is required for gene expression and the maintenance of higher order chromatin structure in vivo.** *Mol Cell* 2000, **5**:355-365.
106. Eskeland R, Eberharter A, Imhof A: **HP1 binding to chromatin methylated at H3K9 is enhanced by auxiliary factors.** *Mol Cell Biol* 2007, **27**:453-465.
107. Vignali M, Hassan AH, Neely KE, Workman JL: **ATP-dependent chromatin-remodeling complexes.** *Mol Cell Biol* 2000, **20**:1899-1910.
108. Kadam S, Emerson BM: **Transcriptional specificity of human SWI/SNF BRG1 and BRM chromatin remodeling complexes.** *Mol Cell* 2003, **11**:377-389.
109. Yang JG, Madrid TS, Sevastopoulos E, Narlikar GJ: **The chromatin-remodeling enzyme ACF is an ATP-dependent DNA length sensor that regulates nucleosome spacing.** *Nat Struct Mol Biol* 2006, **13**:1078-1083.
-

110. Gong F, Fahy D, Smerdon MJ: **Rad4-Rad23 interaction with SWI/SNF links ATP-dependent chromatin remodeling with nucleotide excision repair.** *Nat Struct Mol Biol* 2006, **13**:902-907.
  111. Tyler JK: **Chromatin assembly. Cooperation between histone chaperones and ATP-dependent nucleosome remodeling machines.** *Eur J Biochem* 2002, **269**:2268-2274.
  112. Polo SE, Almouzni G: **Chromatin assembly: a basic recipe with various flavours.** *Curr Opin Genet Dev* 2006, **16**:104-111.
  113. Sharp JA, Fouts ET, Krawitz DC, Kaufman PD: **Yeast histone deposition protein Asf1p requires Hir proteins and PCNA for heterochromatic silencing.** *Curr Biol* 2001, **11**:463-473.
  114. Green EM, Antczak AJ, Bailey AO, Franco AA, Wu KJ, Yates JR, 3rd, Kaufman PD: **Replication-independent histone deposition by the HIR complex and Asf1.** *Curr Biol* 2005, **15**:2044-2049.
  115. Polo SE, Roche D, Almouzni G: **New histone incorporation marks sites of UV repair in human cells.** *Cell* 2006, **127**:481-493.
  116. Mello JA, Sillje HH, Roche DM, Kirschner DB, Nigg EA, Almouzni G: **Human Asf1 and CAF-1 interact and synergize in a repair-coupled nucleosome assembly pathway.** *EMBO Rep* 2002, **3**:329-334.
  117. Green CM, Almouzni G: **Local action of the chromatin assembly factor CAF-1 at sites of nucleotide excision repair in vivo.** *Embo J* 2003, **22**:5163-5174.
  118. Kaufman PD, Kobayashi R, Stillman B: **Ultraviolet radiation sensitivity and reduction of telomeric silencing in *Saccharomyces cerevisiae* cells lacking chromatin assembly factor-I.** *Genes Dev* 1997, **11**:345-357.
  119. Tyler JK, Adams CR, Chen SR, Kobayashi R, Kamakaka RT, Kadonaga JT: **The RCAF complex mediates chromatin assembly during DNA replication and repair.** *Nature* 1999, **402**:555-560.
  120. Reinberg D, Sims RJ, 3rd: **de FACTo nucleosome dynamics.** *J Biol Chem* 2006, **281**:23297-23301.
  121. Zlatanova J, Seebart C, Tomschik M: **Nap1: taking a closer look at a juggler protein of extraordinary skills.** *Faseb J* 2007, **21**:1294-1310.
  122. Heo K, Kim H, Choi SH, Choi J, Kim K, Gu J, Lieber MR, Yang AS, An W: **FACT-mediated exchange of histone variant H2AX regulated by phosphorylation of H2AX and ADP-ribosylation of Spt16.** *Mol Cell* 2008, **30**:86-97.
  123. Kantor GJ, Hull DR: **An effect of ultraviolet light on RNA and protein synthesis in nondividing human diploid fibroblasts.** *Biophys J* 1979, **27**:359-370.
  124. Mone MJ, Volker M, Nikaido O, Mullenders LH, van Zeeland AA, Verschure PJ, Manders EM, van Driel R: **Local UV-induced DNA damage in cell nuclei results in local transcription inhibition.** *EMBO Rep* 2001, **2**:1013-1017.
  125. Kruhlak M, Crouch EE, Orlov M, Montano C, Gorski SA, Nussenzweig A, Misteli T, Phair RD, Casellas R: **The ATM repair pathway inhibits RNA polymerase I transcription in response to chromosome breaks.** *Nature* 2007, **447**:730-734.
  126. Rockx DA, Mason R, van Hoffen A, Barton MC, Citterio E, Bregman DB, van Zeeland AA, Vrieling H, Mullenders LH: **UV-induced inhibition of transcription involves repression of transcription initiation and phosphorylation of RNA polymerase II.** *Proc Natl Acad Sci U S A* 2000, **97**:10503-10508.
-

127. Woudstra EC, Gilbert C, Fellows J, Jansen L, Brouwer J, Erdjument-Bromage H, Tempst P, Svejstrup JQ: **A Rad26-Def1 complex coordinates repair and RNA pol II proteolysis in response to DNA damage.** *Nature* 2002, **415**:929-933.
128. Mannhaupt G, Stucka R, Ehnle S, Vetter I, Feldmann H: **Molecular analysis of yeast chromosome II between *CMD1* and *LYS2*: the excision repair gene *RAD16* located in this region belongs to a novel group of finger proteins.** *Yeast* 1992, **8**:397-408.
129. Kapoor M, Lozano G: **Functional activation of p53 via phosphorylation following DNA damage by UV but not gamma radiation.** *Proc Natl Acad Sci U S A* 1998, **95**:2834-2837.
130. Lu H, Taya Y, Ikeda M, Levine AJ: **Ultraviolet radiation, but not gamma radiation or etoposide-induced DNA damage, results in the phosphorylation of the murine p53 protein at serine-389.** *Proc Natl Acad Sci U S A* 1998, **95**:6399-6402.



## Chapter 2

# Fluorescence Microscopy and Live-cell Imaging

Live cell microscopy is one of the most direct techniques to study biological processes, as it allows one to visualize structures and objects as they appear in nature, or to manipulate the processes under surveillance and draw conclusions from the cellular response. In this chapter different microscopy techniques will be introduced focusing on fluorescence microscopy as it is by far the most frequently used in live cell imaging. Specific attention will go to the techniques that were used in the research described in this dissertation.

### Fluorescence microscopy

Microscopy has been a very important tool in science ever since the development of the first microscopes by Zacharias Jansen (~1585 – 1632) and Cornelis Drebbel (1572 – 1633) and the discovery of bacteria by Antoni van Leeuwenhoek (1632 – 1723). In time, more sophisticated microscopes were built with higher resolution and visualization techniques were developed to show structures that were invisible before. For instance, phase contrast microscopy uses the change in phase of a light wave passing through a sample to visualize it (Zernike, 1955), electron microscopy (EM) uses electrons instead of photons to illuminate objects that are too small to be illuminated with visible wavelengths of light and histological staining and immunohistochemistry use colors to show specific structures in fixed samples. With immunohistochemical techniques, these colors usually come from antibodies bound to fluorescent molecules. Fluorescence is the process that occurs when fluorescent molecules absorb light of a certain wavelength and, following this absorption, emit light at a higher wavelength. The difference between the absorption and emission wavelength of a fluorescent

molecule is often referred to as the Stokes shift. Immunofluorescence, like histological stainings and EM, is typically applied to fixed samples, which

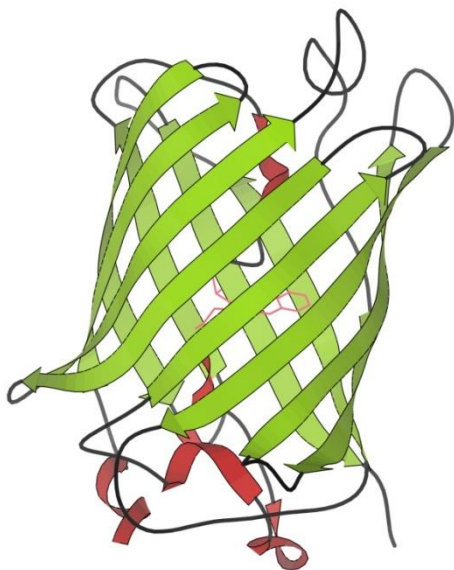


**Fig 1.** GFP displayed as a ribbon diagram. In the center of the beta sheet barrel (green) the single alpha helix contains the three amino acids that form the fluorophore (red). The image was captured with KING display software version 2.13 from <http://kinemage.biochem.duke.edu/>.

excludes the possibility to study biological processes in their most relevant context, the living cell. In order to study for instance the movement and activity of a protein in a living cell, this protein has to be visualized directly by chemical or genetic labeling with a dye, preferably a fluorescent one. Arguably the most important discovery in cell biology in recent history is of one such molecule that can be directly tagged to proteins of interest by means of molecular cloning, the green fluorescent protein (GFP).

### **GFP**

GFP is a 27 kDa protein (Fig 1), originally isolated from the jellyfish *Aequoria victoria*, which emits green light ( $\lambda_{\text{max}} = 508 \text{ nm}$ ) when excited by blue light ( $\lambda_{\text{max}} = 395 \text{ nm}$  and a minor peak at 475 nm) (Cubitt et al., 1995; Shimomura et al., 1962). An important breakthrough for molecular and cell biology came when GFP was first cloned and shown to be non-toxic and stable in cells of other organisms than *A. victoria*, without requiring any external cofactors (Chalfie et al., 1994; Prasher et al., 1992). This made it possible to fuse the coding sequence of GFP to that of virtually any other protein and study the behavior of these proteins in their natural environment by expressing GFP fusion genes in living cells.

Wild-type GFP (wtGFP) can be ectopically expressed and visualized in probably all cell types, however detection suffers from poor photostability, delayed folding at 37°C, inefficient translation due to jelly-fish specific codon usage and a dual peak excitation spectrum. To overcome these disadvantages, many GFP variants with enhanced properties both at coding and protein level were engineered (Cramer et al., 1996; Heim et al., 1995; Tsien, 1998). Also, to enable multicolor experiments, variants of wtGFP and GFP-like proteins from other organisms, such as DsRed (from *Discosoma striata*), with different emission and excitation peaks are continuously being generated (Kremers et al., 2007; Kremers et al., 2006; Matz et al., 1999; Merzlyak et al., 2007; Shaner et al., 2004). The currently available panel of GFP variants covers most of the visual spectrum.

### **Confocal microscopy**

Fluorescence microscopes use filters that block or reflect light of certain wavelengths and transmit light of other wavelengths to specifically illuminate and detect fluorescent molecules. In modern fluorescence microscopy, excitation occurs through the same objective as detection of fluorescence. With this so-called epifluorescence microscopy most of the excitation light (which can be  $<10^4$  times stronger than fluorescence) passes through the specimen, and is therefore not detected. Dichroic mirrors reflect light below a certain wavelength (including the excitation wavelength) and transmit light at higher wavelengths (including the emission wavelength). Excitation light is reflected off the dichroic mirror onto the specimen. Emitted fluorescence light then passes back through the dichroic mirror to a detector while reflected excitation light off the specimen is reflected by the dichroic mirror. An emission filter blocks most of the remaining reflected excitation light, further

---

increasing the signal to noise ratio. Different excitation and emission filters can be combined to allow for simultaneous imaging of multiple colours. This makes fluorescence microscopy a very powerful tool to study the localization of different proteins relative to each other in one specimen. One disadvantage of conventional fluorescence microscopy compared with improved fluorescence microscopy techniques such as confocal laser scanning microscopy (CLSM), is the problem of out-of-focus light. In conventional fluorescence microscopy, besides in-focus fluorophores, light from fluorophores out of the focal plane of the objective will be detected by the photodetector or CCD camera as well, resulting in blurred images. This especially becomes a problem with thicker samples that produce more out of focus light that will be recorded together with the in focus image. The confocal microscope was developed to block out of focus light (Marvin Minsky, 1961, US patent 3013467; (Davidovits and Egger, 1969; Grond et al., 1982). Confocal microscopy uses point illumination by a laser, as opposed to widefield illumination by conventional fluorescence microscopes, and fluorescence is detected through a pinhole in front of the detector, which blocks out-of-focus light (Fig 2). The detection pinhole and the focus of the objective are in **conjugate focal** planes, thus explaining the word confocal. Only in-focus fluorescence is detected, resulting in higher image quality than conventional fluorescence microscopy. Because the specimen is illuminated by a point source (generally a laser) and only photons from the illuminated point are detected, samples have to be scanned to produce a complete image. Computers are used to store this sequentially recorded point-by-point information.



Because out-of-focus information is largely blocked by the confocal pinhole, only a thin slice of the sample is actually scanned. The thickness of this slice depends on the wavelength of the fluorophores that are used but in practice the minimum thickness of a confocal slice is  $\sim 0.5 \mu\text{m}$  (Schrader et al., 1998). The ability of confocal microscopes to make thin optical slices is used to create 3D reconstructions of scanned samples. By taking a series of images at different depths of a sample a so-called z-stack is created, which can be used to analyze fluorescent objects in 3D. This extra (z-) dimension is especially important for determining colocalization of proteins visualized with different colored tags, because for accurate determination of the location of an object, three dimensions are required. When time is added as a fourth dimension, movement of fluorescent objects can be tracked, providing a wealth of information about proteins and biological structures that is not possible to study with other techniques.

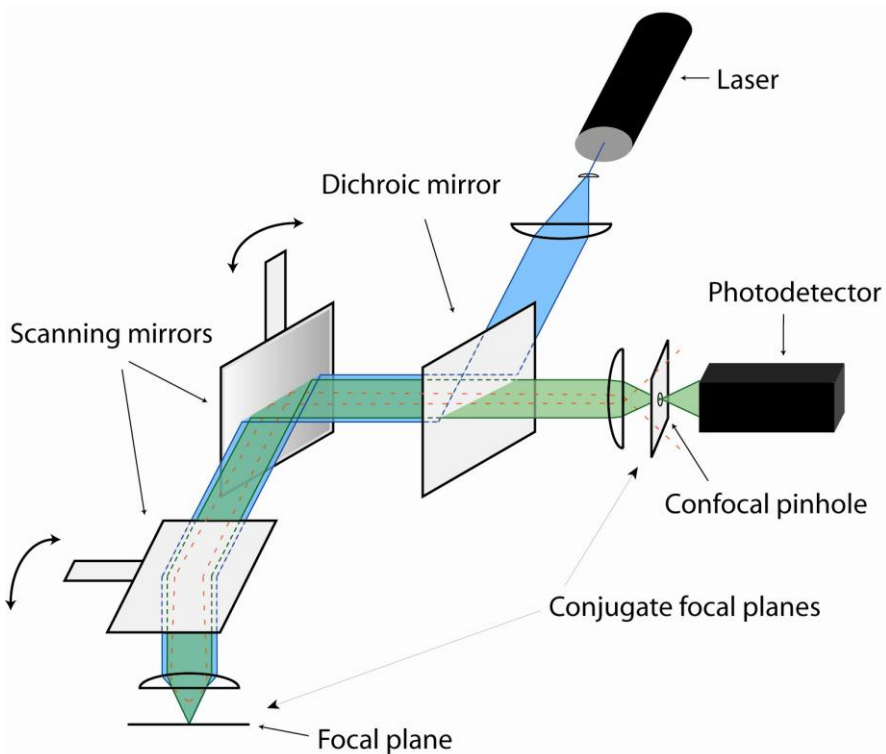


**Fig 2.** Confocal microscope schematic. The (blue) excitation laser reflects off a dichroic mirror and hits two motor-mounted mirrors that scan the laser light across the focal plane. Emission light (green) from excited fluorophores is descanned by the same mirrors, and passes through the dichroic mirror. Light that comes through the confocal pinhole is detected by the photodetector, while light coming from above (or below) the focal plane (red dotted lines), is not focused on the pinhole and therefore only a very small fraction is detected.

**Photobleaching techniques**

Fluorophores have a limited number of excitation-emission cycles they can go through before they become non-fluorescent (e.g.  $\leq 4 \cdot 10^5$  for GFP in solution (Kubitscheck et al., 2000)). This process is called photobleaching. Photobleaching is caused by photochemical reactions of the fluorophore in the excited state with surrounding molecules to produce irreversible covalent modifications. This photobleachable quality of GFP or any other fluorophore has become an important tool in studies of proteins in living cells. Fluorescence recovery after photobleaching (FRAP) and fluorescence loss in photobleaching (FLIP) are two such techniques (Houtsmuller and Vermeulen, 2001; Reits and Neefjes, 2001). With FRAP, fluorescent molecules in an area in the cell are photobleached by a high-intensity laser pulse, and the redistribution of fluorescence in the photobleached region is

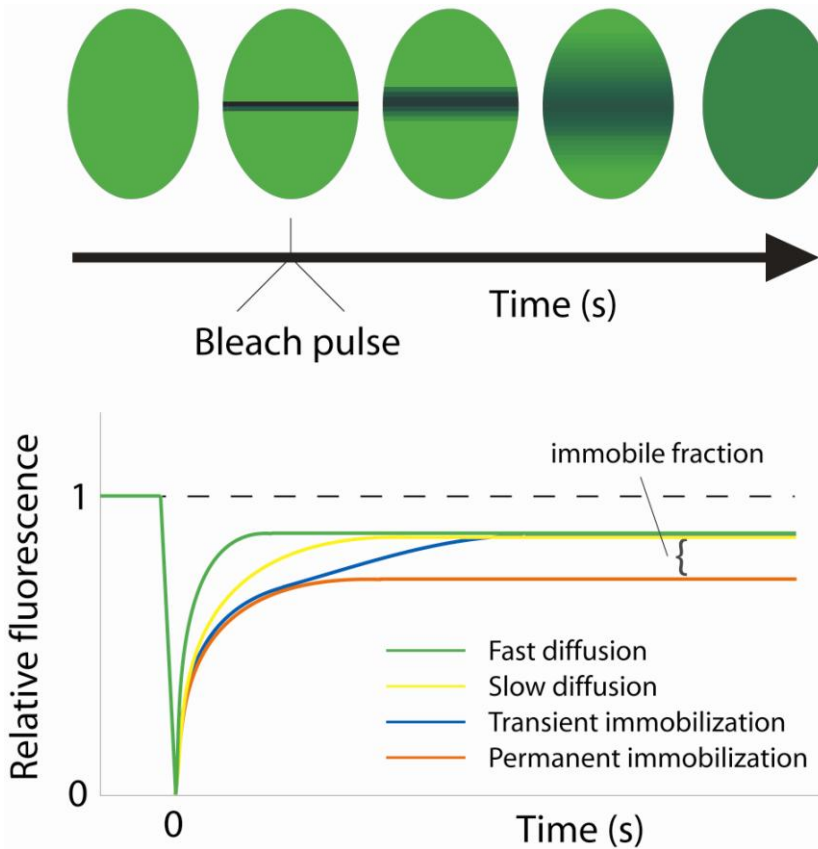


**Fig 3.** FRAP principle. Green ellipsoids represent a cell nucleus that expresses GFP. A strip in the center of the nucleus is photobleached by a high intensity laser pulse and the redistribution of fluorescence in this strip is measured in time. By plotting this redistribution in a graph, different characteristics of a fluorescently tagged protein can be determined, such as the diffusion speed, the immobile fraction and the length of immobilization.

monitored in time. When GFP-tagged proteins are moving freely through the cell, the area that was photobleached quickly becomes green again due to diffusion, while GFP-tagged proteins that are slowed down, for instance because they are continuously binding large structures such as DNA, take much longer to diffuse back into the bleached area and consequently the bleached area will recover its initial intensity much slower. Quantitative FRAP data in which the relative fluorescence (fluorescence after photobleaching/fluorescence before photobleaching) is plotted against time, provides detailed insight into the mobility parameters of fluorescently tagged proteins (Fig 3). A variant of FRAP is FLIP, in which, instead of monitoring the photobleached region, the loss of fluorescence outside a bleached region is measured. The speed with which fluorescence decreases in

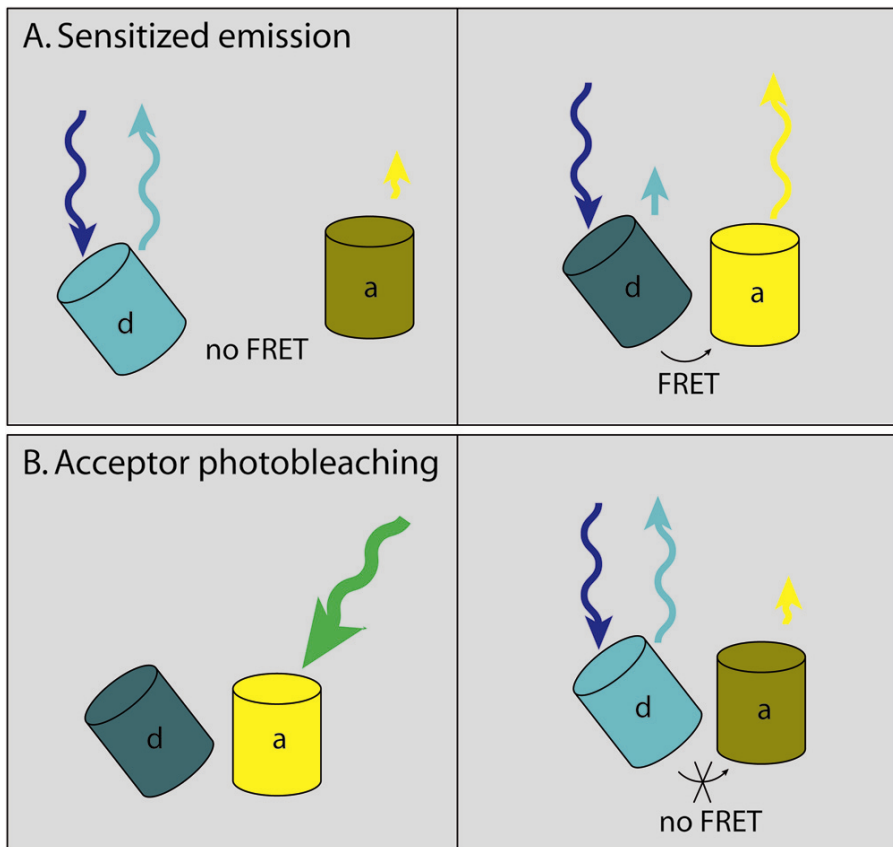


**Fig 4.** FRET detection. A. Sensitized emission. When the donor (d) and acceptor (a) fluorophores come into close proximity ( $< 10$  nm), energy from the excited donor is transferred to the acceptor, resulting in an increase of acceptor fluorescence and a decrease of donor fluorescence. The FRET efficiency can be determined from these fluorescence intensity changes (sensitized emission detection). B. Acceptor photobleaching. Acceptor fluorophores are photobleached by a high intensity laser pulse so that they cannot accept energy from the donor anymore. This results in an increase of donor fluorescence concurrent with the decrease of acceptor fluorescence.

regions outside of the bleached area, by redistribution of fluorescent and nonfluorescent molecules, is a measure for the mobility of tagged proteins. FRAP and FLIP are both used to study kinetic behavior of GFP-tagged proteins, but a combination of the two methods can generate more accurate data and allow the distinction between long-term binding events and slow diffusion (Farla et al., 2004; Farla et al., 2005; Hoogstraten et al., 2002; van den Boom et al., 2004).

In combination with methods that manipulate cellular processes such as transcription inhibition or DNA damage induction, photobleaching techniques can provide a lot of extra information. Changes in protein mobility upon for example DNA damage induction can be evidence for the involvement of this protein in DNA damage repair and parameters such as the amount of proteins involved in DNA repair events and the duration of this involvement can be extracted.

### **Fluorescence resonance energy transfer**

When two fluorophores are in close proximity to each other (less than 10 nm), a process known as fluorescence resonance energy transfer (FRET) can occur. The distances between fluorophores that allow FRET are so short that fluorescently-tagged proteins that exhibit FRET are considered to be interacting with each other. This makes the measurement of FRET a powerful technique to study protein-protein interactions and, when a protein is tagged at two sides with fluorophores, protein conformational changes with.

In FRET, energy is transferred from an excited donor fluorophore to an acceptor molecule, usually also a fluorophore, with a higher excitation wavelength. The efficiency of this process depends on several factors (Fig 4). The most important factors for FRET in biological systems are 1) the overlap between donor emission and acceptor excitation spectra; 2) The fluorescence quantum yield of the donor in the absence of an acceptor and 3) The distance between the fluorophores (Lakowicz, 1999; Piston and Kremers, 2007). The third factor weighs very heavy in FRET determinations, because FRET decreases with the 6<sup>th</sup> power of the distance between the fluorophores. Because of this strong dependence on distance between the fluorophores, FRET is high at very small distances and with increasing distance energy transfer quickly drops to zero. Therefore, FRET can essentially be seen as an all or nothing measurement of protein-protein interaction.

A number of methods have been described to measure FRET in cells. These methods take advantage of a number of characteristic changes that occur in fluorophores when they participate in FRET. For example, the average lifetime of the excited state of donor fluorophores decreases when energy is transferred to an acceptor. Fluorescence lifetime imaging microscopy (FLIM) is a method that measures this excited state lifetime of donor fluorophores in a sample and thereby determines the FRET efficiency (Clegg et al., 2003; Clegg et al., 1992; Hink et al., 2002). Another change

---

that occurs during FRET is in the fluorescence intensity of the donor and the acceptor. The donor fluorescence intensity decreases because part of its energy is transferred to the acceptor and the acceptor intensity increases because of indirect excitation by the donor. These changes in fluorescence intensity are measured by a method called sensitized emission detection (Honda et al., 2001; Ponsioen et al., 2004). A third method to determine FRET efficiencies is by photobleaching the acceptor fluorophores (acceptor bleaching FRET or abFRET). Photobleaching acceptor fluorophores abrogates the energy transfer from a donor. Because the donor does not transfer energy to an acceptor anymore it will emit a photon at its specific wavelength instead. The resulting increase in average donor fluorescence intensity is measured by abFRET (Karpova et al., 2003; van Royen et al., 2007).

### Signal separation by filters versus spectral imaging

One of the greatest advantages of the GFP revolution is the possibility to fuse different proteins with different colored GFP variants and examine their behavior in living cells. Colocalization and FRET studies can be used to study the function and possible interactions of proteins thereby providing

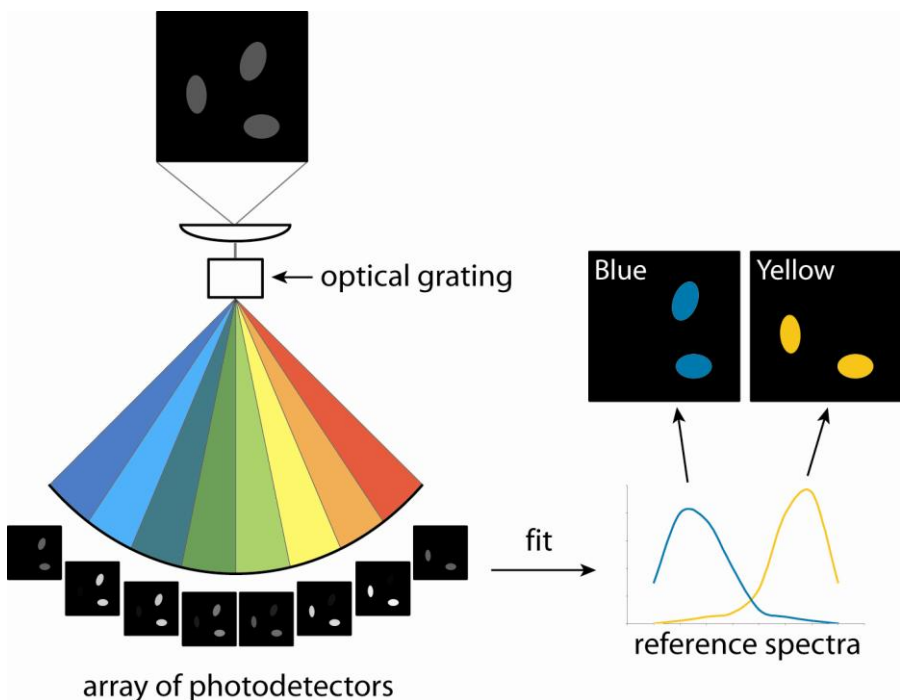


**Fig 5.** Spectral imaging and unmixing. Spectral imaging of three cells containing yellow, blue or both yellow and blue fluorescence. The optical grating separates the light in its spectrum and wavelength packages are detected by separate photodetectors. By fitting reference spectra of the blue and yellow fluorophores to the spectral images, a reconstruction of the fluorescence in each cell is created in one blue and one yellow image.

complementary information to biochemical methods such as co-immunoprecipitation. To get accurate results from such multicolor GFP experiments, microscopes have to be able to separate signals from all the fluorophores that are used. To his end, most (confocal) microscopes apply band-pass filters. A band-pass filter only transmits light of a certain wavelength range. All light of other wavelengths is blocked. To detect fluorophores with different colors simultaneously, confocal microscopes are equipped with two or more channels for image collection. Different band-pass filters in front of photodetectors of each channel allow detection of one specific wavelength per channel. The use of band-pass filters to separate signals of different fluorophores is limited by the wavelength range that is transmitted and the overlap between the emission spectra of the fluorophores. For example, GFP and a red-shifted variant of GFP, yellow fluorescent protein (YFP), are practically inseparable by band-pass filters because of the strong overlap of emission spectra. The only way to separate fluorophores with such overlapping spectra is by spectral imaging (Dickinson et al., 2001; Zimmermann et al., 2002). With spectral imaging, emission light from every pixel is passed through an optical grating or prism that breaks up the light into its component wavelengths (Fig 5). Different wavelengths are sent to separate photodetectors. For example, with the Zeiss LSM 510 META confocal microscope, 10.7 nm of a spectrum is sent to each of (maximum) 32 PMTs, spanning a wavelength range of 342 nm. Thus, a spectrum of the fluorescence in a sample is obtained. To determine the contribution of each fluorophore to this spectrum, separate reference spectra of the fluorophores are used. A computer algorithm determines the contribution of each reference spectra to each pixel and reconstructs separate images for each of the fluorophores. Spectral imaging is not limited to two highly overlapping fluorophores, such as GFP and YFP, but it can also be used to detect and separate multiple fluorophores.

### **DNA damage induction with lasers**

Genetically tagging proteins with GFP (and variants) allows the study of biological processes as they occur in their natural environment, the living cell. Some of these processes, such as DNA replication, involve changes in protein distribution that can be visualized by simply recording a time series of a living cell that expresses a protein-GFP fusion involved in this process. For example, proliferating cell nuclear antigen (PCNA), a protein involved in replication, changes its distribution in the nucleus from a homogeneous pattern to a focal pattern when the cell enters S-phase. Fusing PCNA to GFP makes it possible to study this redistribution in time as the cell goes through the cell cycle (Essers et al., 2005). Studying DNA repair has the advantage that it can be activated at any time in the cell cycle by using genotoxic drugs such as cisplatin or camptothecin, or irradiating a cell with a DNA damaging source, such as UV light or  $\gamma$ -irradiation (Jacob et al., 2005; Nelms et al., 1998; Zamble et al., 1996). Different damage sources generally induce a collection of different types of DNA damage that can activate a

---

---

number of repair pathways, each dedicated to the removal of a subset of lesions (Essers et al., 2006b; Hoeijmakers, 2001; Wyman and Kanaar, 2006). Such DNA damaging methods have been extensively used in combination with photobleaching techniques to study the involvement of DNA repair proteins (Essers et al., 2006b). More recently, DNA repair research has been boosted by the development of several methods to locally inflict DNA damage in living cells, enabling the direct visualization of GFP-tagged repair factors accumulating at the sub-nuclear region where the damage is caused. Local damage induction has an enormous benefit over global damage induction because it allows the determination of many extra parameters, such as the concentration of a protein at sites of DNA damage, the speed at which it is recruited to damage and the amount of time that it is involved. Local DNA damage induction can be accomplished by irradiating partially shielded cells (Kannouche et al., 2001; Katsumi et al., 2001; Mone et al., 2001; Nelms et al., 1998; Volker et al., 2001) or focusing laser beams inside nuclei (Essers et al., 2006a; Lukas et al., 2005). Particularly laser-irradiation has become a popular tool in DNA damage response studies, because it allows the user to specify the size and the location of the damaged region as well as the damage dose. Not every laser is suitable to induce DNA damage with. DNA has an absorption peak in the UV-C range ( $\lambda_{\text{max}} = 266 \text{ nm}$ ). At this wavelength, cyclobutane pyrimidine dimers (CPD) and 6-4 photoproducts (6-4PP) are the two main DNA lesions that are induced. In mammals, CPDs and 6-4PPs are repaired by the nucleotide excision repair (NER) pathway. Therefore, irradiation with UV-C light, allowing induction of a large amount of DNA lesions in a very short time, is a widely used tool in studies of NER (Dinant et al., 2007; Houtsmuller et al., 1999; Mone et al., 2001). For studies to other DNA damage response pathways that are activated by, for example, double or single strand breaks, lasers of different wavelengths are generally used (Cremer et al., 1980; Lan et al., 2004), often in combination with a damage sensitizing agent. For example, UV-A laser irradiation of cells that have been incubated with halogenated nucleotides, more or less specifically induces DNA double strand breaks (DSB) (Bekker-Jensen et al., 2006; Bekker-Jensen et al., 2005; Lukas et al., 2005; Lukas et al., 2003; Tashiro et al., 2000). Besides UV-C and UV-A lasers, near infrared (NIR,  $\pm 800 \text{ nm}$ ) lasers have also been used to induce DNA damage (Dinant et al., 2007; Mari et al., 2006; Meldrum et al., 2003). Damage induction with NIR lasers relies on the absorption of multiple photons by the DNA at the same time. Absorption of two photons doubles the energy deposition, resulting in irradiation with an effective wavelength half of the original emitted wavelength. Therefore, three-photon absorption of 800 nm laser light is equivalent to irradiation with UV-C ( $800 \text{ nm}/3 = 267 \text{ nm}$ ). The very high light intensity that is required to achieve a detectable multiphoton effect is generally brought about by using pulsed lasers. That is because concentrating the laser power in pulses gives much higher peak intensities than a non-pulsed laser does. In contrast to UV-C lasers, a multiphoton laser induces not only UV-C type damages, such as

---

CPDs and 6-4PPs, but also other lesions including DSBs (Dinant et al., 2007; Mari et al., 2006). Likely, these other lesions are induced by the strong temperature increase caused by irradiating a small nuclear volume with NIR light.

In conclusion, fluorescence microscopy, and particularly confocal microscopy, has become a very important tool in cell biological studies, especially in the quantitative study of living cells. In combination with GFP and GFP-variants as fluorescent tags, many properties of proteins can be studied, such as diffusion speed, interactions with other proteins and speed and time of involvement in DNA repair, in the protein's natural environment, the living cell. The following chapters in this dissertation each describe studies that have applied live-cell imaging techniques to investigate activities of proteins involved in the DNA damage response.

#### References

- Bekker-Jensen, S., Lukas, C., Kitagawa, R., Melander, F., Kastan, M. B., Bartek, J. and Lukas, J.** (2006). Spatial organization of the mammalian genome surveillance machinery in response to DNA strand breaks. *J Cell Biol* **173**, 195-206.
- Bekker-Jensen, S., Lukas, C., Melander, F., Bartek, J. and Lukas, J.** (2005). Dynamic assembly and sustained retention of 53BP1 at the sites of DNA damage are controlled by Mdc1/NFBD1. *J Cell Biol* **170**, 201-11.
- Chalfie, M., Tu, Y., Euskirchen, G., Ward, W. W. and Prasher, D. C.** (1994). Green fluorescent protein as a marker for gene expression. *Science* **263**, 802-5.
- Clegg, R. M., Holub, O. and Gohlke, C.** (2003). Fluorescence lifetime-resolved imaging: measuring lifetimes in an image. *Methods Enzymol* **360**, 509-42.
- Clegg, R. M., Murchie, A. I., Zechel, A., Carlberg, C., Diekmann, S. and Lilley, D. M.** (1992). Fluorescence resonance energy transfer analysis of the structure of the four-way DNA junction. *Biochemistry* **31**, 4846-56.
- Crameri, A., Whitehorn, E. A., Tate, E. and Stemmer, W. P.** (1996). Improved green fluorescent protein by molecular evolution using DNA shuffling. *Nat Biotechnol* **14**, 315-9.
- Cremer, C., Cremer, T., Fukuda, M. and Nakanishi, K.** (1980). Detection of laser-UV microirradiation-induced DNA photolesions by immunofluorescent staining. *Hum Genet* **54**, 107-10.
- Cubitt, A. B., Heim, R., Adams, S. R., Boyd, A. E., Gross, L. A. and Tsien, R. Y.** (1995). Understanding, improving and using green fluorescent proteins. *Trends Biochem Sci* **20**, 448-55.
- Davidovits, P. and Egger, M. D.** (1969). Scanning laser microscope. *Nature* **223**, 831.
- Dickinson, M. E., Bearman, G., Tille, S., Lansford, R. and Fraser, S. E.** (2001). Multi-spectral imaging and linear unmixing add a whole new dimension to laser scanning fluorescence microscopy. *Biotechniques* **31**, 1272, 1274-6, 1278.
- Dinant, C., de Jager, M., Essers, J., van Cappellen, W. A., Kanaar, R., Houtsmuller, A. B. and Vermeulen, W.** (2007). Activation of multiple DNA repair pathways by sub-nuclear damage induction methods. *J Cell Sci* **120**, 2731-40.
- Essers, J., Theil, A. F., Baldeyron, C., van Cappellen, W. A., Houtsmuller, A. B., Kanaar, R. and Vermeulen, W.** (2005). Nuclear dynamics of PCNA in DNA replication and repair. *Mol Cell Biol* **25**, 9350-9.
- Essers, J., Vermeulen, W. and Houtsmuller, A. B.** (2006a). DNA damage repair: anytime, anywhere? *Curr Opin Cell Biol*.
- Essers, J., Vermeulen, W. and Houtsmuller, A. B.** (2006b). DNA damage repair: anytime, anywhere? *Curr Opin Cell Biol* **18**, 240-6.
- Farla, P., Hersmus, R., Geverts, B., Mari, P. O., Nigg, A. L., Dubbink, H. J., Trapman, J. and Houtsmuller, A. B.** (2004). The androgen receptor ligand-binding domain stabilizes DNA binding in living cells. *J Struct Biol* **147**, 50-61.
-



- Farla, P., Hersmus, R., Trapman, J. and Houtsmuller, A. B.** (2005). Antiandrogens prevent stable DNA-binding of the androgen receptor. *J Cell Sci* **118**, 4187-98.
- Grond, C. J., Derksen, J. and Brakenhoff, G. J.** (1982). The banding pattern of the segment 46A-48C in *Drosophila hydei* polytene chromosomes as studied by confocal scanning light microscopy (CSLM). *Exp Cell Res* **138**, 458-62.
- Heim, R., Cubitt, A. B. and Tsien, R. Y.** (1995). Improved green fluorescence. *Nature* **373**, 663-4.
- Hink, M. A., Bisselin, T. and Visser, A. J.** (2002). Imaging protein-protein interactions in living cells. *Plant Mol Biol* **50**, 871-83.
- Hoeijmakers, J. H.** (2001). Genome maintenance mechanisms for preventing cancer. *Nature* **411**, 366-74.
- Honda, A., Adams, S. R., Sawyer, C. L., Lev-Ram, V., Tsien, R. Y. and Dostmann, W. R.** (2001). Spatiotemporal dynamics of guanosine 3',5'-cyclic monophosphate revealed by a genetically encoded, fluorescent indicator. *Proc Natl Acad Sci U S A* **98**, 2437-42.
- Hoogstraten, D., Nigg, A. L., Heath, H., Mullenders, L. H., van Driel, R., Hoeijmakers, J. H., Vermeulen, W. and Houtsmuller, A. B.** (2002). Rapid Switching of TFIIH between RNA Polymerase I and II Transcription and DNA Repair In Vivo. *Mol Cell* **10**, 1163-74.
- Houtsmuller, A. B., Rademakers, S., Nigg, A. L., Hoogstraten, D., Hoeijmakers, J. H. J. and Vermeulen, W.** (1999). Action of DNA repair endonuclease ERCC1/XPF in living cells. *Science* **284**, 958-961.
- Houtsmuller, A. B. and Vermeulen, W.** (2001). Macromolecular dynamics in living cell nuclei revealed by fluorescence redistribution after photobleaching. *Histochem Cell Biol* **115**, 13-21.
- Jacob, S., Miquel, C., Sarasin, A. and Praz, F.** (2005). Effects of camptothecin on double-strand break repair by non-homologous end-joining in DNA mismatch repair-deficient human colorectal cancer cell lines. *Nucleic Acids Res* **33**, 106-13.
- Kannouche, P., Broughton, B. C., Volker, M., Hanaoka, F., Mullenders, L. H. and Lehmann, A. R.** (2001). Domain structure, localization, and function of DNA polymerase eta, defective in xeroderma pigmentosum variant cells. *Genes Dev* **15**, 158-72.
- Karpova, T. S., Baumann, C. T., He, L., Wu, X., Grammer, A., Lipsky, P., Hager, G. L. and McNally, J. G.** (2003). Fluorescence resonance energy transfer from cyan to yellow fluorescent protein detected by acceptor photobleaching using confocal microscopy and a single laser. *J Microsc* **209**, 56-70.
- Katsumi, S., Kobayashi, N., Imoto, K., Nakagawa, A., Yamashina, Y., Muramatsu, T., Shirai, T., Miyagawa, S., Sugiura, S., Hanaoka, F. et al.** (2001). In situ visualization of ultraviolet-light-induced DNA damage repair in locally irradiated human fibroblasts. *J Invest Dermatol* **117**, 1156-61.
- Kremers, G. J., Goedhart, J., van den Heuvel, D. J., Gerritsen, H. C. and Gadella, T. W., Jr.** (2007). Improved green and blue fluorescent proteins for expression in bacteria and mammalian cells. *Biochemistry* **46**, 3775-83.
- Kremers, G. J., Goedhart, J., van Munster, E. B. and Gadella, T. W., Jr.** (2006). Cyan and yellow super fluorescent proteins with improved brightness, protein folding, and FRET Forster radius. *Biochemistry* **45**, 6570-80.
- Kubitschek, U., Kuckmann, O., Kues, T. and Peters, R.** (2000). Imaging and tracking of single GFP molecules in solution. *Biophys J* **78**, 2170-9.
- Lakowicz, J. R.** (1999). Principles of fluorescence spectroscopy. New York: Kluwer Academic/Plenum Publishers.
- Lan, L., Nakajima, S., Oohata, Y., Takao, M., Okano, S., Masutani, M., Wilson, S. H. and Yasui, A.** (2004). In situ analysis of repair processes for oxidative DNA damage in mammalian cells. *Proc Natl Acad Sci U S A* **101**, 13738-43.
- Lukas, C., Bartek, J. and Lukas, J.** (2005). Imaging of protein movement induced by chromosomal breakage: tiny 'local' lesions pose great 'global' challenges. *Chromosoma* **114**, 146-54.
- Lukas, C., Falck, J., Bartkova, J., Bartek, J. and Lukas, J.** (2003). Distinct spatiotemporal dynamics of mammalian checkpoint regulators induced by DNA damage. *Nat Cell Biol* **5**, 255-60.
- Mari, P. O., Florea, B. I., Persengiev, S. P., Verkaik, N. S., Bruggenwirth, H. T., Modesti, M., Giglia-Mari, G., Bezstarosti, K., Demmers, J. A., Luijck, T. M. et al.** (2006).

Dynamic assembly of end-joining complexes requires interaction between Ku70/80 and XRCC4. *Proc Natl Acad Sci U S A* **103**, 18597-602.

**Matz, M. V., Fradkov, A. F., Labas, Y. A., Savitsky, A. P., Zaraisky, A. G., Markelov, M. L. and Lukyanov, S. A.** (1999). Fluorescent proteins from nonbioluminescent Anthozoa species. *Nat Biotechnol* **17**, 969-73.

**Meldrum, R. A., Botchway, S. W., Wharton, C. W. and Hirst, G. J.** (2003). Nanoscale spatial induction of ultraviolet photoproducts in cellular DNA by three-photon near-infrared absorption. *EMBO Rep* **4**, 1144-9.

**Merzlyak, E. M., Goedhart, J., Shcherbo, D., Bulina, M. E., Shcheglov, A. S., Fradkov, A. F., Gaintzeva, A., Lukyanov, K. A., Lukyanov, S., Gadella, T. W. et al.** (2007). Bright monomeric red fluorescent protein with an extended fluorescence lifetime. *Nat Methods* **4**, 555-7.

**Mone, M. J., Volker, M., Nikaido, O., Mullenders, L. H., van Zeeland, A. A., Verschure, P. J., Manders, E. M. and van Driel, R.** (2001). Local UV-induced DNA damage in cell nuclei results in local transcription inhibition. *EMBO Rep* **2**, 1013-1017.

**Nelms, B. E., Maser, R. S., MacKay, J. F., Lagally, M. G. and Petrini, J. H.** (1998). In situ visualization of DNA double-strand break repair in human fibroblasts. *Science* **280**, 590-2.

**Piston, D. W. and Kremers, G. J.** (2007). Fluorescent protein FRET: the good, the bad and the ugly. *Trends Biochem Sci* **32**, 407-14.

**Ponsioen, B., Zhao, J., Riedl, J., Zwartkruis, F., van der Krogt, G., Zaccolo, M., Moolenaar, W. H., Bos, J. L. and Jalink, K.** (2004). Detecting cAMP-induced Epac activation by fluorescence resonance energy transfer: Epac as a novel cAMP indicator. *EMBO Rep* **5**, 1176-80.

**Prasher, D. C., Eckenrode, V. K., Ward, W. W., Prendergast, F. G. and Cormier, M. J.** (1992). Primary structure of the *Aequorea victoria* green-fluorescent protein. *Gene* **111**, 229-233.

**Reits, E. A. and Neefjes, J. J.** (2001). From fixed to FRAP: measuring protein mobility and activity in living cells. *Nat Cell Biol* **3**, E145-7.

**Schrader, M., Bahlmann, K., Giese, G. and Hell, S. W.** (1998). 4Pi-confocal imaging in fixed biological specimens. *Biophys J* **75**, 1659-68.

**Shaner, N. C., Campbell, R. E., Steinbach, P. A., Giepmans, B. N., Palmer, A. E. and Tsien, R. Y.** (2004). Improved monomeric red, orange and yellow fluorescent proteins derived from *Discosoma* sp. red fluorescent protein. *Nat Biotechnol* **22**, 1567-72.

**Shimomura, O., Johnson, F. H. and Saiga, Y.** (1962). Extraction, purification and properties of aequorin, a bioluminescent protein from the luminous hydromedusan, *Aequorea*. *J Cell Comp Physiol* **59**, 223-39.

**Tashiro, S., Walter, J., Shinohara, A., Kamada, N. and Cremer, T.** (2000). Rad51 accumulation at sites of DNA damage and in postreplicative chromatin. *J Cell Biol* **150**, 283-91.

**Tsien, R. Y.** (1998). The green fluorescent protein. *Annu Rev Biochem* **67**, 509-44.

**van den Boom, V., Citterio, E., Hoogstraten, D., Zotter, A., Egly, J. M., van Cappellen, W. A., Hoeijmakers, J. H., Houtsmuller, A. B. and Vermeulen, W.** (2004). DNA damage stabilizes interaction of CSB with the transcription elongation machinery. *J Cell Biol* **166**, 27-36.

**van Royen, M. E., Cunha, S. M., Brink, M. C., Mattern, K. A., Nigg, A. L., Dubbink, H. J., Verschure, P. J., Trapman, J. and Houtsmuller, A. B.** (2007). Compartmentalization of androgen receptor protein-protein interactions in living cells. *J Cell Biol* **177**, 63-72.

**Volker, M., Moné, M. J., Karmakar, P., Hoffen, A., Schul, W., Vermeulen, W., Hoeijmakers, J. H. J., van Driel, R., Zeeland, A. A. and Mullenders, L. H. F.** (2001). Sequential Assembly of the Nucleotide Excision Repair Factors In Vivo. *Molecular Cell* **8**, 213-224.

**Wyman, C. and Kanaar, R.** (2006). DNA double-strand break repair: all's well that ends well. *Annu Rev Genet* **40**, 363-83.

**Zamble, D. B., Mu, D., Reardon, J. T., Sancar, A. and Lippard, S. J.** (1996). Repair of cisplatin-DNA adducts by the mammalian excision nuclease. *Biochemistry* **35**, 10004-13.

**Zernike, F.** (1955). How I discovered phase contrast. *Science* **121**, 345-9.

**Zimmermann, T., Rietdorf, J., Girod, A., Georget, V. and Pepperkok, R.** (2002). Spectral imaging and linear un-mixing enables improved FRET efficiency with a novel GFP2-YFP FRET pair. *FEBS Lett* **531**, 245-9.

---

## Chapter 3

# Fluorescence Resonance Energy Transfer of GFP and YFP by Spectral Imaging and Quantitative Acceptor Photobleaching

Christoffel Dinant, Martin E. van Royen, Wim  
Vermeulen and Adriaan B. Houtsmuller

*J. Micr.* 231 (Pt 1): 97-104, July 2008

### **Abstract**

In order to study protein-protein interactions by fluorescence energy transfer (FRET), the proteins of interest are tagged with either a donor or an acceptor fluorophore. For efficient FRET, fluorophores need to have a reasonable overlap of donor emission and acceptor excitation spectra. However, given the relatively small Stokes shift of conventional fluorescent proteins, donor and acceptor pairs with high FRET efficiencies have emission spectra that are difficult to separate. GFP and YFP are widely used in fluorescence microscopy studies. The spectral qualities of GFP and YFP make them one of the most efficient FRET donor-acceptor couples available. However, the emission peaks of GFP (510 nm) and YFP (527 nm) are spectrally too close for separation by conventional fluorescence microscopy. Difficulties in simultaneous detection of GFP and YFP with a fluorescence microscope are eliminated when spectral imaging and subsequent linear unmixing are applied. This allows FRET microscopy using these tags to study protein-protein interactions. We adapted the linear unmixing procedure from commercially available software (Zeiss) for use with acceptor photobleaching FRET using GFP and YFP as FRET-pair. FRET efficiencies up to 52% for a GFP-YFP fusion protein were measured. To investigate the applicability of the procedure we used two constituents of the nucleotide excision repair (NER) system, which removes UV-induced single strand DNA damage. ERCC1 and XPF form a heterodimeric 5' endonuclease in NER. FRET between ERCC1-GFP and XPF-YFP occurs with an efficiency of 30%.

### **Introduction**

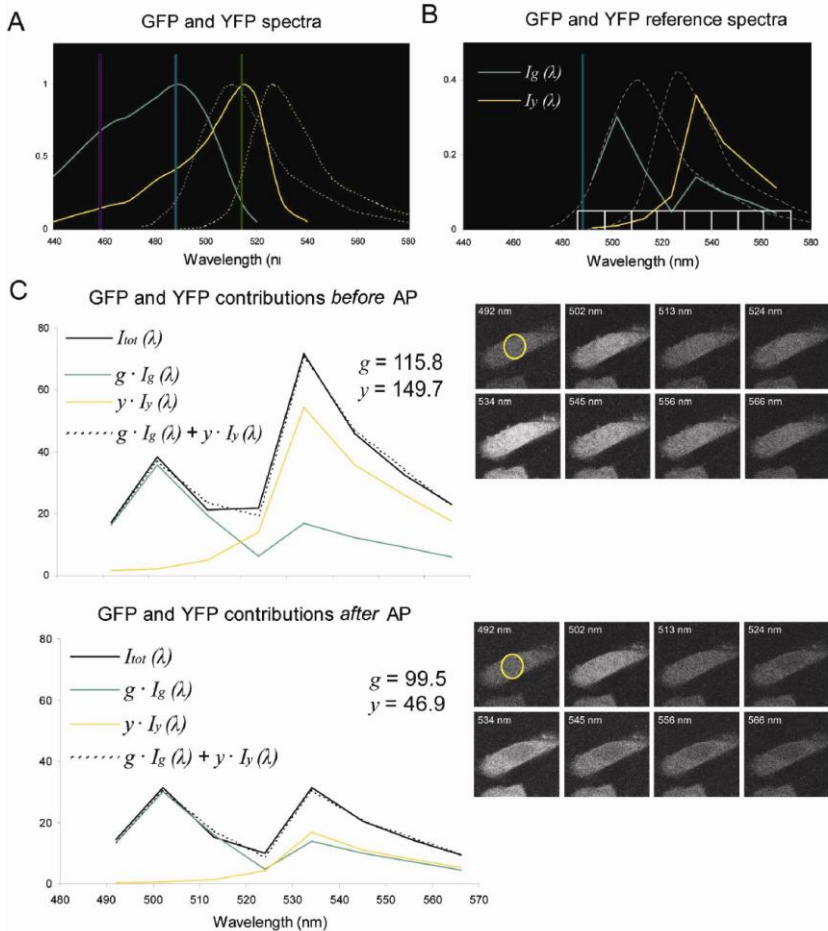
Protein-protein interactions can be detected in living cells in real-time with fluorescence resonance energy transfer (FRET) microscopy (Jares-Erijman and Jovin 2003). FRET is the non-radiative energy transfer from an excited donor fluorophore to an acceptor, which then emits photons at its emission wavelength. The efficiency of this energy transfer depends on several factors: the overlap between donor emission and acceptor excitation spectra, relative orientation of the transition dipoles, the quantum yield of the donor, the extinction coefficient of the acceptor and the (sixth power of the) distance between the fluorophores (Lakowicz 1999; Piston and Kremers 2007).

FRET induces a number of characteristic changes in the donor and acceptor fluorescence, which can be detected in various ways: 1) Fluorescence lifetime imaging (FLIM) can be used to determine FRET since the fluorescence lifetime of the donor is reduced when energy transfer to an appropriate acceptor occurs (Hink et al. 2002; Clegg et al. 2003). 2) FRET can also be quantitatively assessed by measuring the indirect excitation of acceptor fluorophores resulting from energy transfer by a directly excited donor at the appropriate wavelength (Honda et al. 2001; Ponsioen et al. 2004). This method is generally referred to as sensitized emission. A number of correction protocols have been described for the accurate microscope calibration and data collection which is required with this technique (Gordon et al. 1998; Hoppe et al. 2002; Jares-Erijman and Jovin 2003). 3) Acceptor

---

photobleaching (abFRET) is a technique that measures FRET by irreversibly photobleaching the acceptor through application of high intensity light at the acceptor excitation wavelength, and thereby abrogating the energy transfer. When the acceptor is made non-fluorescent by intense irradiation of the excitation wavelength (acceptor photobleaching) the donor will regain its original fluorescence. This resulting increase of donor fluorescence after abFRET can therefore be used to quantitatively determine FRET efficiency (Bastiaens et al. 1996; Karpova et al. 2003; Gu et al. 2004; Van Munster et al. 2005).

At present, there is a large availability of possible donor-acceptor pairs that can be used to study FRET in living cells, but most live cell FRET studies have employed the cyan and yellow variants of GFP, CFP and YFP, as donor and acceptor fluorophores, respectively (Karpova et al. 2003; Gu et al. 2004; Ponsioen et al. 2004; Van Munster et al. 2005). A potential problem of the CFP-YFP FRET couple is that the fluorescence intensity or brightness (quantum yield x molar extinction coefficient) of CFP is approximately 4 times lower than that of YFP (Rizzo et al. 2004). This makes it difficult to detect FRET signals in cells expressing small amounts of tagged proteins. In contrast to CFP, GFP has a quantum yield comparable to YFP and its emission spectrum overlaps more closely with the excitation spectrum of YFP than CFP. This higher overlap results in an increase in FRET efficiency (Patterson et al. 2000). Moreover, many research groups have generated numerous GFP fusions of different proteins of interest and extension of research to interaction studies only requires generation of YFP-tagged potential interaction partners if GFP-YFP could be used as a FRET couple. However, simultaneous imaging of GFP and YFP is not possible using conventional microscopy because of the large overlap of the two emission spectra. Here we describe a quantitative acceptor photobleaching method, based on spectral imaging, for live cell interaction studies using GFP and YFP as a FRET couple.



## Results

### Experimental set up

In order to study protein-protein interactions in living cell nuclei, we have setup a system to measure fluorescence energy transfer from GFP to YFP. First, we optimized a linear unmixing procedure to separate GFP and YFP signals using spectral confocal microscopy. Subsequently we investigated the possibility to use this FRET pair in a quantitative live cell abFRET assay by determining FRET values in cells expressing GFP-YFP fusion protein and unfused GFP and YFP at different ratios. Finally we validated the applicability of the method in living cells expressing two interacting DNA repair proteins (ERCC1 and XPF) tagged with GFP and YFP.

### Linear unmixing

**Fig 1.** GFP and YFP absorption and reference spectra and unmixing. (A) Absorption (continuous line) and emission (dotted line) spectra of GFP (green) and YFP (yellow). The 458 nm line (purple vertical line) was used for excitation and the 514 nm line (green vertical line) for acceptor photobleaching. The 488 nm line (light blue) was not used for excitation because it interfered with spectral imaging. The GFP and YFP emission spectra (dotted lines) show a large overlap, which makes these two fluorophores inseparable with conventional microscopy using band-pass filters. Reference for *gfp* and *yfp* spectra: Asahi Spectra USA inc, <http://www.asahi-spectra.com/>. (B) Background corrected normalized reference spectra of GFP and YFP ( $I_g(\lambda)$  and  $I_y(\lambda)$  respectively). Black boxes indicate spectral channels. The light blue vertical line represents the 488 nm laser and indicates that this laser line was detected in the first spectral channel. Actual GFP and YFP emission spectra are shown as dashed lines. (C) Unmixing example before and after acceptor photobleaching. Black continuous lines represent measured spectra ( $I(\lambda)$ ) containing GFP and YFP signals. Green lines are fits of the GFP reference spectrum ( $I_g(\lambda)$ ) to  $I_{tot}(\lambda)$  and yellow lines are fits of the YFP reference spectrum ( $I_y(\lambda)$ ) to  $I_{tot}(\lambda)$ . Dotted lines are the sum of the GFP and YFP fits. The similarity of the black continuous and the dotted lines show the accuracy of the fits. Images on the right show the fluorescence signal in each of the eight spectral channels before and after photobleaching. Yellow circles represent the region of acceptor photobleaching and  $I_{tot}(\lambda)$  measurement (the nucleus). Values for  $g$  and  $y$  are given.

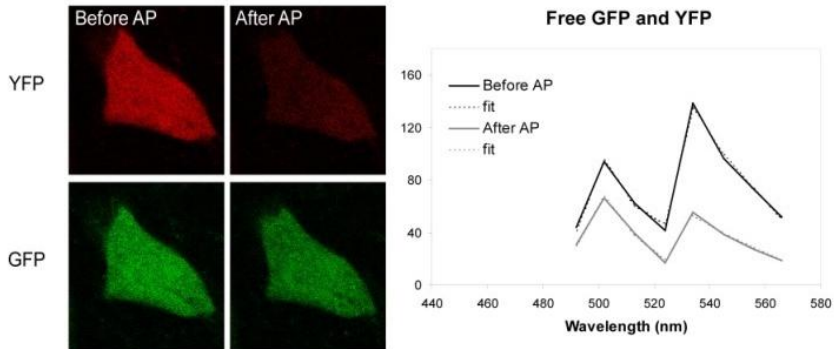
The spectral overlap between GFP and YFP is too large to allow separate detection using conventional microscopy (Fig 1A). In order to use GFP and YFP in protein-protein interaction studies by means of FRET we investigated the use of spectral imaging and subsequent linear unmixing to separate these two fluorophores. In linear unmixing, reference spectra are used to determine the contribution of multiple fluorophores to a measured spectrum. We first obtained reference spectra of GFP and YFP by separately recording cells that express either GFP or YFP (Fig 1B). Using spectral imaging settings of a Zeiss LSM 510 META (Zeiss, Jena, Germany), GFP and YFP spectra were recorded in eight channels (between 486 nm and 572 nm). Excitation of GFP and YFP by 488 nm or 514 nm (for YFP) resulted in detection of laser-light reflection in the spectral images (data not shown). To avoid this problem, both fluorophores were excited by 458 nm (Fig 1A). Subsequently, spectra of cells expressing both GFP and YFP were recorded and linear unmixing was performed (Fig 1C). The least squares method was used to fit normalized reference spectra of GFP and YFP to the spectrum measured in cells expressing both GFP and YFP (Dickinson et al. 2001; Hiraoka et al. 2002; Gu et al. 2004). The contribution of GFP and YFP to a recorded spectrum is described by

$$(1) \quad I_{tot}(\lambda) = g \cdot I_g(\lambda) + y \cdot I_y(\lambda),$$

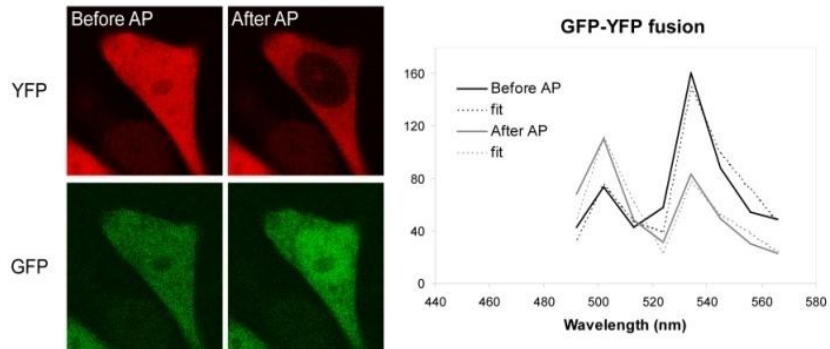
where  $I_{tot}(\lambda)$  is the total fluorescence at wavelength  $\lambda$ ,  $g$  and  $y$  are the relative abundance factors of GFP and YFP respectively, and  $I_g(\lambda)$  and  $I_y(\lambda)$  are the fluorescence intensities at wavelength  $\lambda$  for the GFP and YFP reference spectra, respectively. To fit normalized GFP and YFP reference spectra to measured fluorescence spectra in the nuclei of living cells, values for  $g$  and  $y$  were determined that minimize the sum:

$$(2) \quad \sum_{i=0}^7 = \{I_{tot}(i) - [g \cdot I_g(i) + y \cdot I_y(i)]\}^2$$

**A** Free GFP and YFP



**B** GFP-YFP fusion



**C** Minimum to maximum FRET

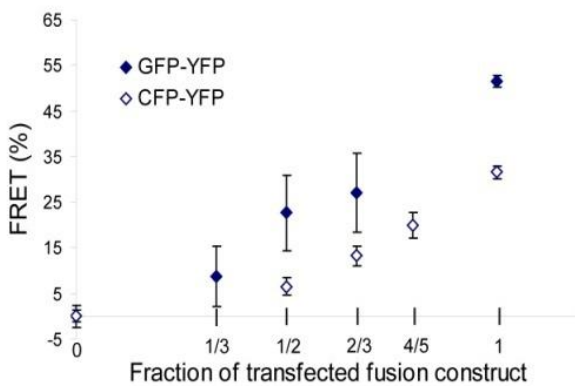




**Fig 2.** GFP-YFP FRET quantification. (A) Cells were transfected with the YFP-IRES-GFP (YIG) construct and acceptor photobleaching (abFRET) was performed. Spectral images were unmixed with the Zeiss unmixing procedure. Red images represent YFP signals and green images GFP. No increase of GFP fluorescence was detected after abFRET. The graph in the right panel shows the measured spectra before and after abFRET of a typical cell transfected with YIG. (B) Cells were transfected with the GFP-YFP fusion construct (GYFP) and acceptor photobleaching (abFRET) was performed. Spectral images were unmixed with the Zeiss unmixing procedure. Red images represent YFP signals and green images GFP. Strong increase of GFP fluorescence was detected after abFRET. The graph in the right panel shows the measured spectra before and after abFRET of a typical cell transfected with GYFP. (C) Cells were transfected with both YIG and GYFP in five different relative concentrations (closed diamonds): (0) Only YIG, (1/3) two thirds YIG and one third GYFP, (1/2) half of each, (2/3) one third YIG and two thirds GYFP and (1) only GYFP. A direct dependence was found between the relative concentration of GYFP (the interacting molecules) and FRET. Maximum FRET efficiency (GYFP only) was 52%. Error bars indicate 2 times the SEM.

where  $i$  indicates a spectral channel (8 channels in total, see above).

For accurate unmixing of fluorophores with large variations in intensities (i.e. before and after acceptor photobleaching) background correction of reference spectra is essential. Because background values differ in every spectral channel, we recorded spectra of the sample background signals and subtracted these from the fluorescence spectra recorded in cells in the same image before applying linear unmixing.

### Acceptor photobleaching

To determine FRET efficiencies we used the acceptor photobleaching method. In this method, images are taken before and after photobleaching of the majority of acceptor molecules of the investigated FRET pair, in our case YFP. If any interactions leading to energy transfer were present in the cell, photobleaching of the acceptor will lead to an increase of donor fluorescence, as it is no longer quenched by the acceptor. Acceptor photobleaching was performed with a high intensity laser pulse at a wavelength of 514 nm. To calculate FRET efficiency  $F$  in acceptor bleaching experiments we calculated the fraction of donor molecules that was quenched by the acceptor before photobleaching as:

$$(3) \quad F = \frac{D_a - D_b}{D_a}$$

where  $D_a$  is the donor intensity after and  $D_b$  the donor intensity before abFRET. Before substituting  $D_a$  and  $D_b$  with the values for GFP after and before abFRET,  $G_a$  and  $G_b$  respectively, two corrections were performed. Since the GFP and YFP excitation spectra overlap to some extent (Fig 1A) a fraction of the GFPs will also be bleached. To determine the fraction of GFP bleached at 514 nm, relative to the fraction of bleached YFP, we subjected cells expressing either YFP or GFP to 514 nm laser pulses of increasing intensity. In the range of 514 nm laser intensities that were typically applied to deplete approximately 70-85% of YFP, the fraction ( $k$ ) of GFP that was photobleached was  $0.32 \pm 0.03$  of the YFP bleached fraction. This  $k$  value can be used to calculate the corrected GFP value after photobleaching YFP,

$G'_a \cdot k \cdot \frac{Y_b - Y_a}{Y_b}$ , with  $Y_b$  the YFP value before photobleaching and  $Y_a$  the YFP value after photobleaching, then defines the fraction of GFP that was bleached and  $G_a$  divided by 1 minus this fraction gives  $G'_a$ :

$$(4) \quad G'_a = G_a / (1 - k \cdot \frac{Y_b - Y_a}{Y_b}).$$

Equation 4 can be rewritten as:

$$(5) \quad G'_a = \frac{G_a \cdot Y_b}{(1 - k) \cdot Y_b + k \cdot Y_a}.$$

To correct for incomplete acceptor photobleaching the difference between GFP before and after bleaching ( $G'_a - G_b$ ) was divided by the fraction of YFP that was bleached ( $\frac{Y_b - Y_a}{Y_b}$ ) and then added to the GFP intensity before photobleaching ( $G_b$ ):

$$(6) \quad G''_a = \frac{(G'_a - G_b) \cdot Y_b}{Y_b - Y_a} + G_b$$

where  $G''_a$  is the corrected GFP intensity. Equation 6 can be rewritten as:

$$(7) \quad G''_a = \frac{G'_a \cdot Y_b - G_b \cdot Y_a}{Y_b - Y_a}$$

Eqs. 5 and 7 were substituted into the general abFRET equation (see Eq. 3):

$$(8) \quad F = \frac{G''_a - G_b}{G''_a}$$

yielding:

$$(9) \quad F = \frac{G_a \cdot Y_b - (1 - k)G_b \cdot Y_b - k \cdot G_b \cdot Y_a}{G_a \cdot Y_b - (1 - k)G_b \cdot Y_a - k \cdot G_b \cdot \frac{Y_a^2}{Y_b}}.$$

Obviously, to get FRET percentages, equation 9 was simply multiplied by 100.

### Quantitative acceptor photobleaching

---

To validate the method we generated fusion constructs of GFP and YFP and of CFP and YFP, both with flexible linkers, as references (van Royen et al. 2007). To determine the efficiency of the GFP-YFP FRET couple, CHO cells were transfected with either a YFP-IRES-GFP (YIG) construct or with the GFP-YFP fusion (GYFP) construct. The internal ribosomal entry site (IRES) between GFP and YFP in YIG ensures that both GFP and YFP are separately translated from the same mRNA molecule. Three images were taken before and three images after acceptor photobleaching. No significant photobleaching was detected owed to making three consecutive images at

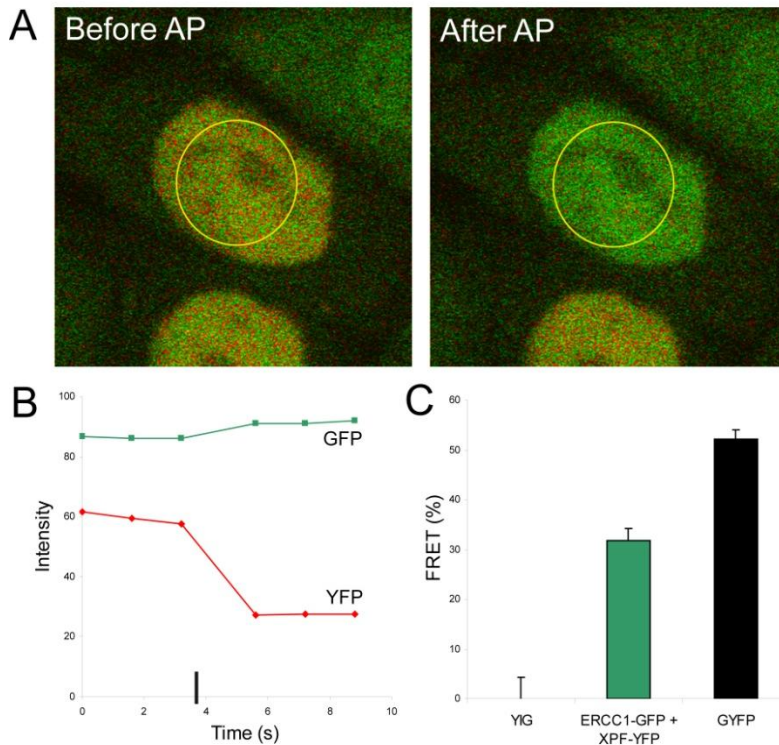


**Fig 3.** ERCC1 and XPF. (A) ERCC1 mutant CHO cells (43-3B) stably expressing ERCC1-GFP were transiently transfected with XPF-YFP and acceptor photobleaching was performed. Spectral images were unmixed with the Zeiss unmixing procedure. Shown are merged images with ERCC1-GFP in green and XPF-YFP in red. Both ERCC1-GFP and XPF-YFP are mainly located in the nucleus. ERCC1-GFP can also be found in the cytoplasm. After abFRET the YFP signal is reduced and the GFP slightly increases. Circles indicate the region that is plotted in (B). (B) Graph of the abFRET procedure of cell shown in (A). Three images were taken before and three after abFRET. The black vertical bar indicates the moment of photobleaching. Upon photobleaching with 514 nm YFP (red) signal is reduced and GFP (green) increases. (C) Average FRET of ten ERCC1-GFP and XPF-YFP expressing cells is plotted in (B). FRET intensities of YIG and GYFP are plotted alongside for comparison. Average FRET between ERCC1-GFP and XPF-YFP is  $30 \pm 2.4\%$ . Error bars indicate standard deviations.

the laser intensity used (data not shown). Transfection with YIG results in the separate expression of free GFP and YFP, which should not show any FRET. The physical linkage between donor and acceptor by means of flexible linker of the GYFP construct should result in a high FRET signal. Indeed, performing abFRET on cells expressing YIG resulted in a small decrease of GFP fluorescence, 32 % of the decrease in YFP fluorescence (see value 0.32 for  $k$  above and in Fig 2A), whereas performing abFRET on cells expressing GYFP resulted in a clear increase of the GFP signal (Fig 2B).

Next, the dependence of measured FRET intensities on the fraction of interacting molecules was studied. Cells were co-transfected with GYFP and YIG in five different concentration ratios (0:1, 1:2, 1:1, 2:1 and 1:0 respectively, Fig 2C). As expected, an increasing relative amount of the GYFP fusion-construct resulted in an increase in FRET (Fig 2C, closed diamonds). Maximum FRET was measured in cells transfected with only the GY construct ( $52 \pm 1.2$  %). As a comparison, the same experiment (with slightly different relative concentrations 0:1, 1:1, 2:1, 4:1 and 1:0) was performed with the CFP-YFP FRET couple (Fig 2C, open diamonds). The same dependence of FRET intensities on relative concentrations of transfected fusion construct was observed, but FRET values were lower than for the GFP-YFP FRET couple ( $32 \pm 1.4$  % for CYFP). These results indicate that abFRET combined with linear unmixing can be used to quantitatively assess molecular interactions. Furthermore, the high maximum efficiency of the GFP-YFP FRET couple makes the dynamic range of detectable changes in FRET larger than for CFP-YFP and probably most other fluorophore couples.

### **Biological example: ERCC1 and XPF**

To study the applicability of abFRET and linear unmixing to biologically relevant proteins expressed at physiological levels we used components of the nucleotide excision repair system (NER), ERCC1 and XPF. ERCC1 and XPF form a heterodimer, which is responsible for the 5' incision of the damaged strand during nucleotide excision repair (NER) (Park et al. 1995; Houtsmuller et al. 1999). Formation of this heterodimer has been shown to be required for the stabilization of both proteins (Sijbers et al. 1996; Yagi et al. 1997; de Laat et al. 1998a). To investigate whether the interaction between ERCC1 and XPF could be detected by FRET we generated two constructs: ERCC1-GFP and XPF-YFP. Both proteins were tagged at the C-termini, which also harbour the mutual interaction domains (de Laat et al. 1998b). Expression of ERCC1-GFP in 43-3B (ERCC1  $-/-$ ) and XPF-YFP in UV47 (XPF  $-/-$ ) Chinese hamster ovary (CHO) cell-lines restores the UV-C sensitivity to wild type levels ((Houtsmuller et al. 1999) and data not shown), indicating the functionality of the tagged proteins. ERCC1-GFP was stably transfected into the ERCC1  $-/-$  CHO cell line 43-3B and this cell line was then transfected with XPF-YFP. Both ERCC1-GFP and XPF-YFP are mainly present in the nucleus but ERCC1-GFP can also be found in the cytoplasm

---

(Fig 3A). After abFRET the GFP signal increased indicating FRET had taken place. (Fig 3A,B). Quantification of the FRET between ERCC1-GFP and XPF-YFP showed a relatively high FRET percentage of  $30 \pm 1.6\%$  (Fig 3C).

Two factors that have to be taken into account when interpreting FRET intensities of protein-protein interactions are 1) the average FRET efficiency of the interacting molecules and 2) the fraction of donor-tagged molecules interacting with acceptor-tagged molecules. Both ERCC1 and XPF were tagged with their fluorophores near the respective interaction domains (Tripsianes et al. 2005), so the average FRET efficiency of the interacting ERCC1-GFP and XPF-YFP was likely close to that of the GFP-YFP fusion construct. Therefore, if every ERCC1-GFP molecule would interact with an XPF-YFP molecule the expected FRET efficiency would be close to 52%, as it is for GFP-YFP. ERCC1 and XPF are known to interact with a stoichiometry of 1 to 1 (Park et al. 1995). However, in this experiment ERCC1-GFP was interacting both with endogenous XPF and with XPF-YFP. The ERCC1-GFP molecules that were interacting with endogenous XPF did not transfer energy through FRET to a YFP but they were partly photobleached by the 514 nm laser pulse. Consequently, the presence of this non-FRETting ERCC1-GFP pool results in an underestimation of FRET values. Therefore, the surprisingly high FRET efficiency of ERCC1-GFP and XPF-YFP of 30%, indicates that a very large fraction of ERCC1-GFP and XPF-YFP molecules were interacting. Most likely no free ERCC1-GFP exists in these cells.

## **Discussion**

We have used linear unmixing combined with acceptor photobleaching FRET to study interaction between the spectrally very close GFP and YFP-tagged molecules in living cells.

### **Spectral imaging**

One of the requirements for efficient FRET is the significant overlap between the emission spectrum of the donor with the excitation spectrum of the acceptor. With conventional two-channel microscopy, separating two highly overlapping fluorophores requires many corrections and is always accompanied by loss of signal, due to use of only 2 channels instead of 8. Spectral imaging reduces the amount of corrective measures and allows collection of light from the whole spectrum of each fluorophore thus resulting in a better signal to noise ratio. Quantitative FRET measurements between CFP and YFP with the aid of spectral imaging have been performed previously (Gu et al. 2004) see also (Neher and Neher 2004). It is concluded that even though FRET studies with these fluorophores are possible on conventional microscopes, spectral unmixing has the advantage of eliminating spectral cross talk as well as providing relative concentrations of the fluorophores.

---

A recent development that eliminates spectral cross talk of GFP and YFP is the dark yellow fluorescent protein called REACh. REACh has retained absorption properties of YFP while having lost its fluorescence (Ganesan et al. 2006). The dynamic range of donor-based FRET detection methods such as donor quenching and FLIM is enhanced with REACh as FRET acceptor since photons from the entire GFP spectrum can be used. An advantage of using YFP over REACh is the direct detection of the acceptor-tagged proteins.

FRET between GFP and YFP has also been measured by FLIM. Positive FRET results in longer average YFP lifetimes which can be detected by FLIM microscopy without the need of spectral separation (Harpur et al. 2001). However, this method is only quantitative in studies of intramolecular FRET (proteins tagged with GFP on one side and YFP on the other) because without spectral separation, the presence of unpaired fluorophores will obscure lifetime measurements.

### **Live cell abFRET**

Acceptor photobleaching implies the destruction of fluorescence from the acceptor fluorophore and is therefore less suitable for longer time-series imaging than other FRET detection methods. However, if a reversibly photobleachable acceptor fluorophore is used, such as the recently developed dronpa (Ando et al. 2004; Habuchi et al. 2005), this technique can possibly be adapted for continuous measurements (Jares-Erijman and Jovin, 2003). When such a fluorophore is used as an acceptor of FRET it can be returned to its fluorescent state by photo-activation after each abFRET pulse in order to obtain a new FRET measurement by abFRET at the next time point. However, in a system as used here, repeated bleaching will lead to loss of the donor so for longer time-series measurements of FRET a different donor would be required.

### **Conclusion**

In conclusion, we present a method that takes full advantage of the optimal energy transfer characteristics of GFP and YFP and straightforward FRET detection by acceptor photobleaching. FRET detection between other closely overlapping fluorophores, such as GFP2 and YFP (Zimmermann et al. 2002) or YFP and mOrange, will also benefit from this method.

### **Material and Methods**

#### **Microscopy**

Microscopy experiments were performed on a Zeiss LSM 510 META confocal microscope. All images were recorded with the same filter settings, objective, detector offset and laser intensities and similar detector gain to ensure proper unmixing. Fluorophores were excited by the 458 nm line of a 30 mW argon laser, a 458/514 dichroic mirror was present in the excitation path and imaging occurred through a 63x 1.4NA objective. For spectral imaging, fluorescence intensities were detected in 8 channels corresponding to the wavelength range between 486 nm and 572 nm.

#### **Cell culture**

---

---

Chinese hamster cells (AA8 and 43-3B) were cultured under standard conditions in DMEM/Ham's F10 complemented with 10% FCS and antibiotics at 37°C and 5% CO<sub>2</sub>.

### Transfections

FuGENE6 (Roche Applied Science, Almere The Netherlands) was used as a transfection reagent. Transfections were performed according to manufacturer's protocol. Total DNA concentrations for double transfections was 1µg per 3µl FuGENE6.

### Data analysis

Data was analyzed with the LSM software of Zeiss (AIM version 3.2) and Microsoft Excel.

### Acknowledgements

This work was supported by the Dutch Organization for Scientific Research (NWO): ZonMW 912-03-012 (CD), 917-46-371 (ABH), 917-46-364 (WV), and by ESF 855-01-072 (MvR).

### References

- Ando, R., Mizuno, H., and Miyawaki, A. 2004. Regulated fast nucleocytoplasmic shuttling observed by reversible protein highlighting. *Science* **306**(5700): 1370-1373.
- Bastiaens, P.I., Majoul, I.V., Verveer, P.J., Soling, H.D., and Jovin, T.M. 1996. Imaging the intracellular trafficking and state of the AB5 quaternary structure of cholera toxin. *Embo J* **15**(16): 4246-4253.
- Clegg, R.M., Holub, O., and Gohlke, C. 2003. Fluorescence lifetime-resolved imaging: measuring lifetimes in an image. *Methods Enzymol* **360**: 509-542.
- de Laat, W.L., Appeldoorn, E., Jaspers, N.G., and Hoeijmakers, J.H. 1998a. DNA structural elements required for ERCC1-XPF endonuclease activity. *J Biol Chem* **273**(14): 7835-7842.
- de Laat, W.L., Sijbers, A.M., Odijk, H., Jaspers, N.G., and Hoeijmakers, J.H. 1998b. Mapping of interaction domains between human repair proteins ERCC1 and XPF. *Nucleic Acids Res* **26**(18): 4146-4152.
- Dickinson, M.E., Bearman, G., Tille, S., Lansford, R., and Fraser, S.E. 2001. Multi-spectral imaging and linear unmixing add a whole new dimension to laser scanning fluorescence microscopy. *Biotechniques* **31**(6): 1272, 1274-1276, 1278.
- Ganesan, S., Ameer-Beg, S.M., Ng, T.T., Vojnovic, B., and Wouters, F.S. 2006. A dark yellow fluorescent protein (YFP)-based Resonance Energy-Accepting Chromoprotein (REACH) for Förster resonance energy transfer with GFP. *Proc Natl Acad Sci U S A* **103**(11): 4089-4094.
- Gordon, G.W., Berry, G., Liang, X.H., Levine, B., and Herman, B. 1998. Quantitative fluorescence resonance energy transfer measurements using fluorescence microscopy. *Biophys J* **74**(5): 2702-2713.
- Gu, Y., Di, W.L., Kellsell, D.P., and Zicha, D. 2004. Quantitative fluorescence resonance energy transfer (FRET) measurement with acceptor photobleaching and spectral unmixing. *J Microsc* **215**(Pt 2): 162-173.
- Habuchi, S., Ando, R., Dedecker, P., Verheijen, W., Mizuno, H., Miyawaki, A., and Hofkens, J. 2005. Reversible single-molecule photoswitching in the GFP-like fluorescent protein Dronpa. *Proc Natl Acad Sci U S A* **102**(27): 9511-9516.
- Harpur, A.G., Wouters, F.S., and Bastiaens, P.I. 2001. Imaging FRET between spectrally similar GFP molecules in single cells. *Nat Biotechnol* **19**(2): 167-169.
- Hink, M.A., Bisselin, T., and Visser, A.J. 2002. Imaging protein-protein interactions in living cells. *Plant Mol Biol* **50**(6): 871-883.
- Hiraoka, Y., Shimi, T., and Haraguchi, T. 2002. Multispectral imaging fluorescence microscopy for living cells. *Cell Struct Funct* **27**(5): 367-374.
- Honda, A., Adams, S.R., Sawyer, C.L., Lev-Ram, V., Tsien, R.Y., and Dostmann, W.R. 2001. Spatiotemporal dynamics of guanosine 3',5'-cyclic monophosphate revealed by a genetically encoded, fluorescent indicator. *Proc Natl Acad Sci U S A* **98**(5): 2437-2442.
- Hoppe, A., Christensen, K., and Swanson, J.A. 2002. Fluorescence resonance energy transfer-based stoichiometry in living cells. *Biophys J* **83**(6): 3652-3664.
-

Houtsmuller, A.B., Rademakers, S., Nigg, A.L., Hoogstraten, D., Hoeijmakers, J.H.J., and Vermeulen, W. 1999. Action of DNA repair endonuclease ERCC1/XPF in living cells. *Science* **284**(5416): 958-961.

Jares-Erijman, E.A. and Jovin, T.M. 2003. FRET imaging. *Nat Biotechnol* **21**(11): 1387-1395.

Karpova, T.S., Baumann, C.T., He, L., Wu, X., Grammer, A., Lipsky, P., Hager, G.L., and McNally, J.G. 2003. Fluorescence resonance energy transfer from cyan to yellow fluorescent protein detected by acceptor photobleaching using confocal microscopy and a single laser. *J Microsc* **209**(Pt 1): 56-70.

Lakowicz, J.R. 1999. *Principles of fluorescence spectroscopy*. Kluwer Academic/Plenum Publishers, New York.

Neher, R.A. and Neher, E. 2004. Applying spectral fingerprinting to the analysis of FRET images. *Microsc Res Tech* **64**(2): 185-195.

Park, C.-H., Bessho, T., Matsunaga, T., and Sancar, A. 1995. Purification and characterization of the XPF-ERCC1 complex of human DNA repair excision nuclease. *J Biol Chem* **270**: 22657-22660.

Patterson, G.H., Piston, D.W., and Barisas, B.G. 2000. Forster distances between green fluorescent protein pairs. *Anal Biochem* **284**(2): 438-440.

Piston, D.W. and Kremers, G.J. 2007. Fluorescent protein FRET: the good, the bad and the ugly. *Trends Biochem Sci* **32**(9): 407-414.

Ponsioen, B., Zhao, J., Riedl, J., Zwartkruis, F., van der Krogt, G., Zaccolo, M., Moolenaar, W.H., Bos, J.L., and Jalink, K. 2004. Detecting cAMP-induced Epac activation by fluorescence resonance energy transfer: Epac as a novel cAMP indicator. *EMBO Rep* **5**(12): 1176-1180.

Rizzo, M.A., Springer, G.H., Granada, B., and Piston, D.W. 2004. An improved cyan fluorescent protein variant useful for FRET. *Nat Biotechnol* **22**(4): 445-449.

Sijbers, A.M., de Laat, W.L., Ariza, R.R., Biggerstaff, M., Wei, Y.F., Moggs, J.G., Carter, K.C., Shell, B.K., Evans, E., de Jong, M.C., Rademakers, S., de Rooij, J., Jaspers, N.G., Hoeijmakers, J.H., and Wood, R.D. 1996. Xeroderma pigmentosum group F caused by a defect in a structure-specific DNA repair endonuclease. *Cell* **86**(5): 811-822.

Tripsianes, K., Folkers, G., Ab, E., Das, D., Odijk, H., Jaspers, N.G., Hoeijmakers, J.H., Kaptein, R., and Boelens, R. 2005. The structure of the human ERCC1/XPF interaction domains reveals a complementary role for the two proteins in nucleotide excision repair. *Structure* **13**(12): 1849-1858.

Van Munster, E.B., Kremers, G.J., Adjobo-Hermans, M.J., and Gadella, T.W., Jr. 2005. Fluorescence resonance energy transfer (FRET) measurement by gradual acceptor photobleaching. *J Microsc* **218**(Pt 3): 253-262.

van Royen, M.E., Cunha, S.M., Brink, M.C., Mattern, K.A., Nigg, A.L., Dubbink, H.J., Verschure, P.J., Trapman, J., and Houtsmuller, A.B. 2007. Compartmentalization of androgen receptor protein-protein interactions in living cells. *J Cell Biol* **177**(1): 63-72.

Yagi, T., Wood, R.D., and Takebe, H. 1997. A low content of ERCC1 and a 120 kDa protein is a frequent feature of group F xeroderma pigmentosum fibroblast cells. *Mutagenesis* **12**(1): 41-44.

Zimmermann, T., Rietdorf, J., Girod, A., Georget, V., and Pepperkok, R. 2002. Spectral imaging and linear un-mixing enables improved FRET efficiency with a novel GFP2-YFP FRET pair. *FEBS Lett* **531**(2): 245-249.

---



## Chapter 4

### Activation of Multiple DNA Repair Pathways by Sub-nuclear Damage Induction Methods

Christoffel Dinant, Martijn de Jager, Jeroen Essers,  
Wiggert A. van Cappellen, Roland Kanaar, Adriaan B.  
Houtsmuller and Wim Vermeulen

*J. Cell. Sc.* 120 (Pt 15): 2731-40, August 2007

### **Abstract**

Live cell studies of DNA repair mechanisms are greatly enhanced by new developments in real-time visualization of repair factors in living cells. Combined with recent advances in local sub-nuclear DNA damage induction procedures these methods have yielded detailed information on the dynamics of damage recognition and repair. Here we analyze and discuss the various types of DNA damage induced in cells by three different local damage induction methods: pulsed 800 nm laser irradiation, Hoechst 33342 treatment combined with 405 nm laser irradiation and UV-C (266 nm) laser irradiation. A wide variety of damages was detected with the first two methods, including pyrimidine dimers, single- and double-strand breaks. However, many aspects of the cellular response to presensitization by Hoechst 33342 and subsequent 405 nm irradiation were aberrant from every other DNA damaging method described here or in the literature. Whereas, application of low-dose 266 nm laser irradiation induced only UV-specific DNA photo-lesions allowing the study of the UV-C-induced DNA damage response in a user-defined area in cultured cells.

### **Introduction**

The mammalian genome is protected against the continuous stress of both exogenous and endogenous DNA damaging agents by a number of DNA damage response mechanisms, including different DNA repair pathways. Unresolved DNA lesions may introduce mutations, which can lead to cancer (Mitchell et al., 2003). In addition, unrepaired damages may result in disturbed transcription and replication, which eventually causes cell death contributing to aging. The severe clinical consequences associated with hereditary disorders that harbor defects in DNA repair systems underscore the importance of efficient DNA repair (Bootsma and Hoeijmakers, 1994; Hoeijmakers, 2001).

Genetic and biochemical analysis of repair processes have culminated in detailed mechanistic insight into the distinct DNA repair processes. To study the interaction of the different DNA repair processes with each other and with other cellular processes such as transcription and replication, spatiotemporal analysis of different DNA repair systems in intact living cells is required and has been used extensively with the aid of GFP-tagged repair factors (Essers et al., 2002b; Hoogstraten et al., 2002; Houtsmuller et al., 1999; Rademakers et al., 2003). Recently, DNA repair research has been boosted substantially by the development of several methods to locally inflict DNA damage in cultured living cells, enabling the direct visualization of GFP-tagged repair factors accumulating at the sub-nuclear region where the damage is caused. These methods range from irradiating partially shielded cells (Kannouche et al., 2001; Katsumi et al., 2001; Mone et al., 2001; Nelms et al., 1998; Volker et al., 2001) to focusing laser beams inside living cell nuclei (Essers et al., 2006; Lukas et al., 2005).

By irradiation of cultured cells through a polycarbonate filter with UV-C-light, either prior to or after mounting on the microscope stage, and

---

subsequently measuring the accumulation of repair proteins, the kinetics of nucleotide excision repair (NER) have been determined previously (Hoogstraten et al., 2002; Mone et al., 2004; Politi et al., 2005; Zotter et al., 2006). In addition, alternative methods have been developed where DNA damage is introduced by focused laser beams, at user-defined regions within the nucleus (Cremer et al., 1980; Lan et al., 2004; Meldrum et al., 2003; Walter et al., 2003). This approach allowed great flexibility not only with respect to position, but also size and shape of the local damage induced in individual cells.

**Table 1. Overview of induced damages and protein accumulations: DSB and SSB repair**

Treatment	TUNEL	γH2AX	γPKcs	MDC1	Rad54	Ku70	PARP-1
Pulsed 800	+	+	+	+	+	+	+
H+405	+	+	-	+ <sup>1</sup>	+ <sup>1</sup>	+	+
UV-C	- <sup>2</sup>	- <sup>3</sup>	-	- <sup>4</sup>	- <sup>4</sup>	- <sup>2</sup>	-

<sup>1</sup> DSB repair proteins that do not accumulate in foci but in a homogenous pattern; <sup>2</sup> UV-C irradiation without attenuation resulted in positive TUNEL staining and Ku-GFP accumulation; <sup>3</sup> At higher UV-C doses γH2AX accumulation can be found; <sup>4</sup> Accumulation of DSB repair proteins on UV-C damage is dependent on ongoing replication.

Tuned localized intense laser irradiation with 365 nm light causes different types of DNA lesions ranging from oxidized base damages, single-strand breaks (SSBs) up to double-strand breaks (DSBs) (Lan et al., 2004). Another powerful method uses pulsed near infrared laser (multiphoton) technology. In this case 2 or 3 lower energy-photons are absorbed simultaneously resulting in twice or three times the energy deposition. Meldrum et al. (2003) applied this procedure using a pulsed 750 nm laser (with an effective wavelength of 250 nm) and showed that this method is able to create UV-like DNA lesions in living cells as shown by in situ immuno staining using antibodies against cyclobutane pyrimidine dimers (CPDs). Recently, it has been shown that with a pulsed near infrared laser DSBs are created as well (Mari et al., 2006), indicating the broad spectrum of DNA lesions induced with this procedure.

More indirect methods rely on local relatively low energy UV-A irradiation. These methods require cells to be pretreated with halogenated thymidine analogs such as BrdU or IdU, which are incorporated in DNA, and induce SSBs and DSBs when exposed to UV-A (Lukas et al., 2003; Tashiro et al., 2000). A variant of this method employs the DNA-binding dyes like Hoechst either in combination with (Rogakou et al., 1999; Walter et al., 2003), or without thymidine analogs (Bradshaw et al., 2005). Although, a number of these in situ local damage-inducing systems have been applied to study

**Table 2. Overview of induced damages and protein accumulations: NER**

Treatment	CPD	6-4PP	XPC	XPA
Pulsed 800	+	+	+	+
H+405	+	-	+	+
UV-C	+	+	+	+

DNA damage response mechanisms the spectrum of DNA lesion induced by these procedures has not been analyzed in great detail.

Here we have systematically analyzed and compared different procedures to locally inflict DNA damage in cultured cells. We show that pulsed 800 nm irradiation introduces a broad variety of DNA lesions at which proteins involved in different pathways accumulate. The combination of Hoechst 33342 incorporation and 405 nm irradiation induced a cellular response that strongly differs from the response to other damaging methods. In addition, we have developed a microscope setting using focused UV-C (266 nm) laser irradiation, which induces predominantly UV-C specific photolesions such as cyclobutane pyrimidine dimers (CPD) and 6-4 photoproducts (6-4PP).

## **Results**

### **Experimental setup**

We have investigated local DNA damage induction in cultured living cells with confocal microscopy using lasers of different wavelengths: 800 nm, 405 nm and 266 nm. The types of damages created with these methods and the assembly of different repair proteins after local irradiation were first analyzed using immunocytological procedures directed against lesions (CPD, 6-4PP and TUNEL) or the consequences of lesions (accumulation of phosphorylated H2AX, phosphorylated DNA-PKcs, PARP-1) as well as protein-GFP fusions. The results of these studies are summarized in Tables 1 and 2. In addition, the kinetics of protein assembly to DNA damage complexes were analyzed in living cells expressing fluorescently tagged repair factors involved in both early and late steps of the reaction of both nucleotide excision repair (XPC and XPA) and DSB repair (MDC1 and Rad54). All cell lines expressing GFP- or YFP-tagged proteins have previously been characterized and published (see Material and Methods section and references therein).

### **Response of the NER machinery to pulsed 800 nm irradiation**

To investigate the types of DNA damage created by pulsed near infrared (NIR) laser irradiation, cells were subjected to high intensity 800 nm laser pulses. To provide an internal control for the immunofluorescent detection of pyrimidine dimers, we irradiated XPC-GFP expressing cells with UV-C light through a filter before irradiation with a NIR laser. Pulsed 800 nm laser irradiation resulted in the formation of CPDs (Fig. 1A), as reported previously (Meldrum et al., 2003). In addition to CPDs, also 6-4PPs were formed (Fig. 1B; arrowheads). XPC-GFP (Politi et al., 2005) accumulated on areas irradiated with a UV lamp through a micro-porous filter as well as areas irradiated with a pulsed 800 nm laser. (Fig. 1A,B). GFP-XPA (Rademakers et al., 2003) also accumulated with both methods, but its response to UV lamp irradiation was much stronger than to pulsed 800 nm irradiation (Fig. 1C).

---

### Response of the DSB repair machinery to pulsed 800 nm irradiation

To determine whether DSBs are induced by a pulsed 800 nm laser we stained locally irradiated nuclei of XPC deficient fibroblasts (XP4PA) expressing XPC-GFP (Politi et al., 2005) with an antibody against phosphorylated DNA-PKcs ( $\gamma$ PKcs). DNA-PKcs is the catalytic subunit of the DNA dependent protein kinase (DNA-PK), which is autophosphorylated in response to ionizing radiation (Chan et al., 2002). The presence of  $\gamma$ PKcs suggested the formation of DSBs by a pulsed 800 nm laser (Fig. 2A). In

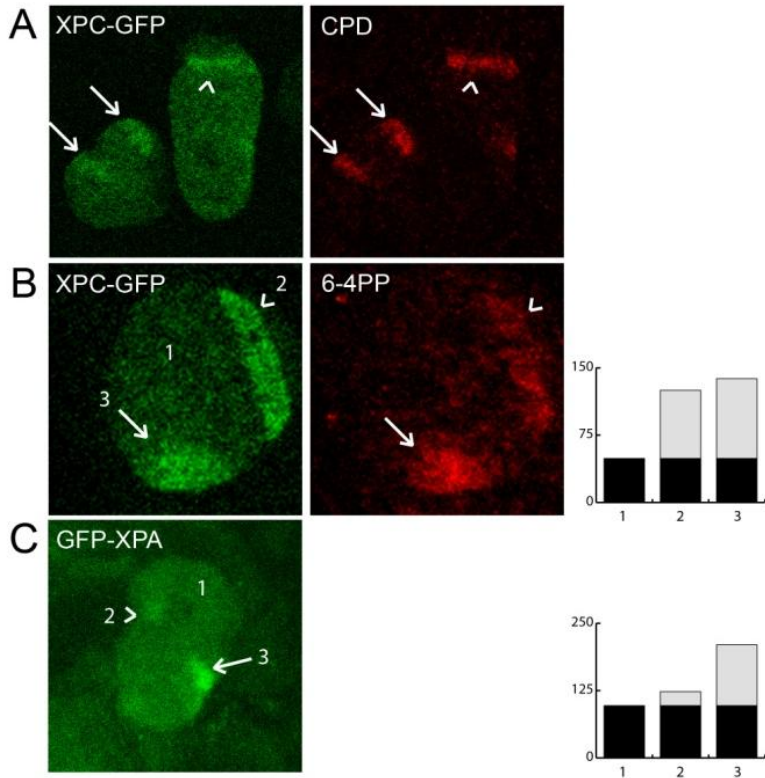
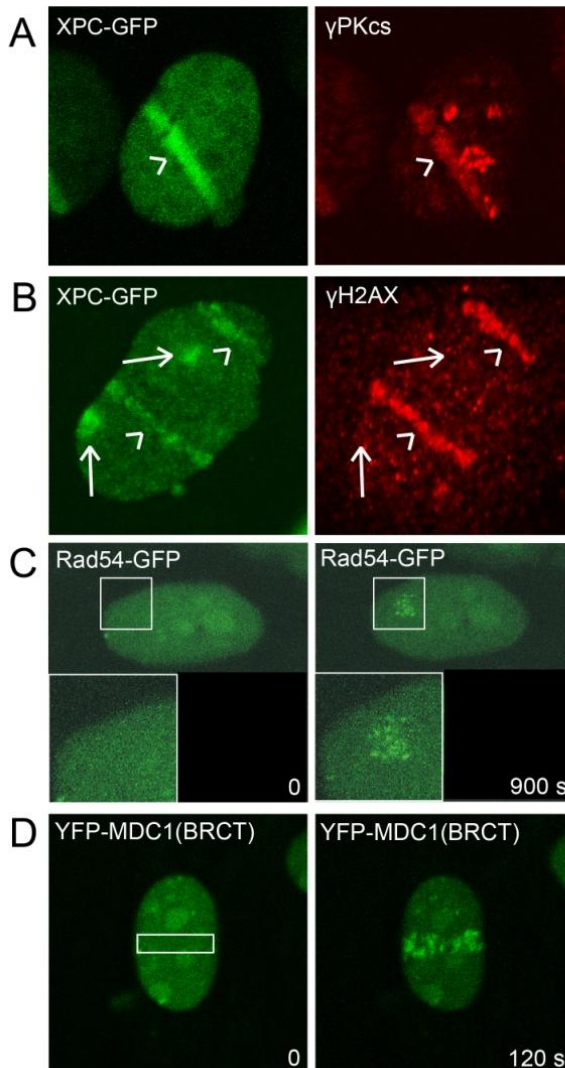


**Fig. 1.** The NER response to local pulsed 800 nm laser irradiation. (A) XPC-GFP-expressing cells were irradiated through a filter with UV-C light (spots indicated by arrows) and subsequently treated with 800 nm laser pulses (lines indicated by arrowheads). Induction of CPDs is shown by staining with the CPD antibody (red, middle panel) both on UV-C and pulsed 800 nm locally irradiated areas. In both areas XPC-GFP accumulated (green, left and merge, right panel). (B) XPC-GFP-expressing cells were treated as in panel A and stained for the presence of 6-4PPs (red, middle panel). Pulsed 800 nm irradiation is able to induce 6-4PP-formation as shown by the lines indicated by the arrowheads (middle panel). The bar graph indicates fluorescence intensities of the nucleus (1), pulsed 800 nm induced local damage (2) and UV-C induced local damage (3). (C) GFP-XPA accumulates to a limited extent on pulsed 800 nm induced damaged areas (arrowhead) compared to UV-C irradiated areas (arrow). The bar graph indicates fluorescence intensities of the nucleus (1), pulsed 800 nm induced local damage (2) and UV-C induced local damage (3).



addition,  $\gamma$ H2AX (Fig. 2B) and Ku80-GFP (Mari et al., 2006) were also found at these sites, indicative of the presence of DSBs. Under similar conditions local UV-C irradiation through pores in a filter failed to induce DSBs as indicated by the absence of  $\gamma$ PKcs positive signal (Table 1) and  $\gamma$ H2AX staining (Fig. 2B).

Rad54 is implicated in multiple steps of DSB repair through homologous recombination (HR). Previous research has shown that in response to DSB induction by ionizing radiation HR proteins accumulate in nuclear foci (Essers et al., 2002b; Rouse and Jackson, 2002; van Veelen et al., 2005a; van Veelen et al., 2005b). Accordingly, Rad54-GFP accumulated in a focal pattern at the damaged area (Fig. 2C, right panel), similar to what has been

**Fig. 2.** The DSB repair response to local pulsed 800 nm laser irradiation. (A) XPC-GFP-expressing cells were treated with pulsed 800 nm irradiation and presence of DSBs is shown by immunohistochemical staining with a  $\gamma$ PKcs antibody (lines in middle panel indicated by arrowheads). The bright spots outside the damaged area in the middle and right panel are nucleolar structures of unknown origin and it is unknown if they exist in a living cell as well. (B) XPC-GFP-expressing cells were treated as in panel A and stained for the presence of phosphorylated histone H2AX ( $\gamma$ H2AX). Accumulation of  $\gamma$ H2AX at areas irradiated by the pulsed 800 nm laser confirms the presence of DSBs (red, middle panel, arrowheads). No accumulation of  $\gamma$ H2AX is found on UV-C irradiated spots (arrows). Earlier it was shown that phosphorylation of H2AX takes place after UV-C irradiation (Marti et al., 2006; O'Driscoll et al., 2003) and we have found this as well in other experiments (data not shown). It is possible that in this case the specific immunohistochemical staining of  $\gamma$ H2AX at UV-C damage was not strong enough to be detected over background signals. (C) Rad54-GFP expressing cells were irradiated in an area of approximately  $5 \mu\text{m}^2$  with pulsed 800 nm light and the redistribution of fluorescence was studied in time. The boxed area is two times enlarged in the right bottom of both panels. Rad54-GFP accumulates in small foci at the damaged area. (D) YFP-MDC1(BRCT) expressing cells were irradiated in a rectangular line through the nucleus and fluorescence redistribution was followed in time. YFP-MDC1(BRCT) accumulates in large foci at the damaged area (boxed area, left panel).

described for multiple HR proteins after DNA damage induction (Bekker-Jensen et al., 2006). Whereas HR is thought to be predominantly active during the S and G2 phases of the cell-cycle, we found accumulation of Rad54-GFP in virtually all cells. Similarly, Rad51 was found to accumulate at locally damaged areas regardless of cell-cycle phase (Kim et al., 2005). These observations suggest that part of the HR machinery is loaded onto DSBs in G1. However, this recruitment might not reflect ongoing repair. Interestingly, the BRCT domain of MDC1 tagged with YFP (YFP-MDC1(BRCT)) also accumulated on pulsed 800 nm induced damage, but with faster kinetics and in much bigger foci than Rad54 (Fig. 2D, right panel, versus Fig. 2C, right panel). These large foci are likely indicative of the interaction between MDC1 and  $\gamma$ H2AX (Bekker-Jensen et al., 2006).

To determine a dose of pulsed 800 nm irradiation with which specifically one repair pathway was induced and not another, we lowered the laser intensity. At slightly lower doses than used above, both GFP-XPA (NER) and Rad54-GFP (HR) remained undetectable at irradiated areas (data not shown). This indicates that under the conditions used we did not observe preferential formation of one type of lesion over the other by changing the applied dose.

### **NER response to Hoechst 33342 + 405 nm damage induction**

The DNA binding agents Hoechst 33258 and 33342 are known to induce DNA breaks when activated by UV-A irradiation (Lecoecur, 2002). Surprisingly, also the NER protein XPC-GFP, which detects 6-4PPs and to a lesser extent CPDs induced by UV-C (<300nm), was targeted to 405 nm (UV-A)-irradiated spots in Hoechst 33342 containing cells (Fig. 3A). In the absence of Hoechst 33342, DNA damage induction with a 405 nm laser required more than ten fold higher laser intensity (data not shown). This localization of the UV damage sensor XPC prompted us to further analyze the types of DNA lesions introduced by this procedure. XPC-GFP expressing cells were UV-C irradiated through a filter as an internal control for the

pyrimidine dimer antibody staining before addition of Hoechst. After Hoechst 33342 treatment, cells were irradiated in a rectangular area through the nucleus with 405 nm. This resulted in abundant CPD formation (Fig. 3A) identical to pulsed 800 nm-induced damage (Fig. 1C). Remarkably, no 6-4PPs were found (Fig. 3B). Apparently this method specifically induced minor helix distorting lesions such as CPDs but not the more severely helix distorting 6-4PPs. Similar to its response to pulsed 800 nm irradiation, XPC-

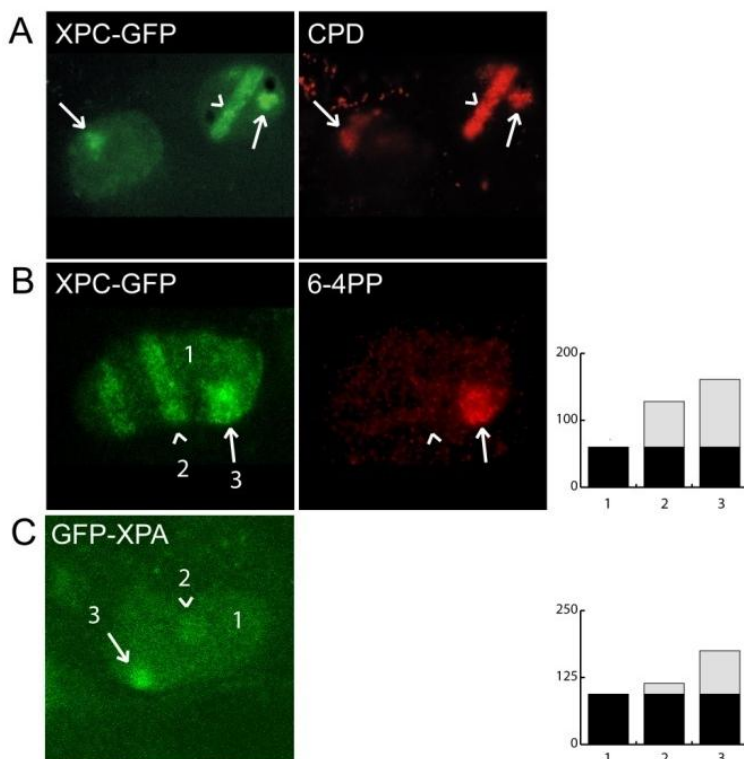


**Fig. 3.** NER response to local Hoechst 33342 treatment + 405 nm irradiation. (A) XPC-GFP-expressing cells were irradiated through a filter with UV-C light (spots indicated by arrows), sensitized with Hoechst 33342 and subsequently locally treated with 405 nm irradiation in the nucleus (lines indicated by arrowheads). Induction of CPDs is shown by the CPD antibody staining (middle panel) both on UV-C and H+405 treated areas. XPC-GFP accumulated on both areas irradiated through a filter with UV-C light (arrows) and irradiated with 405 nm in combination with Hoechst 33342 (arrowheads). (B) Treatment as in panel A, here cells were stained with an antibody that recognizes 6-4PPs (middle panel). Surprisingly, no 6-4PP-staining can be detected on laser-irradiated areas (lines indicated by arrowheads), while the UV-C treated areas show a clear induction with UV-C light (arrows). The bar graph indicates fluorescence intensities of the nucleus (1), 405 nm combined with Hoechst 33342 treatment induced local damage (2) and UV-C induced local damage (3). (C) GFP-XPA accumulates to a low level on local damage induced by 405 nm laser irradiation in combination with Hoechst 33342 treatment (arrowhead) compared with local UV-C irradiated areas (arrow). The bar graph indicates fluorescence intensities of the nucleus (1), 405 nm combined with Hoechst 33342 treatment induced local damage (2) and UV-C induced local damage (3).



---

GFP responded very strongly to these damages (Fig. 3A,B) but GFP-XPA accumulation was much less intense on Hoechst + 405 nm irradiated areas than on UV lamp irradiated areas (Fig. 3C). This suggests that XPC responds to a wider variety of lesions than only those typically repaired by NER.

### **Response of the DSB repair machinery to Hoechst 33342 + 405 nm damage induction**

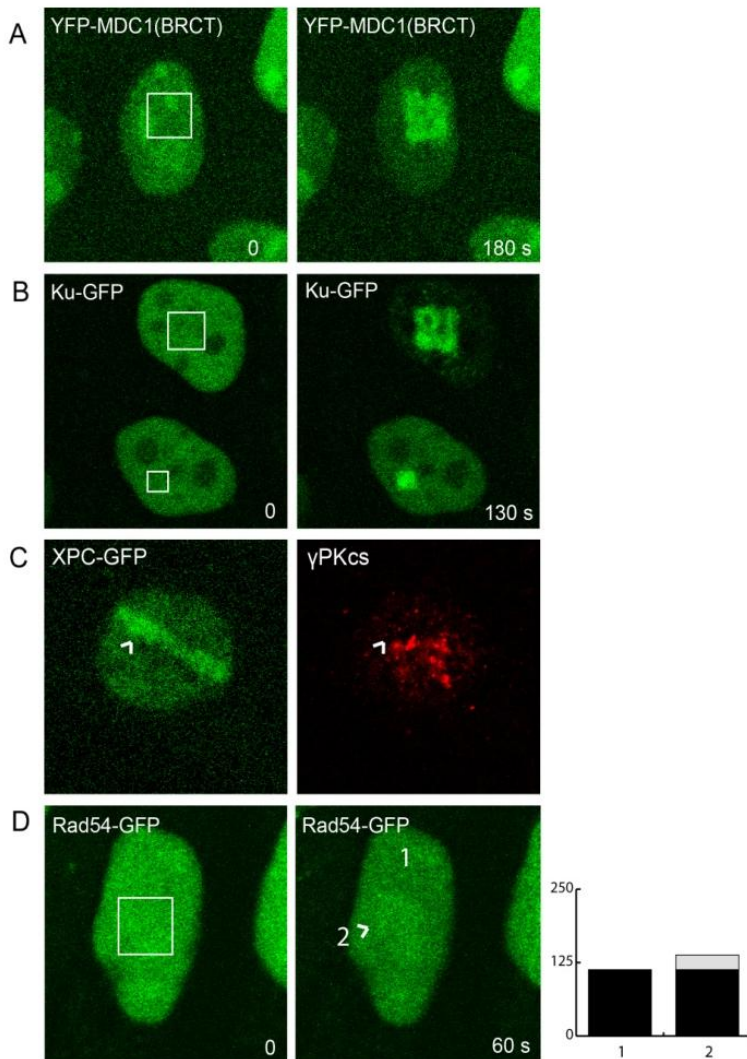
In Hoechst 33342-sensitized CHO9 cells locally irradiated at 405 nm, YFP-MDC1(BRCT) as well as the NHEJ-specific Ku80-GFP quickly accumulated in the 405 nm irradiated areas in very high numbers (Fig. 4A,B, see Supplemental Fig. S1 for co-localisation of XPC-mCherry and YFP-MDC1(BRCT)), indicating that DSBs were present. The presence of phosphorylated H2AX confirmed the creation of DSBs (Table 1). DNA-PKcs is recruited to DNA damage by Ku (Downs and Jackson, 2004) and damage-induced autophosphorylation of DNA-PKcs is regulated by MDC1 (Lou et al., 2004) so we expected to find  $\gamma$ PKcs on local Hoechst 33342 + 405 nm damage. In contrast to its response to pulsed 800 nm irradiation,  $\gamma$ PKcs did not localize to Hoechst 33342-induced DNA damage in any of the irradiated cells above background levels of the immunohistochemical staining (Fig. 4C). Apparently the types of lesions created with this method are not a good substrate for  $\gamma$ PKcs. This indicates an activity of Ku70/Ku80 that is independent of DNA-PKcs as was previously described for its proposed function at telomeres (Hsu et al., 2000).

Furthermore YFP-MDC1(BRCT) accumulation did not show a focal pattern but rather was homogeneously distributed within the damaged area (Fig. 4A, right panel). Similarly Rad54-GFP accumulated on damages induced by 405 nm in combination with Hoechst 33342, albeit in low numbers (bargraph Fig. 4D), but it did not appear in foci (Fig. 4D, right panel), not even after 40 minutes (data not shown). Together with the absence of  $\gamma$ PKcs at irradiated areas this indicates that the combination of Hoechst 33342 sensitization and 405 nm light triggers a hitherto unknown response of DSB repair proteins.

### **NER and DSBs upon local UV-C irradiation**

To induce local UV damage, we installed a pulsed 2 mW 266 nm laser on a confocal microscope adapted for UV-C transmission with all-quartz optics. Local UV-light induced DNA damage infliction by irradiation through a microporous filter is technically a fairly easily applicable procedure, but includes a number of drawbacks that are overcome with the use of a laser. First, unless a set-up is used where irradiation takes place on the microscope stage (Mone et al., 2004), irradiation through a filter is unsuitable for the study of accumulation rates. Even with the application of the on-the-microscope-stage set-up, early or quick assembly rates are hard to monitor due to the relatively long irradiation times required (>12s). Second, irradiation through a filter induces damage in all cells in the preparation simultaneously, making it

---



very difficult to monitor protein accumulations in multiple cells in one experiment. Laser irradiation provides much more flexibility, allowing local damage infliction at specific locations in individual cells, e.g. specific sub-nuclear hetero- or euchromatic regions or even multiple irradiations in one cell or different doses in different cells in the same view, which is not possible with filter irradiation.

UV-C light is known to directly induce helix-distorting lesions such as CPDs 6-4PPs but not SSBs or DSBs (Perdiz et al., 2000; Rodrigo et al., 2000). However, at high UV-C intensity positive TUNEL staining was found next to the accumulation of the NER factor XPA (Fig. 5A, arrowhead). In

**Fig. 4.** DSB repair response to Hoechst 33342 + 405 nm damage. (A) YFP-MDC1(BRCT) expressing cells were incubated with Hoechst 33342 and irradiated in an area of approximately  $5 \mu\text{m}^2$  (white box) with 405 nm laser-light and the fluorescence redistribution was followed in time. YFP-MDC1(BRCT) accumulates in a non-focal/homogenous pattern at the damaged area (right panel). (B) Ku-GFP expressing cells were incubated with Hoechst 33342 and irradiated with 405 nm light in a big (top cell) or small (lower cell) area in the nucleus (white boxes). The accumulation of Ku-GFP was followed in time (right panel). (C)  $\gamma$ PKcs does not accumulate at Hoechst 33342 + 405 nm treated sites (line in the nucleus indicated by arrowhead). The bright spots in the  $\gamma$ PKcs channel are described in Figure 2A and are also found in cells that were not damaged. (D) Rad54-GFP expressing cells were treated with Hoechst 33342 and 405 nm irradiation (white boxes) and fluorescence redistribution was followed in time (right panel). Rad54-GFP accumulates in very low numbers at locally damaged areas in a non-focal/homogenous pattern. The bar graph indicates the fluorescence intensity in the nucleus (1) and at the locally damaged area (2).

addition, the DSB factor Ku80-GFP accumulated in the irradiated area (footnote Table 1). At  $\sim 12$  fold lower irradiation intensity, only the NER factors accumulated in the damaged region, indicating that NER-specific lesions were created both at high and at low intensities (Fig. 5A,B). Dose-dependency studies showed that up to 6 seconds irradiation with 12 fold attenuation induces accumulation of GFP-XPA but not of Ku80-GFP and that without attenuation 1-second irradiation was sufficient to induce DSBs (Supplemental Table 1). In the remaining experiments, the UV-C dose used was 0.5 s with 12 fold attenuation. After inflicting local irradiation with this dose, GFP-PCNA expressing cells (Essers et al., 2005) were still able to go through mitosis (Supplemental Figure S2 and online video), suggesting that under the conditions used we did not trigger apoptosis.

During S-phase, replication forks can stall when they encounter a UV-induced lesion. HR is suggested to be involved in resolving these stalled replication forks. Therefore we examined the response of Rad54 to UV-C laser irradiation at different stages of the cell-cycle in cells expressing both Rad54-GFP and mCherry-PCNA. In cells that showed a homogeneous mCherry-PCNA staining (G1- or G2-phases), no accumulation of Rad54-GFP at damaged areas was found (Fig. 5C). In cells with a focal mCherry-PCNA pattern, Rad54-GFP accumulated at irradiated areas (Fig. 5D), suggesting that HR is only activated by UV-C laser irradiation during replication.

### Accumulation kinetics with laser assisted DNA damaging methods

We have measured the kinetic behavior of four DNA damage repair proteins, XPC, XPA, MDC1 and Rad54, upon recruitment to the various local laser-damaged areas discussed above. To this end we monitored protein redistribution for up to 20 minutes after local damage induction with either pulsed 800 nm irradiation, 405 nm combined with Hoechst 33342 or 266 nm laser irradiation and compared fold increase of fluorescence in the damaged area over time for these three damaging methods (Fig. 6 A-D).

XPC-GFP responded quickly with both the pulsed 800 nm and 266 nm irradiation methods but it accumulated slower at Hoechst 33342 + 405 nm induced damage (Fig. 6A). This unexpected behavior of XPC is most likely

caused by an inhibitory effect of the presence of Hoechst on XPC mobility (Hoogstraten, manuscript in preparation). XPC appeared to very transiently and frequently bind to Hoechst-stained DNA thus limiting the speed of its accumulation in the damaged area.

GFP-XPA was not visibly retarded by Hoechst 33342 addition, but it accumulated to a much lesser extent than XPC-GFP in areas irradiated with either pulsed 800 nm or Hoechst combined with 405 nm. Both GFP-XPA (Fig. 6B) and XPC-GFP (Fig. 6A) showed a stronger increase in fluorescence intensity with the 266 nm method than with the other two, indicating that a UV-C laser can induce a high concentration of lesions that are specifically repaired by NER without creating DSBs at the same time (Tables 1 and 2). Note that GFP-XPA took much longer to reach a plateau level in response to 266 nm irradiation than XPC-GFP ( $t_{1/2}$  values of ~140 and ~40s respectively). Two scenarios can explain this difference between XPA and XPC: (i) at individual repair sites XPC is released before repair is complete (Park and Choi, 2006; Riedl et al., 2003; You et al., 2003), whereas XPA remains longer bound. This difference in residence time makes that XPC kinetics reaches equilibrium between binding and dissociation earlier than XPA. (ii) Alternatively, the association of XPA with locally damaged areas is delayed because it depends on the presence or enzymatic activity of an earlier factor (Mone et al., 2004; Politi et al., 2005).

MDC1 has been found to interact with proteins of both the non-homologous end-joining (NHEJ) and HR pathways (Bekker-Jensen et al., 2005; Lou et al., 2004; Zhang et al., 2005) and is involved in early events in the DSB repair process, serving as an intermediary between the Mre11/Rad50/Nbs1 complex and chromatin (Lukas et al., 2004; Stucki et al., 2005). In agreement with its early association with damage sites, we found rapid accumulation of this protein at both pulsed 800 nm- and Hoechst + 405 nm-irradiated sites (Fig. 6C). Contrary to XPC, MDC1 accumulated faster on Hoechst treated cells than on 800 nm irradiated cells.

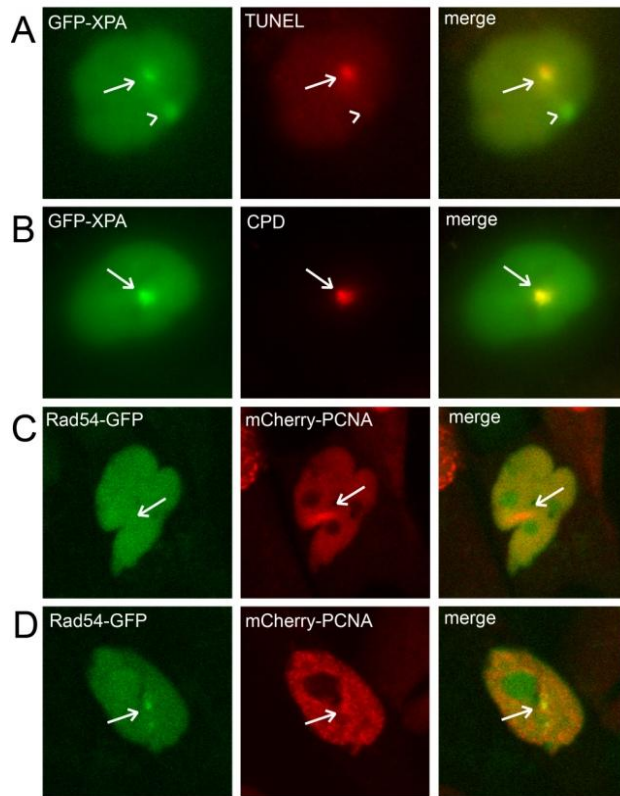


**Fig. 5.** UV-C laser irradiation. (A) GFP-XPA expressing cells were irradiated with 266 nm either without (arrow) or with attenuation (arrowhead). GFP-XPA accumulates on both areas (green, left panel) whereas TUNEL (red, middle panel) only stains positive on the spot that was created without attenuation. (B) GFP-XPA expressing cells were irradiated by attenuated UV-C laser light (arrow). Presence of CPDs was shown by immunohistochemical staining with  $\alpha$ -CPD (red, middle panel). (C) Cells that were irradiated in G1 or G2 phase (homogeneous PCNA pattern, red, middle panel) show no accumulation of Rad54-GFP (green, left panel) 2 hours after irradiation (arrow). (D) In cells that were irradiated in S phase (PCNA pattern in foci, red, middle panel) Rad54-GFP (green, left panel) accumulates at locally irradiated areas within 1 hour after irradiation (arrow).

Interestingly, Rad54-GFP displayed a delayed response to pulsed 800 nm damage, only visibly accumulating after 10 minutes (Fig. 6D). This is consistent with its proposed function later in the DSB repair process and suggests that the kinetics of HR are slower than that of NER of UV lesions (Essers et al., 2002a; Houtsmuller et al., 1999; Mone et al., 2004). It has been shown previously that Rad51, another HR factor, appears at local damage in a comparable timeframe (30 minutes) after DSB induction by a 532 nm laser and that it still is found at these sites after at least 24 hours (Kim et al., 2005). Rad54-GFP accumulated to a lesser extent but with faster kinetics in areas irradiated at 405 nm in Hoechst-treated cells than in areas

irradiated by pulsed 800 nm. In combination with the homogeneous pattern of accumulation for both Rad54 and MDC1 and the absence of detectable  $\gamma$ PKCs accumulation this suggests that the cellular response to 405 nm irradiation and Hoechst 33342 treatment is very different than the response to pulsed 800 nm irradiation. In addition, it suggests that different types of DNA damage are created with these methods and not just different amounts of the same damage.

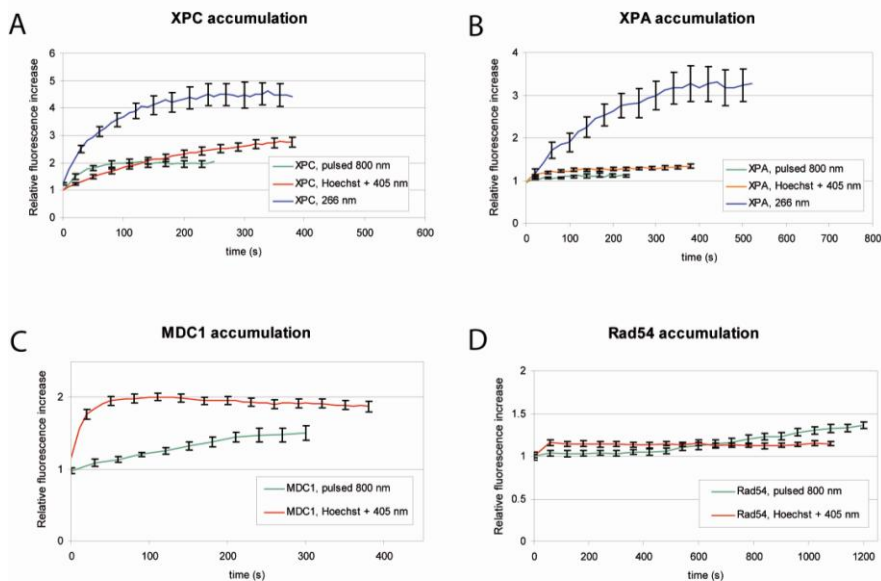


**Fig. 6.** Recruitment of DNA repair factors to various types of DNA damage. (A) XPC-GFP accumulates most efficiently in areas damaged with 266 nm laser light. The presence of Hoechst 33342 causes slower diffusion of XPC thus retarding its recruitment to DNA damage. (B) GFP-XPA also accumulates most efficiently in areas damaged with 266 nm laser light. GFP-XPA responds to a very small extent to pulsed 800 nm irradiation and 405 nm irradiation combined with Hoechst 33342. (C) YFP-MDC1(BRCT) is recruited quicker and in higher numbers to damaged areas in cells irradiated with 405 nm combined with Hoechst 33342 than in pulsed 800 nm-irradiated cells. (D) Rad54-GFP has a delayed response to pulsed 800 nm irradiation but it accumulates to a larger extent to these damages than to 405 nm combined with Hoechst 33342 irradiation.

## Discussion

We have investigated the response of several DNA repair factors, involved in either NER or DSB break repair, to different types of DNA damage induction (Tables 1 and 2). We show that the NER-factor XPC responds to many different types of lesions. This is for instance illustrated by the strong response of XPC-GFP to pulsed 800 nm irradiation and 405 nm irradiation after Hoechst-treatment, whereas GFP-XPA is recruited to irradiated areas to a much lesser extent. Upon 266 nm irradiation this difference is much

smaller. Interestingly, XPC-GFP seemed to be the only NER factor that accumulated after irradiation with a 365 nm laser (Lan et al., 2004), confirming that it binds to a wide range of DNA lesions and not only to lesions that are repaired by NER. This is in accordance with previous *in vitro* DNA binding experiments showing low specificity of XPC for various aberrant DNA structures (Sugasawa et al., 1998). In addition, live cell studies using fluorescence recovery after photobleaching on XPC-GFP expressing cells exposed to a variety of DNA damaging agents known to induce lesions other than pyrimidine dimers showed participation of XPC-GFP similar to its behavior after UV-exposure (Hoogstraten D, manuscript in preparation).

This observed affinity of XPC for a variety of DNA-lesions suggests the rapid formation of pre-repair complexes on DNA. Such a quick response may initiate rapid activation of cell-cycle checkpoints after damage detection. The initial, weakly specific response is then followed by a more lesion-specific, but slower acting damage verification step, which in case of positive verification, in its turn may activate a fully specific repair pathway required for the type of damage encountered. In addition, rapid exchange of damage recognition proteins with more pathway-specific factors may ensure that a repair pathway can quickly become completely activated. Recently, such differential dynamic interactions have been suggested transcription initiation (Hager et al., 2006; Metivier et al., 2006). It was suggested that this prevents slowing down the entire transcription machinery due to too many non-productive long-lasting associations. A bipartite damage-recognition step for NER has been suggested previously (Dip et al., 2004; Sugasawa et al., 2001) with quick binding of a low-specificity initiating factor (XPC) and subsequent lesion verification. Our current data supports this model.

### **Damaging mechanisms by laser-assisted techniques**

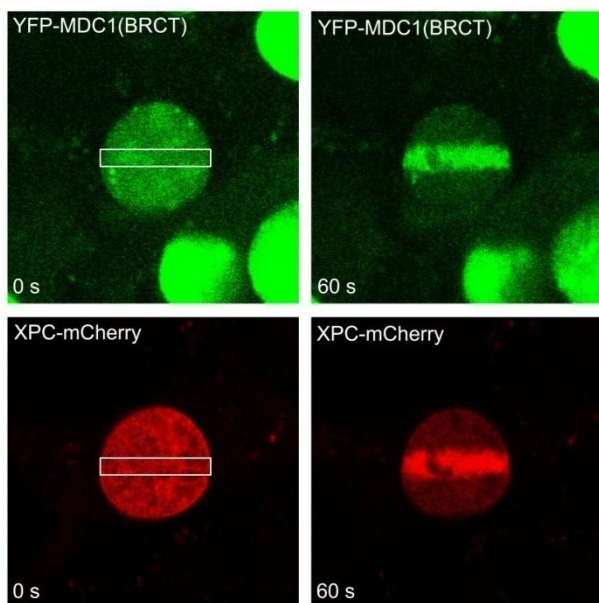
Formation of DSBs by a pulsed 800 nm laser has been reported previously (König et al., 2001; Tirlapur and König, 2001) and is thought to be caused by ablation of the DNA at the highly focused laser spot. In metaphase chromosomes this multiphoton ablation introduces gaps of approximately 100 nm corresponding to ~65 kb (König et al., 2001). Most likely such gaps, i.e. DSBs, will be created in interphase chromosomes as well, explaining the accumulation of DSB repair proteins observed here. Recently, also the induction and repair of DSBs in living cultured cells has been described using this DNA damage induction method (Mari et al., 2006).

A pulsed 800 nm laser beam has been shown to efficiently induce CPDs (Meldrum et al., 2003) and here we show that also 6-4PPs are efficiently formed with a pulsed 800 nm laser. The formation of these lesions which are typically created by UV-C is likely caused by three-photon absorption on the DNA, the effective wavelength being ~267 nm.

Many studies have been published in which DNA is sensitized prior to local irradiation. Sensitization of DNA can be accomplished by incorporation of a halogenated thymidine analogue in combination with Hoechst (Limoli

---

and Ward, 1993; Paull et al., 2000; Rogakou et al., 1999), by incorporation of halogenated Hoechst (Martin et al., 1994; Martin et al., 1990) or of halogenated thymidine analogues alone (Lukas et al., 2003; Tashiro et al., 2000). Halogenation is thought to be required for DSB induction. However, Hoechst (either 33258 or 33342) by itself can also sensitize DNA to UV-A irradiation resulting in DSB formation (Bradshaw et al., 2005; Celeste et al., 2003; Kruhlak et al., 2006). Similarly, we have shown here that in the absence of halogen intermediates, irradiation of Hoechst 33342 sensitized cells at 405 nm induced DSBs, although it invokes a different response of



**S1.** Co-localisation of YFP-MDC1(BRCT) and XPC-mCherry at local damage induced by 405 nm irradiation in combination with Hoechst treatment (rectangular area).

photoproduct that is not recognized by the 6-4PP antibody (Kobayashi et al., 2001). However, the optimum wavelength for photoisomerization is between 280 and 360 nm, so 405 nm laser irradiation probably does not induce DewarPP formation. Instead, Hoechst binding induces local structural changes in the DNA, which might not allow the bending angle that is necessary for 6-4PP formation (Chen et al., 1993). We and others have noted that pre-sensitization of cells with Hoechst 33343 induces a very broad spectrum of events associated with structural changes in the DNA conformation, ranging from chromosome decondensation (Turner and Denny, 1996) to transcription inhibition (White et al., 2000). The aberrant responses shown here are: (1) Absence of phosphorylated DNAPKcs from

Rad54 and  $\gamma$ PKcs, i.e. non-focal accumulation and absence at damaged sites respectively, than those induced by a pulsed 800 nm laser. Another remarkable effect of 405 nm irradiation of Hoechst 33342 sensitized cells is the specific induction of CPDs but not 6-4PPs. Photoisomerization of 6-4PPs results in the formation of the DewarPP, a



damaged areas, whereas DSBs are formed as judged by the Ku70-GFP accumulation; (2) reduced mobility of XPC; (3) homogenous accumulation of DSB repair proteins, rather than the common focal pattern and (4) very rapid accumulation of YFP-MDC1(BRCT) and Rad54-GFP compared with pulsed 800 nm irradiation. Recently, also an aberrant accumulation response of TRF2, a telomere binding protein, to local damage inflicted by pre-sensitization with Hoechst combined with high intensity 800 nm laser irradiation has been described compared to multiple other local damage techniques (Williams et al, Nature Genetics 2007 in press (May 2007)). We conclude that treatment with Hoechst 33343 as a sensitizer for DNA damage induction may have considerable consequences for the cellular response.

Sensitization with halogenated nucleotides instead of Hoechst prior to UV-A irradiation induces a response that is much more similar to ionizing radiation and pulsed 800 nm irradiation as repair proteins accumulate in foci (Lukas et al., 2003; Bekker-Jensen et al., 2006). One striking difference between pulsed 800 nm irradiation and UV-A irradiation of halogenated thymidine-sensitized nuclei is the response of NHEJ factors such as Ku80 and DNA-PKcs, which clearly accumulate in damaged areas created by the first but not by the latter method. Probably, these methods induce a different spectrum of DNA lesions, for example blunt-ended DSBs versus breaks with overhangs. Perhaps the relative concentration of these two types of DSBs determines the extent to which NHEJ or HR becomes activated. We show that UV-C laser irradiation can induce pyrimidine dimers as well as DSBs, however the latter only after high intensity irradiation.



**S2.** Time-lapse of CHO cells expressing GFP-PCNA. After local UV damage induction by the 266 nm laser (yellow circle) the cell proceeds through mitosis.

### Specific DNA damage induction

We show here that UV-C laser irradiation at the appropriate intensity is the most specific method to induce 6-4PPs and CPDs. In contrast, induction of exclusively DSBs seems not possible with currently existing laser-assisted damaging methods. This problem was overcome by a method specifically inducing DSBs using a recombination reporter system involving an *HO* or *I-SceI* endonuclease-site adjacent to a Lac- or Tet-operon repeat (Lisby et al., 2003; Miyazaki et al., 2004; Rodrigue et al., 2006). After induction of expression of the appropriate endonuclease, accumulation of repair proteins at the single DSB can be studied. This method has provided insight in the

nature of repair foci, showing that multiple DSBs can colocalize within one focus in yeast (Lisby et al., 2003). Production of a known amount of well-specified DSBs will become a valuable tool in the study of DSB repair, especially since it has recently been effectively applied in mammalian cells (Rodrigue et al., 2006). However, the study of accumulation kinetics of DSB repair factors may be more complicated with this method because the timing of the activity of restriction enzymes is difficult to control.

**Supplemental Table 1. Dose-dependency of the 266 nm laser.**

	0.5s OD1	1s OD1	6s OD1	20s OD1	1s	6s
XPA	+	+	+	+	+	+
Ku	-	-	-	+	+	+
TUNEL	n.d.	n.d.	-	n.d.	n.d.	+

## Conclusion

Summarizing, we have shown that most presently available and widely used laser-assisted DNA damaging methods induce a wide response of cellular repair mechanisms. The relative proportion of the induced damages, which determines the extent to which different repair pathways become activated, is shown to differ for the three studied methods. Proteins that respond to a variety of lesions, like XPC, will exhibit different kinetic behaviors depending on the damaging method used. In future studies, using more than one source of DNA damage to study cellular responses, with accurate analysis of the types of lesions induced with these methods, will greatly help our understanding of DNA repair *in vivo*.

## Material & Methods

### Preparation and culture of cell lines

XPC-GFP and GFP-XPA were expressed in the human cell lines XP4PA-SV and XP2OS-SV, deficient in XPC and XPA, respectively (Politi et al., 2005; Rademakers et al., 2003). Rad54-GFP expressing cell lines were created by stable expression of Rad54-GFP in CHO9 cells as described (Essers et al., 2002a). In this cell line mCherry-PCNA was transfected. The YFP-MDC1 (BRCT) cell line was created by stable expression of a construct encoding an YFP fusion to the BRCT domains of hMdc1 into CHO9. This construct was shown to be functional as a marker for MDC1 localization (O'Driscoll et al., 2003). GFP-Ku80 was transfected into Ku deficient XR-V15B cells (Mari et al., 2006). GFP-PCNA was expressed in CHO9 cells as described in (Essers et al., 2005). All cell lines were cultured under standard conditions in DMEM/F10 medium supplemented with 10% fetal calf serum and antibiotics at 37°C and 5% CO<sub>2</sub>.

### Local UV induction with UV-C lamps

To induce local UV damage, cells were grown on coverslips, washed with PBS, covered with a polycarbonate-filter (5 µm pore size, Millipore), radiated with 100 J/m<sup>2</sup> (overall dose) and incubated in standard growth medium for 30 minutes before fixation or further treatment.

### **Laser-induction of local damage**

A Coherent Mira modelocked Ti:Sapphire laser was used at 800 nm with a pulselength of 200 fs and repetition rate of 76 MHz. Maximum output power on the cells for DNA damage induction was approximately 80 mW.

For the Hoechst + 405 nm damage a 30 mW 405 nm diode laser supplied by Zeiss was used. Damage was induced at 60% of maximum power.

For UV laser irradiation a 2 mW pulsed (7.8 kHz) diode pumped solid state laser emitting at 266 nm (Rapp OptoElectronic, Hamburg GmbH) was connected to a Zeiss LSM 510 confocal microscope with an Axiovert 200 M housing adapted for UV by all-quartz optics. A special adaptor (ZSI-A200, Rapp OptoElectronic) to fit in the aperture slider position of an Axiovert 200 microscope was developed by Rapp OptoElectronic to focus the laser on a sample. For local UV-C irradiation experiments cells were grown on 25 mm diameter quartz coverslips (010191T-AB, SPI supplies).

### **Imaging of cells using confocal microscopy**

Cells expressing GFP-tagged repair factors were grown on coverslips and imaged at 37°C using Zeiss confocal microscope setup (Zeiss LSM510). In the case of cells to be treated with a combination of Hoechst and 405 nm light, Hoechst 33342 was added to the medium (final concentration 0.5 µg/ml) shortly before treatment. Cells with an intermediate fluorescence level were selected to be treated with either 405 nm or 800 nm light. All treated cells were analyzed at the same magnification and zoom factor using low laser power to minimize photobleaching during data collection. The region to be damaged was always the same size and shape, while laser treatment was done with calibrated lasers at the same laser output to exclude variations in dose.

### **Immunofluorescence analysis**

For immunohistochemical analysis cells were washed with PBS and fixed 15 minutes in 2% paraformaldehyde in PBS 30-60 minutes after damage induction. Next, the cells were washed with 3% BSA in PBS. In the case of antibodies directed against CPDs (TDM2, Mori et al., 1991) or 6-4PPs (6-4-M-2 Mori et al 1991) cells were treated with 0.07 M NaOH in PBS for 5 minutes at room temperature to denature the DNA. Next, the cells were washed three times with P-buffer (0.1% Triton X-100 in PBS) and washed once using I-buffer (0.1% glycine, 1% BSA in PBS). Then, cells were incubated with primary antibodies (diluted in I-buffer) for one hour at 20°C for detection of protein epitopes or 12 hours at 4°C for detection of DNA lesions. The rabbit anti-γH2AX (Ser138) antibody was from Upstate Biotechnology, Charlottesville, VA. After incubation, cells were washed three times using P-buffer, once using I-buffer, and incubated for one hour at 20°C with secondary antibody conjugated to Alexa-488 or Alexa-594 (or multiple antibodies for double staining) diluted in I-buffer. Next, cells were washed three times using P-buffer, once with PBS and embedded in vectashield (Vector Laboratory). The rabbit anti-γPKcs antibody was a kind gift from D. Chen (Chan et al., 2002). TUNEL-staining method was acquired from Roche Applied Science, Penzberg Germany (Cat. No. 12156792910). PARP-1 accumulation was detected with anti-Poly(ADP-ribose) Polymerase-1 (human) polyclonal antibody (ALX-210-895) from Alexis (Breda, The Netherlands).

### **Data analysis**

Images obtained with the confocal microscope were analyzed using AIM software (Zeiss). Fluorescent levels were determined of the specified region where damage was induced in addition to the complete nucleus. From these datapoints the relative amount of protein in de damaged area was determined in time. Curves were normalized to 1 for the first datapoints prior to damage induction. Brightness and contrast of images obtained with the confocal microscope were set to show optimal accumulation through time in the images shown here, and do not necessarily represent the levels used during imaging.

### **Acknowledgements**

---

The authors would like to thank Dr. Roald van der Laan for helpful discussion on pulsed 800 nm laser technology, Professor Goldberg for the MDC1 construct, Professor D. Chen for the antibody against phosphorylated DNA-PKcs and Nicole Verkaik for the Ku-GFP cell line. This work was supported by the Dutch Organisation for Scientific Research (NWO): ZonMW 912-03-012 (CD), 917-46-371 (ABH), 917-46-364 (WV) and 901-01-229, and by ESF 855-01-072, EU LSHG-CT-2005-512113, RGP0007/2004-C (HFSP) and by an Erasmus University research fellowship (MdJ).

### References

- Bekker-Jensen, S., Lukas, C., Kitagawa, R., Melander, F., Kastan, M. B., Bartek, J. and Lukas, J.** (2006). Spatial organization of the mammalian genome surveillance machinery in response to DNA strand breaks. *J Cell Biol* **173**, 195-206.
- Bekker-Jensen, S., Lukas, C., Melander, F., Bartek, J. and Lukas, J.** (2005). Dynamic assembly and sustained retention of 53BP1 at the sites of DNA damage are controlled by Mdc1/NFBD1. *J Cell Biol* **170**, 201-11.
- Bootsma, D. and Hoeijmakers, J. H. J.** (1994). The molecular basis of nucleotide excision repair syndromes. *Mut. Res.* **307**, 15-23.
- Bradshaw, P. S., Stavropoulos, D. J. and Meyn, M. S.** (2005). Human telomeric protein TRF2 associates with genomic double-strand breaks as an early response to DNA damage. *Nat Genet* **37**, 193-7.
- Celeste, A., Fernandez-Capetillo, O., Kruhlak, M. J., Pilch, D. R., Staudt, D. W., Lee, A., Bonner, R. F., Bonner, W. M. and Nussenzweig, A.** (2003). Histone H2AX phosphorylation is dispensable for the initial recognition of DNA breaks. *Nat Cell Biol* **5**, 675-9.
- Chan, D. W., Chen, B. P., Prithivirajasingh, S., Kurimasa, A., Story, M. D., Qin, J. and Chen, D. J.** (2002). Autophosphorylation of the DNA-dependent protein kinase catalytic subunit is required for rejoining of DNA double-strand breaks. *Genes Dev* **16**, 2333-8.
- Chen, A. Y., Yu, C., Gatto, B. and Liu, L. F.** (1993). DNA minor groove-binding ligands: a different class of mammalian DNA topoisomerase I inhibitors. *Proc Natl Acad Sci U S A* **90**, 8131-5.
- Cremer, C., Cremer, T., Fukuda, M. and Nakanishi, K.** (1980). Detection of laser-UV microirradiation-induced DNA photolesions by immunofluorescent staining. *Hum Genet* **54**, 107-10.
- Dip, R., Camenisch, U. and Naegeli, H.** (2004). Mechanisms of DNA damage recognition and strand discrimination in human nucleotide excision repair. *DNA Repair (Amst)* **3**, 1409-23.
- Downs, J. A. and Jackson, S. P.** (2004). A means to a DNA end: the many roles of Ku. *Nat Rev Mol Cell Biol* **5**, 367-78.
- Essers, J., Hendriks, R. W., Wesoly, J., Beerens, C. E., Smit, B., Hoeijmakers, J. H., Wyman, C., Dronkert, M. L. and Kanaar, R.** (2002a). Analysis of mouse Rad54 expression and its implications for homologous recombination. *DNA Repair (Amst)* **1**, 779-93.
- Essers, J., Houtsmuller, A. B., van Veelen, L., Paulusma, C., Nigg, A. L., Pastink, A., Vermeulen, W., Hoeijmakers, J. H. and Kanaar, R.** (2002b). Nuclear dynamics of RAD52 group homologous recombination proteins in response to DNA damage. *Embo J* **21**, 2030-7.
- Essers, J., Theil, A. F., Baldeyron, C., van Cappellen, W. A., Houtsmuller, A. B., Kanaar, R. and Vermeulen, W.** (2005). Nuclear dynamics of PCNA in DNA replication and repair. *Mol Cell Biol* **25**, 9350-9.
- Essers, J., Vermeulen, W. and Houtsmuller, A. B.** (2006). DNA damage repair: anytime, anywhere? *Curr Opin Cell Biol.*
- Hager, G. L., Elbi, C., Johnson, T. A., Voss, T., Nagaich, A. K., Schiltz, R. L., Qiu, Y. and John, S.** (2006). Chromatin dynamics and the evolution of alternate promoter states. *Chromosome Res* **14**, 107-16.
- Hoeijmakers, J. H.** (2001). Genome maintenance mechanisms for preventing cancer. *Nature* **411**, 366-74.
- Hoogstraten, D., Nigg, A. L., Heath, H., Mullenders, L. H., van Driel, R., Hoeijmakers, J. H., Vermeulen, W. and Houtsmuller, A. B.** (2002). Rapid Switching of TFIIH between RNA Polymerase I and II Transcription and DNA Repair In Vivo. *Mol Cell* **10**, 1163-74.

- Houtsmuller, A. B., Rademakers, S., Nigg, A. L., Hoogstraten, D., Hoeijmakers, J. H. J. and Vermeulen, W. (1999). Action of DNA repair endonuclease ERCC1/XPF in living cells. *Science* **284**, 958-961.
- Hsu, H. L., Gilley, D., Galande, S. A., Hande, M. P., Allen, B., Kim, S. H., Li, G. C., Campisi, J., Kohwi-Shigematsu, T. and Chen, D. J. (2000). Ku acts in a unique way at the mammalian telomere to prevent end joining. *Genes Dev* **14**, 2807-12.
- Kannouche, P., Broughton, B. C., Volker, M., Hanaoka, F., Mullenders, L. H. and Lehmann, A. R. (2001). Domain structure, localization, and function of DNA polymerase  $\eta$ , defective in xeroderma pigmentosum variant cells. *Genes Dev* **15**, 158-72.
- Katsumi, S., Kobayashi, N., Imoto, K., Nakagawa, A., Yamashina, Y., Muramatsu, T., Shirai, T., Miyagawa, S., Sugiura, S., Hanaoka, F. et al. (2001). In situ visualization of ultraviolet-light-induced DNA damage repair in locally irradiated human fibroblasts. *J Invest Dermatol* **117**, 1156-61.
- Kim, J. S., Krasieva, T. B., Kurumizaka, H., Chen, D. J., Taylor, A. M. and Yokomori, K. (2005). Independent and sequential recruitment of NHEJ and HR factors to DNA damage sites in mammalian cells. *J Cell Biol* **170**, 341-7.
- Kobayashi, N., Katsumi, S., Imoto, K., Nakagawa, A., Miyagawa, S., Furumura, M. and Mori, T. (2001). Quantitation and visualization of ultraviolet-induced DNA damage using specific antibodies: application to pigment cell biology. *Pigment Cell Res* **14**, 94-102.
- Konig, K., Riemann, I. and Fritzsche, W. (2001). Nanodissection of human chromosomes with near-infrared femtosecond laser pulses. *Optics Letters* **26**, 819-821.
- Kruhlak, M. J., Celeste, A., Dellaire, G., Fernandez-Capetillo, O., Muller, W. G., McNally, J. G., Bazett-Jones, D. P. and Nussenzweig, A. (2006). Changes in chromatin structure and mobility in living cells at sites of DNA double-strand breaks. *J Cell Biol* **172**, 823-34.
- Lan, L., Nakajima, S., Oohata, Y., Takao, M., Okano, S., Masutani, M., Wilson, S. H. and Yasui, A. (2004). In situ analysis of repair processes for oxidative DNA damage in mammalian cells. *Proc Natl Acad Sci U S A* **101**, 13738-43.
- Lecoeur, H. (2002). Nuclear apoptosis detection by flow cytometry: influence of endogenous endonucleases. *Exp Cell Res* **277**, 1-14.
- Limoli, C. L. and Ward, J. F. (1993). A new method for introducing double-strand breaks into cellular DNA. *Radiat Res* **134**, 160-9.
- Lisby, M., Mortensen, U. H. and Rothstein, R. (2003). Colocalization of multiple DNA double-strand breaks at a single Rad52 repair centre. *Nat Cell Biol* **5**, 572-7.
- Lou, Z., Chen, B. P., Asaithamby, A., Minter-Dykhouse, K., Chen, D. J. and Chen, J. (2004). MDC1 regulates DNA-PK autophosphorylation in response to DNA damage. *J Biol Chem* **279**, 46359-62.
- Lukas, C., Bartek, J. and Lukas, J. (2005). Imaging of protein movement induced by chromosomal breakage: tiny 'local' lesions pose great 'global' challenges. *Chromosoma* **114**, 146-54.
- Lukas, C., Falck, J., Bartkova, J., Bartek, J. and Lukas, J. (2003). Distinct spatiotemporal dynamics of mammalian checkpoint regulators induced by DNA damage. *Nat Cell Biol* **5**, 255-60.
- Lukas, C., Melander, F., Stucki, M., Falck, J., Bekker-Jensen, S., Goldberg, M., Lerenthal, Y., Jackson, S. P., Bartek, J. and Lukas, J. (2004). Mdc1 couples DNA double-strand break recognition by Nbs1 with its H2AX-dependent chromatin retention. *Embo J* **23**, 2674-83.
- Mari, P. O., Florea, B. I., Persengiev, S. P., Verkaik, N. S., Bruggenwirth, H. T., Modesti, M., Giglia-Mari, G., Bezstarosti, K., Demmers, J. A., Luijck, T. M. et al. (2006). Dynamic assembly of end-joining complexes requires interaction between Ku70/80 and XRCC4. *Proc Natl Acad Sci U S A* **103**, 18597-602.
- Marti, T. M., Hefner, E., Feeney, L., Natale, V. and Cleaver, J. E. (2006). H2AX phosphorylation within the G1 phase after UV irradiation depends on nucleotide excision repair and not DNA double-strand breaks. *Proc Natl Acad Sci U S A* **103**, 9891-6.
- Martin, R. F., Kelly, D. P., Roberts, M., Nel, P., Tursi, J., Denison, L., Rose, M., Reum, M. and Pardee, M. (1994). Comparative studies of UV-induced DNA cleavage by analogues of iodoHoechst 33258. *Int J Radiat Biol* **66**, 517-21.

- Martin, R. F., Murray, V., D'Cunha, G., Pardee, M., Kampouris, E., Haigh, A., Kelly, D. P. and Hodgson, G. S.** (1990). Radiation sensitization by an iodine-labelled DNA ligand. *Int J Radiat Biol* **57**, 939-46.
- Meldrum, R. A., Botchway, S. W., Wharton, C. W. and Hirst, G. J.** (2003). Nanoscale spatial induction of ultraviolet photoproducts in cellular DNA by three-photon near-infrared absorption. *EMBO Rep* **4**, 1144-9.
- Metivier, R., Reid, G. and Gannon, F.** (2006). Transcription in four dimensions: nuclear receptor-directed initiation of gene expression. *EMBO Rep* **7**, 161-7.
- Mitchell, J. R., Hoeijmakers, J. H. and Niedernhofer, L. J.** (2003). Divide and conquer: nucleotide excision repair battles cancer and ageing. *Curr Opin Cell Biol* **15**, 232-40.
- Miyazaki, T., Bressan, D. A., Shinohara, M., Haber, J. E. and Shinohara, A.** (2004). In vivo assembly and disassembly of Rad51 and Rad52 complexes during double-strand break repair. *Embo J* **23**, 939-49.
- Mone, M. J., Bernas, T., Dinant, C., Goedvree, F. A., Manders, E. M., Volker, M., Houtsmuller, A. B., Hoeijmakers, J. H., Vermeulen, W. and van Driel, R.** (2004). In vivo dynamics of chromatin-associated complex formation in mammalian nucleotide excision repair. *Proc Natl Acad Sci U S A* **101**, 15933-7.
- Mone, M. J., Volker, M., Nikaido, O., Mullenders, L. H., van Zeeland, A. A., Verschure, P. J., Manders, E. M. and van Driel, R.** (2001). Local UV-induced DNA damage in cell nuclei results in local transcription inhibition. *EMBO Rep* **2**, 1013-1017.
- Nelms, B. E., Maser, R. S., MacKay, J. F., Lagally, M. G. and Petrini, J. H.** (1998). In situ visualization of DNA double-strand break repair in human fibroblasts. *Science* **280**, 590-2.
- O'Driscoll, M., Ruiz-Perez, V. L., Woods, C. G., Jeggo, P. A. and Goodship, J. A.** (2003). A splicing mutation affecting expression of ataxia-telangiectasia and Rad3-related protein (ATR) results in Seckel syndrome. *Nat Genet* **33**, 497-501.
- Park, C. J. and Choi, B. S.** (2006). The protein shuffle. Sequential interactions among components of the human nucleotide excision repair pathway. *Febs J* **273**, 1600-8.
- Paull, T. T., Rogakou, E. P., Yamazaki, V., Kirchgessner, C. U., Gellert, M. and Bonner, W. M.** (2000). A critical role for histone H2AX in recruitment of repair factors to nuclear foci after DNA damage. *Curr Biol* **10**, 886-95.
- Perdiz, D., Grof, P., Mezzina, M., Nikaido, O., Moustacchi, E. and Sage, E.** (2000). Distribution and repair of bipyrimidine photoproducts in solar UV-irradiated mammalian cells. Possible role of Dewar photoproducts in solar mutagenesis. *J Biol Chem* **275**, 26732-42.
- Politi, A., Mone, M. J., Houtsmuller, A. B., Hoogstraten, D., Vermeulen, W., Heinrich, R. and van Driel, R.** (2005). Mathematical modeling of nucleotide excision repair reveals efficiency of sequential assembly strategies. *Mol Cell* **19**, 679-90.
- Rademakers, S., Volker, M., Hoogstraten, D., Nigg, A. L., Mone, M. J., Van Zeeland, A. A., Hoeijmakers, J. H., Houtsmuller, A. B. and Vermeulen, W.** (2003). Xeroderma pigmentosum group A protein loads as a separate factor onto DNA lesions. *Mol Cell Biol* **23**, 5755-67.
- Riedl, T., Hanaoka, F. and Egly, J. M.** (2003). The comings and goings of nucleotide excision repair factors on damaged DNA. *Embo J* **22**, 5293-5303.
- Rodrigo, G., Roumagnac, S., Wold, M. S., Salles, B. and Calsou, P.** (2000). DNA replication but not nucleotide excision repair is required for UVC-induced replication protein A phosphorylation in mammalian cells. *Mol Cell Biol* **20**, 2696-705.
- Rodrigue, A., Lafrance, M., Gauthier, M. C., McDonald, D., Hendzel, M., West, S. C., Jasin, M. and Masson, J. Y.** (2006). Interplay between human DNA repair proteins at a unique double-strand break in vivo. *Embo J* **25**, 222-31.
- Rogakou, E. P., Boon, C., Redon, C. and Bonner, W. M.** (1999). Megabase chromatin domains involved in DNA double-strand breaks in vivo. *J Cell Biol* **146**, 905-16.
- Rouse, J. and Jackson, S. P.** (2002). Interfaces between the detection, signaling, and repair of DNA damage. *Science* **297**, 547-51.
- Stucki, M., Clapperton, J. A., Mohammad, D., Yaffe, M. B., Smerdon, S. J. and Jackson, S. P.** (2005). MDC1 directly binds phosphorylated histone H2AX to regulate cellular responses to DNA double-strand breaks. *Cell* **123**, 1213-26.
- Sugasawa, K., Ng, J. M., Masutani, C., Iwai, S., van der Spek, P. J., Eker, A. P., Hanaoka, F., Bootsma, D. and Hoeijmakers, J. H.** (1998). Xeroderma pigmentosum group C protein complex is the initiator of global genome nucleotide excision repair. *Mol. Cell* **2**, 223-232.

- 
- Sugasawa, K., Okamoto, T., Shimizu, Y., Masutani, C., Iwai, S. and Hanaoka, F.** (2001). A multistep damage recognition mechanism for global genomic nucleotide excision repair. *Genes Dev* **15**, 507-21.
- Tashiro, S., Walter, J., Shinohara, A., Kamada, N. and Cremer, T.** (2000). Rad51 accumulation at sites of DNA damage and in postreplicative chromatin. *J Cell Biol* **150**, 283-91.
- Tirlapur, U. K. and Konig, K.** (2001). Femtosecond near-infrared laser pulse induced strand breaks in mammalian cells. *Cell Mol Biol (Noisy-le-grand)* **47 Online Pub**, OL131-4.
- Turner, P. R. and Denny, W. A.** (1996). The mutagenic properties of DNA minor-groove binding ligands. *Mutat Res* **355**, 141-69.
- van Veelen, L. R., Cervelli, T., van de Rakt, M. W., Theil, A. F., Essers, J. and Kanaar, R.** (2005a). Analysis of ionizing radiation-induced foci of DNA damage repair proteins. *Mutat Res* **574**, 22-33.
- van Veelen, L. R., Essers, J., van de Rakt, M. W., Odijk, H., Pastink, A., Zdzienicka, M. Z., Paulusma, C. C. and Kanaar, R.** (2005b). Ionizing radiation-induced foci formation of mammalian Rad51 and Rad54 depends on the Rad51 paralogs, but not on Rad52. *Mutat Res* **574**, 34-49.
- Volker, M., Moné, M. J., Karmakar, P., Hoffen, A., Schul, W., Vermeulen, W., Hoeijmakers, J. H. J., van Driel, R., Zeeland, A. A. and Mullenders, L. H. F.** (2001). Sequential Assembly of the Nucleotide Excision Repair Factors In Vivo. *Molecular Cell* **8**, 213-224.
- Walter, J., Cremer, T., Miyagawa, K. and Tashiro, S.** (2003). A new system for laser-UVA-microirradiation of living cells. *J Microsc* **209**, 71-5.
- Williams, E. S., Stap, J., Essers, J., Ponnaiya, B., Luijsterburg, M. S., Krawczyk, P. M., Ullrich, R. L., Aten, A., Bailey, S. M.** (2007). DNA double-strand breaks are not sufficient to initiate the recruitment of TRF2. *Nat Gen* in press.
- White, C. M., Heidenreich, O., Nordheim, A. and Beerman, T. A.** (2000). Evaluation of the effectiveness of DNA-binding drugs to inhibit transcription using the c-fos serum response element as a target. *Biochemistry* **39**, 12262-73.
- You, J. S., Wang, M. and Lee, S. H.** (2003). Biochemical analysis of the damage recognition process in nucleotide excision repair. *J Biol Chem* **278**, 7476-85.
- Zhang, J., Ma, Z., Treszezamsky, A. and Powell, S. N.** (2005). MDC1 interacts with Rad51 and facilitates homologous recombination. *Nat Struct Mol Biol* **12**, 902-9.
- Zotter, A., Luijsterburg, M. S., Warmerdam, D. O., Ibrahim, S., Nigg, A., van Cappellen, W. A., Hoeijmakers, J. H., van Driel, R., Vermeulen, W. and Houtsmuller, A. B.** (2006). Recruitment of the nucleotide excision repair endonuclease XPG to sites of UV-induced dna damage depends on functional TFIIH. *Mol Cell Biol* **26**, 8868-79.
-





## Chapter 5

# Accelerated Exchange of H2A and H2B at Sites of DNA Damage Depends on Histone Chaperone FACT

Christoffel Dinant, Jurgen Marteijn, Hiroshi Kimura, Wim  
Vermeulen and Adriaan B. Houtsmuller

## **ABSTRACT**

Chromatin is the natural substrate of all DNA-associated processes in eukaryotes. The basic repeating unit, the nucleosome, forms a barrier for DNA interacting proteins, such as transcription or DNA repair factors. Different mechanisms of chromatin remodeling, including facilitated histone exchange by histone chaperones, such as FACT and NAP1L1, is required for efficient transcription. However, chromatin remodeling by DNA repair processes is less well characterized. Here we show accelerated exchange of H2A and H2B upon UV-induced DNA damage and provide evidence that the histone chaperone FACT, but not NAP1L1 is required for this. UV-induced DNA lesions are mainly repaired by nucleotide excision repair (NER). However, accelerated histone exchange by FACT is independent of this repair process, suggesting that it plays an early role in the UV-induced damage response such as promoting increased chromatin accessibility for NER factors.

## **INTRODUCTION**

Cells are continuously exposed to endogenous metabolites and environmental agents that induce lesions in DNA. DNA lesions interfere with vital DNA transacting process, such as transcription and replication, resulting in cellular malfunction and damage-induced mutagenesis of genetic information. To counteract the severe consequences of DNA damage, different DNA repair systems have evolved, which collectively remove the vast majority of genomic injuries. One such system is the versatile nucleotide excision repair (NER) process, which removes helix-destabilizing lesions such as the UV-C induced cyclobutane pyrimidine dimers (CPD) and 6-4 photoproducts (6-4PP). Repair by NER is achieved by damage recognition, local unwinding of the helix and incisions 5' and 3' of the lesion in order to remove a short single strand DNA patch containing the damage. The resulting gap is filled by repair synthesis and sealed by ligation (Hoeijmakers 2001; Gillet and Scharer 2006). Two damage detection mechanisms are known that activate NER. Lesions located in the transcribed strand of active genes obstruct RNA polymerase II elongation, which activates the process of transcription coupled NER (TC-NER), whereas lesions located anywhere else in the genome are recognized by the concerted action of the XPC and DDB2 complexes that initiate global genome repair (GG-NER) (Mellon et al. 1987; Sugawara et al. 1998; Tang et al. 2000; van den Boom et al. 2002; Hanawalt et al. 2003; Foustari and Mullenders 2008). Aside from the recognition step, TC-NER and GG-NER share the same downstream pathway, which involves unwinding of the DNA double helix by the transcription factor TFIIH, damage verification and complex assembly by RPA and XPA and dual incision by the structure-specific endonucleases XPF-ERCC1 and XPG (de Laat et al. 1999; Friedberg 2001; Hoeijmakers 2001; Park and Choi 2006). DNA resynthesis and ligation is performed by the replication machinery and DNA ligases I and III (Moser et al. 2007).

---

The natural substrate for DNA repair is chromatin, which is organized in arrays of nucleosomes. Nucleosomes consist of two copies of each core histone protein, H2A, H2B, H3 and H4, forming an octamer, that has approximately 146 bp of DNA wrapped around it. Wrapping of DNA around nucleosomes serves as a compaction mechanism and as a way to regulate activity of the genome. Chromatin-associated processes such as transcription and replication are controlled by several mechanisms that influence the compaction of chromatin and promote accessibility of transcription or replication factors. These mechanisms include active ATP-driven chromatin remodeling (Gangaraju and Bartholomew 2007), post-translational histone modifications (Kouzarides 2007) and a group of specialized proteins the histone chaperones (e.g.CAF-1, FACT and NAP1L1) that both catalyze histone deposition to and eviction from nucleosomes (Tyler 2002). Histone chaperone CAF-1 (for Chromatin assembly factor 1) incorporates H3.1 and H4 into chromatin during replication (Polo and Almouzni 2006) and was recently found to deposit H3.1 during NER (Polo et al. 2006). This histone exchange is dependent on active NER indicating that it probably occurs after repair as a chromatin restoration step. Another chaperone, FACT (for FACilitates Chromatin Transcription) is a heterodimer of SSRP1 and hSpt16 and functions in transcription elongation by removing one of the two H2A/H2B dimers from

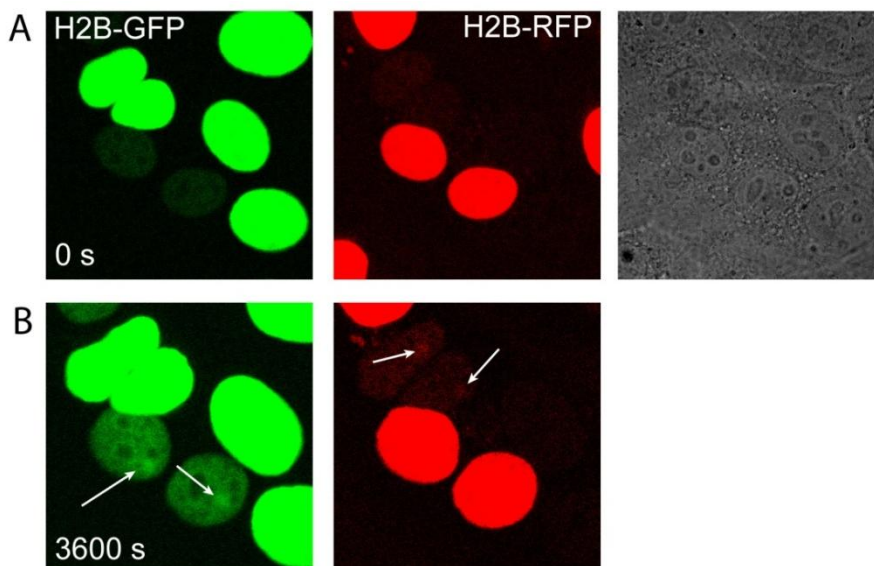


**Fig 1.** Accelerated exchange of H2B-GFP and H2B-RFP at sites of local damage. (A) HeLa cells expressing H2B-GFP (green) and HeLa cells expressing H2B-RFP (red) 30 min after PEG fusion. The right panel shows the widefield image. Images taken immediately after local UV-C laser irradiation. (B) The same fused HeLa cells as in (A), 3600 s after local UV-C laser irradiation. Arrows indicate the location of DNA damage.

nucleosomes (Kireeva et al. 2002; Belotserkovskaya et al. 2003; Reinberg and Sims 2006). FACT is also implicated in DNA repair by binding cisplatin-damaged DNA through SSRP1 and enabling eviction of phosphorylated H2AX from nucleosomes (Bruhn et al. 1992; Yarnell et al. 2001; Heo et al. 2008). NAP1L1 (for nucleosomes assembly protein 1-like 1) also has a function in facilitating transcription by removal of H2A/H2B dimers (Park et al. 2005). Besides removal of histones from nucleosomes, both NAP1L1 and FACT are capable of incorporating H2A/H2B dimers in nucleosomes and unlike CAF-1 they act independently of replication (Mello et al. 2002; Belotserkovskaya et al. 2003; Park et al. 2005).

Here we show that H2A and H2B display accelerated exchange at damaged DNA. However, differently from H3.1 incorporation at DNA damage, this increased exchange of H2A and H2B is independent of active NER. FACT, and not NAP1L1, is required for this accelerated exchange. These results identify FACT as a novel factor involved in the DNA damage response and suggest that remodeling of UV-damaged chromatin does not require components of the repair machinery.

## RESULTS

### Experimental setup

Core histones are stably bound to chromatin in mammalian cells and display only limited exchange between the bound and freely diffusing form. In order to study the mobility of histones upon DNA damage induction, we employed two different methods aimed at measuring differences in histone exchange rates. 1) Cells were fused using polyethyleneglycol (PEG) 1500 (50%). Fusing a cell that expresses fluorescently labeled histones (GFP-tagged) with a cell that does not express this fluorescent histone will result in incorporation of fluorescent histones in the non-fluorescent nucleus, predominantly derived from newly synthesized fluorescent histones. During the incorporation of fluorescent histones in the initially non-fluorescent nucleus, a relative fast histone exchange in specific sub-nuclear will be monitored by a faster accumulation of fluorescent signal in these areas as compared to chromatin in which histone exchange is slower. High resolution quantitative time-lapse confocal imaging of nuclei of fused cells allows measuring the incorporation rate of the histones under surveillance. 2) We used a high-intensity laser to photobleach the fluorescence in half of a nucleus expressing fluorescent histones. Similar to the fusion method, the recovery of fluorescence in the bleached half of the nucleus is faster in chromatin with faster histone exchange.

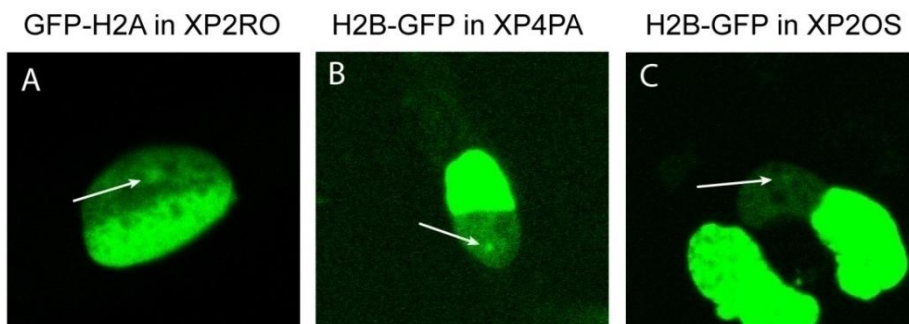


**Fig 2.** Accelerated exchange of H2B and H2A in human fibroblast deficient for NER. (A) XP2OS cells (deficient for XPA) were fused with XP2OS cells expressing H2B-GFP and locally irradiated with UV-C (arrow). 60 min after irradiation an accumulation of H2B-GFP is seen at the irradiated area, indicating faster H2B exchange than in the rest of nucleus. (B) XP4PA cells (deficient for XPC) expressing H2B-GFP were locally irradiated with UV-C (arrow) and GFP was photobleached in half of the nucleus. After 60 min a higher concentration of H2B-GFP is seen at the site of irradiation than in the rest of the photobleached area, indicating accelerated exchange. (C) XP2RO cells (deficient for DDB2) expressing GFP-H2A were locally irradiated with UV-C (arrow) and GFP was photobleached in half of the nucleus. After 60 min a higher concentration of GFP-H2A is seen at the site of irradiation than in the rest of the photobleached area, indicating accelerated exchange.

### H2A and H2B exchange at local damage

To study chromatin remodeling in response to DNA damage we used HeLa cells stably expressing either H2B-GFP or GFP-H2A. Irradiation of these cells with a UV-C laser (Dinant et al. 2007), inducing damage in a small area within the nucleus, does not affect the nuclear H2B-GFP distribution (data not shown). This indicates that there is no change in the amount of H2B and H2A at sites of damaged DNA. In order to study whether the mobility of histones changes when DNA damages has been induced, we used PEG 1500 to fuse cells expressing H2B-GFP with cells expressing H2B-RFP. In the nuclei that initially contained H2B-GFP, the fluorescence intensity of newly incorporated H2B-RFP was higher in the damaged area than the surrounding nucleus. Inversely, in nuclei initially containing H2B-RFP, we observed faster incorporation of H2B-GFP. Core histones are stably bound to chromatin in mammalian cells and display only limited exchange between the bound and freely diffusing form (Fig 1A,B). Accelerated exchange was also found for GFP-H2A (data not shown) This indicates that the mobility of H2B and H2A is increased in chromatin containing damaged DNA compared to non-damaged chromatin, similar to what has been shown for H3.1 (Polo et al. 2006).

### H2B and H2A exchange in NER mutants

Accelerated exchange of H3.1 at damaged areas was shown to occur in a NER-dependent fashion and was suggested to be required for the post-repair re-assembly of histones (Polo et al. 2006). To investigate whether the

accelerated exchange we found for H2B and H2A also occurs during or as a consequence of DNA repair, we used human fibroblast cell-lines that are deficient in repairing UV-induced lesions, i.e. NER-deficient. To that aim we use cells derived from xeroderma pigmentosum (XP) and Cockayne syndrome (CS) patients, which harbor inherited mutations in of the NER genes. In two independent XP-A cells (mutated in XPA, derived from patients XP2OS and XP12RO, respectively) we observed a similar accelerated H2B-GFP exchange at damaged spots as in NER-proficient control cells (Fig. 2A and data not shown). This suggests that the increased H2B exchange at damaged DNA is independent of active NER. It is conceivable however that this accelerated H2B eviction and deposition is dependent on an earlier NER step, preceding the incorporation of XPA into the NER complex, i.e. recognition of lesions. In cells deficient in the GG-NER recognition proteins XPC (XP4PA) or DDB2 (XP2RO) histone H2B showed a

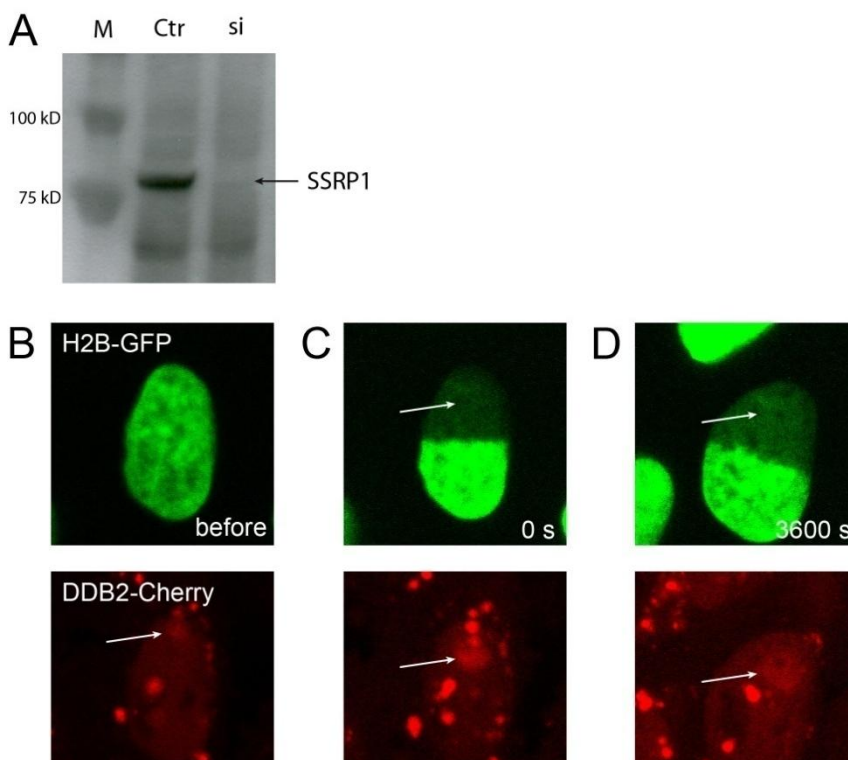


**Fig 3.** Knockdown of FACT by siRNA abolishes accelerated exchange of H2B at areas of DNA damage. (A) SSRP1 expression levels in cells transfected with non-targeting control siRNA (middle lane, Ctr) or siRNA directed against SSRP1 and hSPT16 (right lane, si). (B) A HeLa cell stably expressing H2B-GFP (green) transfected with Cherry-DDB2 (red) and siRNA against SSRP1 and hSPT16 was locally irradiated with UV-C (arrow). Cherry-DDB2 is used as a marker for the location of the DNA damage. (C) Just after photobleaching GFP in half of the nucleus of the same cell as in (B). (D) 3600 s after photobleaching. No accelerated exchange of H2B-GFP is detected at the site of damage.

faster exchange rate in damaged chromatin than in undamaged, similar to wild-type cells (Fig. 2B,C) indicating that increased histone exchange at sites of DNA damage is not a consequence of global damage repair initiated by XPC. Damage detection in the transcription coupled repair pathway does not require XPC. Therefore we also tested TC-NER deficient CSB (CS1AN) cells. Also in these cells exchange of H2B-GFP at damaged areas was not altered (data not shown) indicating that TC-NER is not required for this process either.

### Increased H2A and H2B exchange depends on FACT

FACT is a histone chaperone that facilitates transcription by removal of one H2B/H2A dimer from nucleosomes (Reinberg and Sims 2006). It was recently shown that FACT can promote exchange of histone variant H2AX *in vitro* and that this activity was augmented by activity of the double strand break repair protein DNA-PKcs (Heo et al. 2008). To determine whether FACT also has a function in H2A/H2B exchange in response to UV-induced DNA damage, we used siRNA against both subunits of FACT, SSRP1 and hSPT16. Knockdown of SSRP1 and hSPT16 in HeLa cells expressing H2B-GFP was very efficient (Fig 3A and data not shown). In cells expressing siRNA against FACT we observed a significant decrease in exchange of H2A and H2B at damaged areas compared to cells transfected with non-targeting siRNA (Fig 3B-D). This indicates that FACT is required for increased exchange rate of H2A and H2B upon DNA damage induction.

NAP1L1 is the human counterpart of nucleosome assembly protein 1 in yeast. It is a histone chaperone that has been shown to stimulate both nucleosome assembly and nucleosome disruption (Park and Luger 2006). We used siRNA to transiently knock-down NAP1L1 expression in HeLa cells expressing GFP-H2A (Fig 4A). Knock-down of

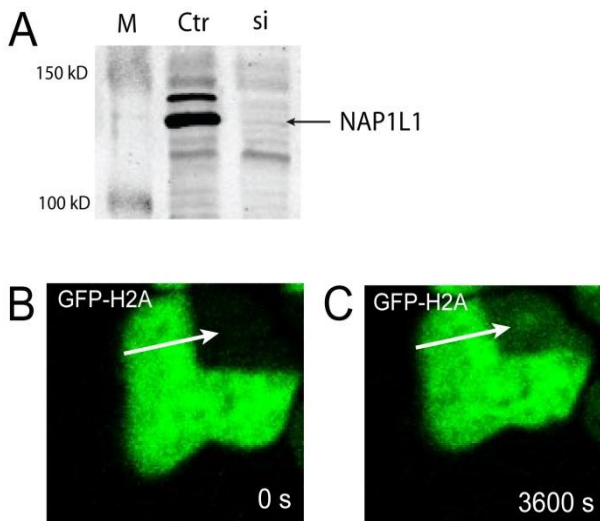


**Fig 4.** Knockdown of NAP1L1 does not influence the exchange of H2B-GFP at areas of DNA damage. (A) NAP1L1 expression levels in cells transfected with non-targeting control siRNA (middle lane, Ctr) or siRNA directed against NAP1L1 (right lane, si). (B) A HeLa cell stably expressing GFP-H2A transfected with siRNA against NAP1L1 was locally irradiated with UV-C followed by photobleaching part of the nucleus containing the damaged area. (C) 3600 s after local DNA damage induction accelerated exchange of GFP-H2A is found at the damaged area.

NAP1L1 had no effect on the rate of exchange of H2A at sites of DNA damage (Fig 4B, C), indicating that in contrast to FACT, NAP1L1 has no function in histone exchange during the response to UV-induced DNA damage.

## DISCUSSION

Here we show an increased exchange rate of core histones H2A and H2B in chromatin containing UV-induced DNA damage. Previously, accelerated exchange of H3.1 was shown in response to DNA damage (Polo et al. 2006). However, there is a considerable mechanistical difference between the H2A/H2B exchange that we describe here and the increased previously described H3.1 exchange. Whereas accelerated H3.1 exchange occurs only in NER proficient cells, increased H2A/H2B exchange at UV-damaged areas is also observed in NER deficient cells.

A model that has been proposed to describe DNA repair in chromatin *in vivo* suggests a three-step repair mechanism: access, repair and restore (Smerdon 1991). Chromatin has to be remodeled to allow access of repair factors, which remove the lesions, and after repair, chromatin structure needs to be restored.

Exchange of H3.1 at damaged areas was suggested to reflect the 'restoration' step in this model, occurring after repair has taken place (Polo et al. 2006). The independency of H2A/H2B exchange on repair suggests that it might reflect the opening of chromatin around DNA lesions by remodeling factors such as FACT, during the 'access' step in this model. The previously described ability of the FACT subunit SSRP1, which we identified to be required for accelerated H2A/H2B exchange, to bind directly to cisplatin-adducts on DNA (Bruhn et al. 1992; Yarnell et al. 2001) further corroborates a possible function of FACT in early damage recognition by initiating the opening-up of damaged chromatin. It is surprising to note that enhanced histone exchange on damaged DNA took relatively long (~ 30 minutes post UV-irradiation) to become microscopically visible. This is for example much slower than the visible early assembly of GG-NER initiation proteins DDB2 (Luijsterburg et al. 2007) and XPC (Hoogstraten et al. 2008). The virtual slow histone exchange as compared to NER factor assembly does not necessarily imply that it occurs at a later step. Rather, it indicates that the mobility of H2B and H2A is only slightly increased at areas of DNA damage and that it takes longer periods of persisting damage to visualize the exchange by microscopy.

Besides binding cisplatin adducts, FACT has been associated with DNA damage through other mechanisms as well. For example, UV irradiation induces the interaction between FACT and CK2 (Keller et al. 2001). CK2 is a serine/threonine kinase that phosphorylates a number of DNA damage response proteins, including p53 (Keller et al. 2001), XRCC1 (Loizou et al. 2004) and HP1 (Ayoub et al. 2008). The interaction of CK2 with FACT alters CK2 such that it selectively phosphorylates p53 (serine 392) over other

---



substrates (Keller et al. 2001; Keller and Lu 2002). Phosphorylation of p53 at serine 392 by CK2 occurs only in response to UV irradiation, and not after treatment with other DNA damage sources such as gamma irradiation. In addition, the FACT subunit SSRP1 is also phosphorylated by CK2 upon UV (and not by gamma irradiation) (Li et al. 2005). It is attractive to speculate that FACT directly interacts with UV-induced DNA damage, resulting in enhanced NER by accelerated histone exchange, and phosphorylation of checkpoint protein p53 by CK2, which induces cell-cycle checkpoint activation or apoptosis.

During transcription, FACT is responsible for the removal of one H2A/H2B dimer from chromatin (Kireeva et al. 2002; Belotserkovskaya et al. 2003; Reinberg and Sims 2006). H3 and H4 on the other hand, appear to remain in place during transcription, only being replaced in S-phase, or after NER (Polo et al. 2006). This is reflected in the higher mobility of H2A/H2B than H3/H4 as measured by FRAP in non-challenged cells (Kimura and Cook 2001). Apparently, dissociation of H2A/H2B is sufficient to allow access of transcription factors to DNA. Similarly, our data suggests that, like during transcription, H2A/H2B exchange upon DNA damage induction might help repair factors to access the DNA, while H3/H4 dimers are only exchanged during the DNA synthesis step of NER. The more stable association of H3/H4 dimers with DNA might also be a reason why there appear much more epigenetic markers on these histones than on H2A and H2B (Kouzarides 2007). This ensures the integrity of the epigenetic code also after RNA polymerases have transcribed the DNA. The exchange of H3.1 during repair synthesis indicates that there must be another mechanism that restores epigenetic information after DNA repair has taken place.

## **MATERIAL & METHODS**

### **Cell lines and constructs**

HeLa cells were cultured under standard conditions in DMEM/F10 medium supplemented with 10% fetal calf serum and antibiotics at 37°C and 5% CO<sub>2</sub>. The H2B-GFP expressing cells have been previously published (Kimura and Cook 2001). GFP-H2A was a kind gift from dr. M. Luijsterburg and Cherry-DDB2 was a kind gift from dr. S. Alekseev. H2B-RFP was stably expressed in HeLa cells.

Cells were fused with 50% polyethyleneglycol 1500 for 1.5 min (see (Schmidt-Zachmann et al. 1993). cDNA constructs were transfected with FuGENE HD (Roche Applied Science).

### **siRNA**

Small interfering RNAs (smartpool) against SSRP1, SPT16 and NAP1L1 were supplied by Dharmacon. Lipofectamine 2000 (Invitrogen) was used to transfect siRNAs.

### **Microscopy**

A 2 mW pulsed (7.8 kHz) diode pumped solid state laser emitting at 266 nm (Rapp OptoElectronic, Hamburg GmbH) was connected to a Zeiss LSM 510 confocal microscope with an axiovert 200 M housing adapted for UV by all-quartz optics. A special adaptor (ZSI-A200, Rapp OptoElectronic) to fit in the aperture slider position of an axiovert 200 microscope was developed by Rapp OptoElectronic to focus the laser on a sample. For local UV-C irradiation experiments cells were grown on 25 or 24 mm diameter quartz coverslips (SPI supplies, USA, or Atoptical, China, respectively). Cells were imaged and irradiated through a 100x 1.2 NA

---

Ultrafluar quartz objective. GFP was excited and photobleached with the 488 nm line of a 30 mW argon laser and mRFP and mCherry were excited with a 1 mW 543 nm HeNe laser.

### ACKNOWLEDGEMENTS

The authors would like to thank Dr. Luijsterburg for constructs and critical reading of the manuscript. This work was supported by the Netherlands Organization for Scientific Research (NWO): ZonMW 912-03-012 (CD), 917-46-371 (ABH), 917-46-364 (WV) and 901-01-229, ESF 855-01-072 and EU LSHG-CT-2005-512113 (JM).

### REFERENCES

- Ayoub, N., Jeyasekharan, A.D., Bernal, J.A., and Venkitaraman, A.R. 2008. HP1-beta mobilization promotes chromatin changes that initiate the DNA damage response. *Nature*.
- Belotserkovskaya, R., Oh, S., Bondarenko, V.A., Orphanides, G., Studitsky, V.M., and Reinberg, D. 2003. FACT facilitates transcription-dependent nucleosome alteration. *Science* **301**(5636): 1090-1093.
- Bruhn, S.L., Pil, P.M., Essigmann, J.M., Housman, D.E., and Lippard, S.J. 1992. Isolation and characterization of human cDNA clones encoding a high mobility group box protein that recognizes structural distortions to DNA caused by binding of the anticancer agent cisplatin. *Proc Natl Acad Sci U S A* **89**(6): 2307-2311.
- de Laat, W.L., Jaspers, N.G., and Hoeijmakers, J.H. 1999. Molecular mechanism of nucleotide excision repair. *Genes Dev* **13**(7): 768-785.
- Dinant, C., de Jager, M., Essers, J., van Cappellen, W.A., Kanaar, R., Houtsmuller, A.B., and Vermeulen, W. 2007. Activation of multiple DNA repair pathways by sub-nuclear damage induction methods. *J Cell Sci* **120**(Pt 15): 2731-2740.
- Fousteri, M. and Mullenders, L.H. 2008. Transcription-coupled nucleotide excision repair in mammalian cells: molecular mechanisms and biological effects. *Cell Res* **18**(1): 73-84.
- Friedberg, E.C. 2001. How nucleotide excision repair protects against cancer. *Nat Rev Cancer* **1**(1): 22-33.
- Gangaraju, V.K. and Bartholomew, B. 2007. Mechanisms of ATP dependent chromatin remodeling. *Mutat Res* **618**(1-2): 3-17.
- Gillet, L.C. and Scharer, O.D. 2006. Molecular mechanisms of mammalian global genome nucleotide excision repair. *Chemical reviews* **106**(2): 253-276.
- Hanawalt, P.C., Ford, J.M., and Lloyd, D.R. 2003. Functional characterization of global genomic DNA repair and its implications for cancer. *Mutat Res* **544**(2-3): 107-114.
- Heo, K., Kim, H., Choi, S.H., Choi, J., Kim, K., Gu, J., Lieber, M.R., Yang, A.S., and An, W. 2008. FACT-mediated exchange of histone variant H2AX regulated by phosphorylation of H2AX and ADP-ribosylation of Spt16. *Mol Cell* **30**(1): 86-97.
- Hoeijmakers, J.H. 2001. Genome maintenance mechanisms for preventing cancer. *Nature* **411**(6835): 366-374.
- Hoogstraten, D., Bergink, S., Verbiest, V.H., Luijsterburg, M.S., Geverts, B., Raams, A., Dinant, C., Hoeijmakers, J.H., Vermeulen, W., and Houtsmuller, A.B. 2008. Versatile DNA damage detection by the global genome nucleotide excision repair protein XPC. *J Cell Sci*.
- Keller, D.M. and Lu, H. 2002. p53 serine 392 phosphorylation increases after UV through induction of the assembly of the CK2.hSPT16.SSRP1 complex. *J Biol Chem* **277**(51): 50206-50213.
- Keller, D.M., Zeng, X., Wang, Y., Zhang, Q.H., Kapoor, M., Shu, H., Goodman, R., Lozano, G., Zhao, Y., and Lu, H. 2001. A DNA damage-induced p53 serine 392 kinase complex contains CK2, hSpt16, and SSRP1. *Mol Cell* **7**(2): 283-292.
- Kimura, H. and Cook, P.R. 2001. Kinetics of core histones in living human cells: little exchange of H3 and H4 and some rapid exchange of H2B. *J Cell Biol* **153**(7): 1341-1353.
- Kireeva, M.L., Walter, W., Tchernajenko, V., Bondarenko, V., Kashlev, M., and Studitsky, V.M. 2002. Nucleosome remodeling induced by RNA polymerase II: loss of the H2A/H2B dimer during transcription. *Mol Cell* **9**(3): 541-552.
- Kouzarides, T. 2007. Chromatin modifications and their function. *Cell* **128**(4): 693-705.
- Li, Y., Keller, D.M., Scott, J.D., and Lu, H. 2005. CK2 phosphorylates SSRP1 and inhibits its DNA-binding activity. *J Biol Chem* **280**(12): 11869-11875.
-

- 
- Loizou, J.I., El-Khamisy, S.F., Zlatanou, A., Moore, D.J., Chan, D.W., Qin, J., Sarno, S., Meggio, F., Pinna, L.A., and Caldecott, K.W. 2004. The protein kinase CK2 facilitates repair of chromosomal DNA single-strand breaks. *Cell* **117**(1): 17-28.
- Luijsterburg, M.S., Goedhart, J., Moser, J., Kool, H., Geverts, B., Houtsmuller, A.B., Mullenders, L.H., Vermeulen, W., and van Driel, R. 2007. Dynamic in vivo interaction of DDB2 E3 ubiquitin ligase with UV-damaged DNA is independent of damage-recognition protein XPC. *J Cell Sci* **120**(Pt 15): 2706-2716.
- Mello, J.A., Sillje, H.H., Roche, D.M., Kirschner, D.B., Nigg, E.A., and Almouzni, G. 2002. Human Asf1 and CAF-1 interact and synergize in a repair-coupled nucleosome assembly pathway. *EMBO Rep* **3**(4): 329-334.
- Mellon, I., Spivak, G., and Hanawalt, P.C. 1987. Selective removal of transcription-blocking DNA damage from the transcribed strand of the mammalian DHFR gene. *Cell* **51**(2): 241-249.
- Moser, J., Kool, H., Giakzidis, I., Caldecott, K., Mullenders, L.H., and Foustari, M.I. 2007. Sealing of chromosomal DNA nicks during nucleotide excision repair requires XRCC1 and DNA ligase III alpha in a cell-cycle-specific manner. *Mol Cell* **27**(2): 311-323.
- Park, C.J. and Choi, B.S. 2006. The protein shuffle. Sequential interactions among components of the human nucleotide excision repair pathway. *Febs J* **273**(8): 1600-1608.
- Park, Y.J., Chodaparambil, J.V., Bao, Y., McBryant, S.J., and Luger, K. 2005. Nucleosome assembly protein 1 exchanges histone H2A-H2B dimers and assists nucleosome sliding. *J Biol Chem* **280**(3): 1817-1825.
- Park, Y.J. and Luger, K. 2006. Structure and function of nucleosome assembly proteins. *Biochem Cell Biol* **84**(4): 549-558.
- Polo, S.E. and Almouzni, G. 2006. Chromatin assembly: a basic recipe with various flavours. *Curr Opin Genet Dev* **16**(2): 104-111.
- Polo, S.E., Roche, D., and Almouzni, G. 2006. New histone incorporation marks sites of UV repair in human cells. *Cell* **127**(3): 481-493.
- Reinberg, D. and Sims, R.J., 3rd. 2006. de FACTo nucleosome dynamics. *J Biol Chem* **281**(33): 23297-23301.
- Schmidt-Zachmann, M.S., Dargemont, C., Kuhn, L.C., and Nigg, E.A. 1993. Nuclear export of proteins: the role of nuclear retention. *Cell* **74**(3): 493-504.
- Smerdon, M.J. 1991. DNA repair and the role of chromatin structure. *Curr Opin Cell Biol* **3**(3): 422-428.
- Sugasawa, K., Ng, J.M., Masutani, C., Iwai, S., van der Spek, P.J., Eker, A.P., Hanaoka, F., Bootsma, D., and Hoeijmakers, J.H. 1998. Xeroderma pigmentosum group C protein complex is the initiator of global genome nucleotide excision repair. *Mol Cell* **2**(2): 223-232.
- Tang, J.Y., Hwang, B.J., Ford, J.M., Hanawalt, P.C., and Chu, G. 2000. Xeroderma pigmentosum p48 gene enhances global genomic repair and suppresses UV-induced mutagenesis. *Mol Cell* **5**(4): 737-744.
- Tyler, J.K. 2002. Chromatin assembly. Cooperation between histone chaperones and ATP-dependent nucleosome remodeling machines. *Eur J Biochem* **269**(9): 2268-2274.
- van den Boom, V., Jaspers, N.G., and Vermeulen, W. 2002. When machines get stuck--obstructed RNA polymerase II: displacement, degradation or suicide. *Bioessays* **24**(9): 780-784.
- Yarnell, A.T., Oh, S., Reinberg, D., and Lippard, S.J. 2001. Interaction of FACT, SSRP1, and the high mobility group (HMG) domain of SSRP1 with DNA damaged by the anticancer drug cisplatin. *J Biol Chem* **276**(28): 25736-25741.
-



## Chapter 6

# Heterochromatin Protein 1 is Involved in the DNA Damage Response

Christoffel Dinant, Martijn S. Luijsterburg, Elżbieta  
Wiernasz, Hannes Lans, Jan Stap, Maria I. Foustero,  
Daniël O. Warmerdam, Maartje C. Brink, Saskia  
Lagerwerf, Jurek W. Dobrucki, Gert Jansen, Wim  
Vermeulen, Leon H.F. Mullenders, Adriaan B.  
Houtsmuller, Pernette J. Verschure, and Roel van Driel

*Submitted*

### **Abstract**

The mammalian genome is protected against genotoxic stress by DNA damage response (DDR) mechanisms that include DNA repair. Heterochromatin protein 1 (HP1) family members are chromatin-associated proteins involved in transcription and replication. In this study we show that the HP1 isoforms HP1 $\alpha$ , HP1 $\beta$  and HP1 $\gamma$  are recruited to DNA lesions in living human cells. This response to DNA damage strictly requires the chromo shadow domain of the HP1 protein and occurs at sites of double strand breaks and at sites of helix-distorting lesions. Evidence is provided that HP1 is not involved DNA repair itself. We show that several HP1-interacting proteins are also recruited to DNA damage, including chromatin remodelling factors and DNA and histone methyltransferases. Loss of HP1 results in high sensitivity to UV-induced damage in the nematode *C. elegans*, providing evidence for involvement of HP1 in a DDR mechanism. These results suggest a novel function of HP1 proteins and reveal a link between maintenance of epigenetic information and DNA damage responses.

### **Introduction**

The genetic component of chromatin (*i.e.* the DNA) can be damaged by various sources including ionizing and ultraviolet (UV) radiation. Cells respond to genotoxic stress by activating interwoven DNA damage response (DDR) systems including DNA repair, cell cycle arrest, repression of transcription, senescence and apoptosis<sup>1-3</sup>. To restore the genetic information after it has been compromised, several sophisticated DNA repair pathways have evolved, each dealing with specific types of lesions<sup>4</sup>. Nucleotide excision repair (NER) removes bulky adducts and UV-induced pyrimidine-pyrimidone (6-4) photoproducts (6-4PPs) and cyclobutane pyrimidine dimers (CPDs) from the genome<sup>5</sup>. NER involves lesion detection by stalled RNA Polymerase II (for transcription-coupled NER or TC-NER) or XPC and DDB2 complexes (for global genome NER or GG-NER) and subsequent unwinding of DNA (TFIIH, RPA, XPA), incision of the damaged strand (XPG and ERCC1-XPF) and DNA resynthesis, which is performed by the DNA replication machinery<sup>4-7</sup>. DNA double strand breaks (DSB) induced by, amongst others, ionizing radiation, are removed by homologous recombination (HR) or non-homologous end-joining (NHEJ). Repair by HR requires a homologous template, which is available during S and G2 phases. Therefore HR is active during these stages of the cell-cycle, whereas NHEJ repairs DSBs mainly in G1<sup>8</sup>.

Chromatin is the substrate for all genome-associated processes in eukaryotes such as replication, transcription and DNA repair. Besides the genetic information, chromatin encodes epigenetic information by means of DNA methylation, incorporation of histone variants and post-translational modifications of histones<sup>9-11</sup>. The maintenance of epigenetic information is crucial to regulate gene expression profiles and maintain cellular identity.

---

How epigenetic information is maintained during DNA repair is currently not understood. A major obstacle for NER in eukaryotic cells is the packaging of damaged DNA into chromatin. In general, chromatin is considered inhibitory to processes associated with DNA and the rate of repair in a chromatin context is about 10% of that on naked DNA<sup>12-14</sup>. To overcome this obstacle, cells employ a number of chromatin modifying activities to create a more permissive environment for repair locally. It has been demonstrated that NER in mono- and di-nucleosomes is considerably enhanced by ATP-dependent remodelling factors like SWI/SNF and ACF1 (containing ISWI)<sup>12,15</sup>, although it is unclear whether these factors also stimulate NER *in vivo*. Several other mechanisms, including histone ubiquitylation<sup>16,17</sup>, histone acetylation<sup>18-20</sup> and small acidic proteins (e.g. GADD45 and ING) that increase the accessibility of nucleosomal DNA, have been suggested to enhance NER in a chromatin environment<sup>21-26</sup>. Following removal of DNA injuries, cells need to restore the original chromatin structure to maintain the epigenetic information, which requires specialized factors<sup>27</sup>. For instance, CAF1 is recruited to NER sites followed by incorporation of histone H3.1, reflecting a chromatin reassembly step after repair<sup>28,29</sup>. Such a model in which chromatin rearrangements precede and follow DNA repair, has been put forward as the access-repair-restore model that has proven very useful for understanding how NER operates on a chromatin template<sup>30,31</sup>. This model is conceptually appealing and predicts that epigenetic regulators are involved in chromatin rearrangements before, during or after DNA repair.

The heterochromatin protein 1 (HP1) isoforms HP1 $\alpha$ , HP1 $\beta$  and HP1 $\gamma$  are versatile epigenetic regulators with functions in chromatin organization, transcription regulation and DNA replication<sup>32,33</sup>. All three HP1 isoforms share a common dimerization motif allowing them to form homo and heterodimers<sup>34</sup>. The versatility of HP1 proteins in various chromatin-interacting processes raises the question whether these proteins are involved in DNA damage response mechanisms. HP1 proteins, amongst others localize to pericentromeric heterochromatin<sup>35,36</sup>. Expression of genes is considerably decreased when HP1 is targeted to them<sup>37,38</sup>. We have previously demonstrated that targeted binding of HP1 triggers formation of heterochromatin<sup>39</sup>. However, depletion of chromatin-bound HP1 did not result in loss of heterochromatin, suggesting that HP1 is not involved in heterochromatin maintenance<sup>35</sup>. Although previous studies have led to the idea that HP1 proteins are mainly involved in heterochromatin formation it is becoming increasingly clear that this view needs revision. For instance, analysis of HP1 binding sites along the *Drosophila* genome revealed that HP1 also associates with actively transcribed genes<sup>40</sup>. Moreover, the HP1 $\gamma$  isoform interacts with RNAPII and is mainly found in euchromatin<sup>41,42</sup>. HP1 proteins directly bind to methylated H3 at Lys9 via their N-terminal chromodomain<sup>43</sup>. In addition, HP1 dimers interact with a plethora of nuclear proteins via their C-terminal chromoshadow domains, including Suv(3-9), Suv(4-20), Dnmt1, CAF1 as well as chromatin remodelling proteins ACF1

---

and BRG1<sup>44-48</sup>. This makes HP1 a candidate to serve as a binding platform for the recruitment of epigenetic regulators that re-establish the correct chromatin state after DNA repair.

In this study, we show that the three HP1 proteins are involved in the response to DNA damage. We demonstrate that the HP1 proteins are recruited to several types of DNA injuries, such as UV-lesions and double strand breaks (DSBs) in living human cells. A comprehensive *in vivo* analysis shows that recruitment of HP1 to UV-induced lesions critically depends on the CSD and is independent of the binding and activity of pre-precision NER proteins. Moreover, we demonstrate that loss of HP1 renders the nematode *C. elegans* highly sensitive to UV irradiation, providing evidence for an essential role of HP1 in the DNA damage response.

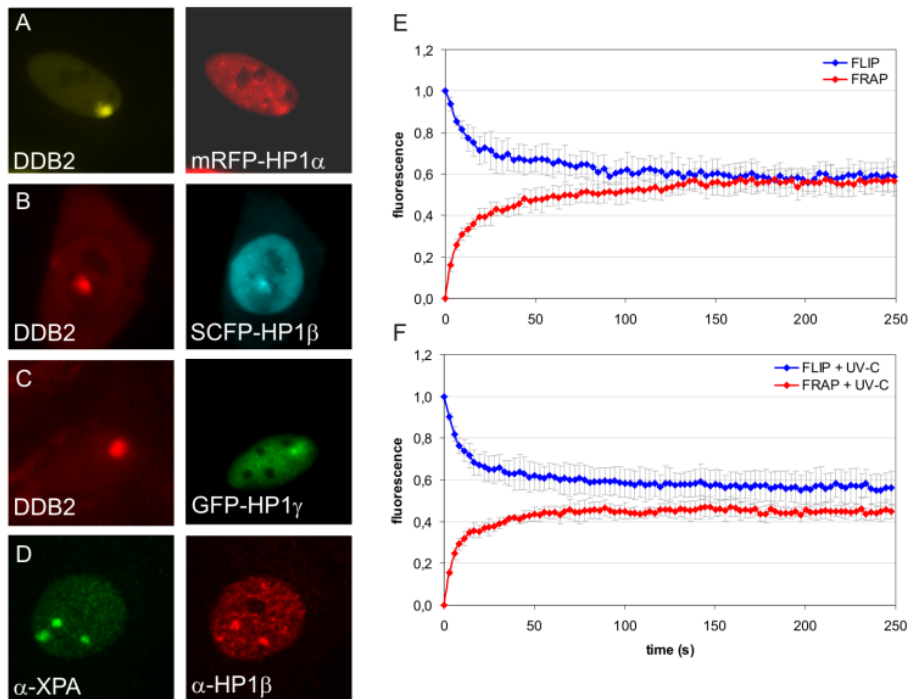


**Fig 1.** Recruitment of HP1s to UV-damage. (A) Nuclear localization of mRFP-HP1 $\alpha$ , (B) SCFP3a-HP1 $\beta$  and (C) EGFP-HP1 $\gamma$  in living HeLa cells locally irradiated at 100 J.m<sup>-2</sup> through 5  $\mu$ m pores or irradiated using a UV-C laser. The site of local DNA damage is indicated by accumulation of DDB2-mVenus or DDB2-mCherry (left column in A,B and C). (D) immunolocalisation of endogenous HP1 $\beta$  in locally UV-irradiated confluent normal human fibroblasts through 3  $\mu$ m pores. UV- damaged sites are visualized by local accumulation of XPA. (E) Combined FLIP-FRAP analysis on NIH-3T3 cells expressing EGFP-HP1 $\beta$ . Cells were either mock treated or globally irradiated at 25 J.m<sup>-2</sup> (F). Half of a cell nucleus was bleached and the loss of fluorescence (FLIP) was measured in the non-bleached half (blue line) while the recovery of fluorescence (FRAP) was measured in the bleached half (red line).



---

## Results

### HP1 proteins are recruited to UV-lesions by the chromoshadow domain

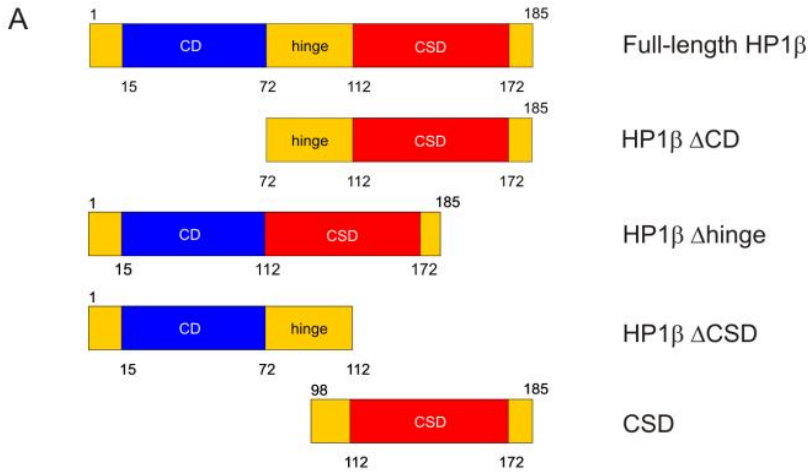
To study if HP1 proteins are recruited to sites of UV-induced DNA damage, we used UV-C light that induces the formation of CPDs and 6-4 PPs. Cell nuclei were locally irradiated with either a UV-C laser (266 nm)<sup>49</sup> or with a UV-C lamp (254 nm) through a polycarbonate mask with pores of 5  $\mu\text{m}$ , resulting in localized DNA damage<sup>50,51</sup>. Both methods trigger recruitment of NER proteins but not of factors involved in other repair pathways, demonstrating that these methods produce bona fide NER-specific lesions. Human HeLa cells and mouse NIH/3T3 were transfected with fluorescent protein-tagged HP1 and mCherry-tagged DDB2 and subsequently irradiated. At irradiated sites that are marked by the accumulation of fluorescent protein-tagged DDB2, we observed recruitment of all three HP1 isoforms (mRFP-HP1 $\alpha$ , SCFP3a-HP1 $\beta$  and EGFP-HP1 $\gamma$ ) in both cell types (Figure 1A-C). In agreement, endogenous HP1 $\beta$  also accumulated after local UV irradiation in primary human fibroblasts (data not shown). To confirm these results, we carried out photobleaching experiments on mouse cells stably expressing EGFP-HP1 $\beta$  that were globally UV-C irradiated at 25  $\text{J}\cdot\text{m}^{-2}$ . Bleaching one half of a cell nucleus ( $n = 5$  cells) and monitoring the equilibration of bleached and non-bleached molecules confirmed that a small fraction of EGFP-HP1 $\beta$  was immobilized in UV-irradiated but not in control cells on a time-scale of several minutes (Figure 1D,E).

HP1 proteins contain three distinct domains: the N-terminal chromo-domain (CD), the C-terminal chromoshadow-domain (CSD) and the hinge region that separates the CD from the CSD. This prompted us to investigate whether a specific HP1 domain is responsible for the recruitment to DNA damage. Different deletion mutants of HP1 $\beta$ , lacking CD, CDS or hinge (Figure 2A), were tagged with EGFP or mCherry and tested for recruitment to UV-irradiated regions. Interestingly, recruitment of mCherry-HP1 $\beta$  ( $\Delta\text{CD}$ ) and EGFP-HP1 $\beta$  ( $\Delta\text{hinge}$ ) following UV irradiation was observed, but EGFP-HP1 $\beta$  ( $\Delta\text{CSD}$ ) failed to accumulate (Figure 2B-D). To test whether the CSD (amino acids 98 – 185 of HP1 $\beta$ ) is sufficient for recruitment, we fused this domain to EYFP and show that CSD-EYFP is indeed recruited to sites of localized UV irradiation (Figure 2E). To verify that the CD is not required for HP1 binding, we examined recruitment of HP1 in MEFs deficient for Suv39h1 and Suv39h2<sup>52,53</sup>. These proteins are methyl-transferases responsible for tri-methylation of H3K9, which is a binding site for HP1 via its CD<sup>54</sup>. Following UV irradiation, SCFP3a-HP1 $\beta$  clearly accumulated at sites of damage, confirming that binding of HP1 does not require the CD (data not shown). These results demonstrate that all three HP1 isoforms are recruited to sites of UV-induced DNA damage and that this recruitment depends on the CSD.

### HP1 recruitment to UV lesions is independent of NER

---

Cells from placental mammals are fully dependent on NER for the removal of UV-induced DNA injuries. Several chromatin-related events are triggered by UV-lesions, such as recruitment of CAF-1 followed by incorporation of histone H3.1 and ubiquitylation of H2A at lysine 119. These events strictly depend on the binding and activity of early binding NER proteins, involved in recognition and stabilising of lesions<sup>28,29,55</sup>. This favours a scenario in which such chromatin rearrangements occur only after repair by NER. To investigate whether HP1 recruitment is a late event following repair we tested accumulation of HP1 $\beta$  in repair-deficient XP-A cells that have



HeLa cells

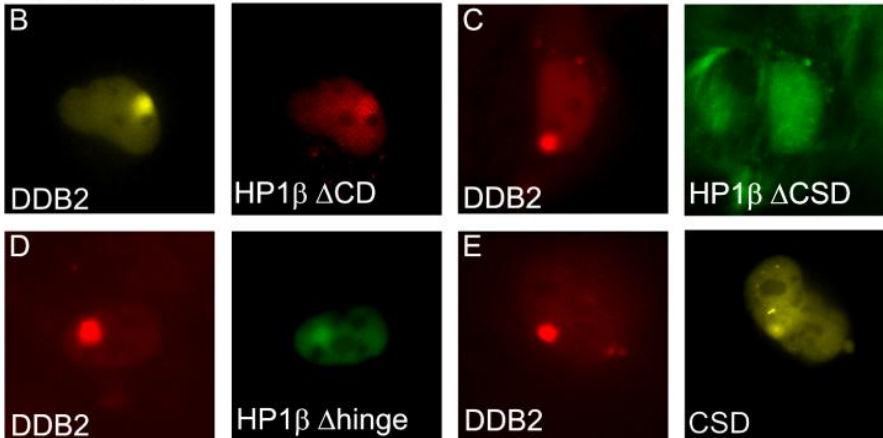


**Fig 2.** HP1 $\beta$  deletion mutants. (A) Representation of DNA constructs encoding fluorescently tagged HP1 $\beta$  deletion mutants. The CD is indicated in red, the CSD in blue and the hinge in yellow. Indicated numbers represent amino acids. (B) Nuclear localization of mCherry-HP1 $\beta$  ( $\Delta$ CD), (C) EGFP-HP1 $\beta$  ( $\Delta$ hinge), (D) EGFP-HP1 $\beta$  ( $\Delta$ CSD) or (E) EYFP-CSD in living HeLa cells locally irradiated at 100 J.m<sup>-2</sup> through 5  $\mu$ m pores or irradiated using a UV-C laser. The site of local DNA damage is indicated by accumulation of DDB2-mVenus or DDB2-mCherry.

compromised GG- and TC-NER. Unexpectedly, SCFP3a-HP1 $\beta$  accumulated in two XPA mutant cell lines upon UV irradiation, showing that its recruitment does not require dual incision (Figure 3A). This shows that HP1 $\beta$  binding is not a late step that occurs after DNA repair is finished. We then considered the possibility that HP1 binding is an early step following damage detection and tested accumulation in DDB2-deficient and XPC-deficient human cells, as well as XPC-inactivated mouse embryonic fibroblasts (MEF), which express very low levels of DDB2. Accumulation of SCFP3a-HP1 $\beta$  was observed in all cell lines, showing that HP1 binding is independent of the activity of GG-NER proteins (Figure 3B-D). Damage detection during TC-NER requires stalled RNAPII and subsequent recruitment of NER factors depends on the coupling-factor CSB<sup>18</sup>. However, recruitment of HP1 was also observed in CSB-deficient cells derived from CS-B patients, indicating that it did not require TC-NER (Figure 3E).

One explanation for recruitment of HP1 to DNA damage in NER deficient cells is that the cells that we monitored were in S-phase. Lesions induced by

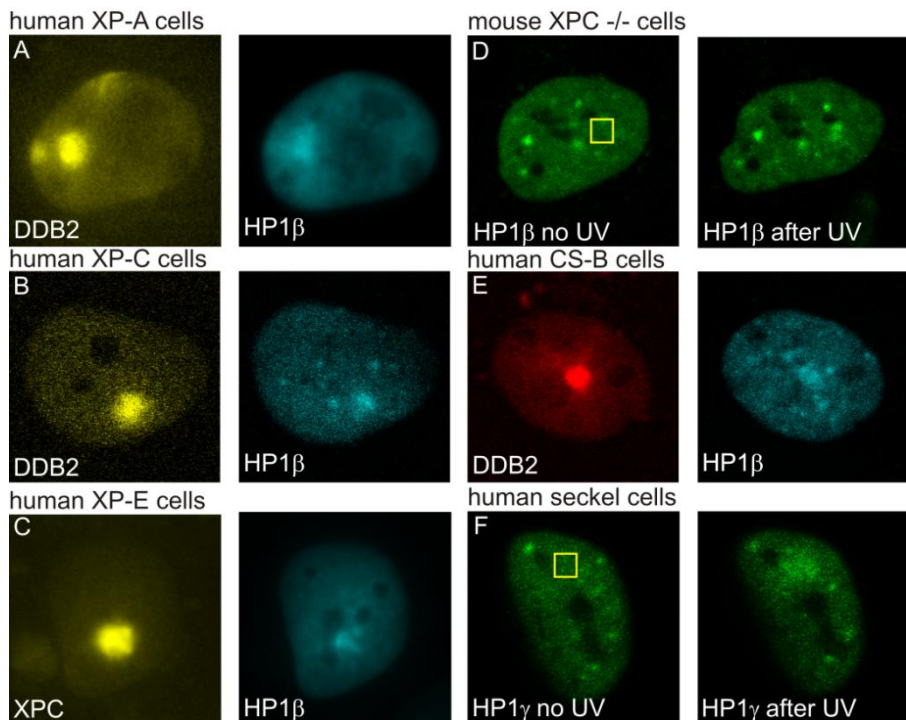


**Fig 3.** Recruitment of HP1 $\beta$  in NER-deficient cells. (A) Nuclear localization of SCFP3a-HP1 $\beta$  or EGFP-HP1 $\beta$  in human fibroblasts deficient for XPA, (B) XPC, (C) DDB2, (D) MEFs deficient for XPC, (E) human fibroblasts deficient for CSB and (F) human seckel cells, which have severely reduced expression of ATR kinase. All cells were locally irradiated at 100 J.m<sup>-2</sup> through 5  $\mu$ m pores or irradiated using a UV-C laser. The site of local DNA damage is indicated by accumulation of DDB2-mVenus, DDB2-mCherry or XPC-mVenus or by a square (in D and F).

UV light can be converted to other types of lesions (e.g. DSBs) during replication, which are removed by other repair pathways than NER. To exclude this possibility, we determined the cell-cycle stage by expressing mCherry-PCNA together with SCFP3a-HP1 $\beta$  and DDB2-mVenus in repair-deficient XP-A cells and wild-type MRC5 cells. Recruitment of HP1 $\beta$  was observed in wild-type and NER-deficient in S-phase as well as non S-phase cells, as shown by the distribution of PCNA (Supplemental figure S1A and -B). To verify these results, we examined the distribution of endogenous HP1 $\beta$  in human cells that do not proliferate (i.e. G0 cells), using Ki67 antigen, as a marker for cell proliferation. Clear accumulation of endogenous HP1 $\beta$  was observed in G0 cells (Ki67 negative cells) at sites of UV irradiation (Supplemental figure S1C), showing that HP1 accumulation is not due to stalled replication. Together, these results show that HP1 binding following UV irradiation occurs in both cycling and quiescent cells and is independent of the activity of pre-incision NER proteins and CSB.

We then investigated whether HP1 accumulates longer on damaged DNA in cells in which UV lesions are not repaired. To test this, accumulation of SCFP3a-HP1 $\beta$  following local UV damage was measured in XPA-deficient cells (XP12RO) for several hours. Accumulation of the fusion protein was still observed ~4 hrs after irradiation (Figure 4A). Conversely, in XPA-deficient cells that were transiently transfected with mVenus-XPA (to restore the repair capacity), bound HP1 $\beta$  levels gradually decreased in time and HP1 accumulation was almost lost 4 hrs following UV irradiation (Figure 4B). Accordingly, accumulation of EYFP-tagged CSD of HP1 $\beta$  in HeLa cells was also lost ~4 hrs after local irradiation (data not shown). These results show that binding of HP1 is mainly triggered by the presence of 6-4PPs because this type of lesion is removed within ~4 hours following repair whereas CPDs are still abundant at this time. To our knowledge, this is the first example of a protein that is recruited to sites of UV-induced DNA damage independent of the known NER factors.

### **HP1 recruitment to UV lesions is independent of ATR**

In addition to DNA repair, cells respond to damaged DNA by activating ATR/ATM kinase signaling pathways resulting in activation of cell cycle checkpoint (e.g. Chk1 and Chk2) and phosphorylation of a plethora of proteins involved in the DDR<sup>1</sup>. UV-induced DNA damage activates ATR, which is required for ubiquitylation of H2A following UV damage<sup>55</sup>. It is currently unclear if ATR activation requires processing of DNA lesion by NER or whether ATR binds directly to damaged DNA<sup>56,57</sup>. Since HP1 recruitment to sites of DNA damage does not require NER, we examined accumulation of HP1 $\alpha$ ,  $\beta$  and  $\gamma$  in Seckel cells, which have severely reduced ATR expression<sup>57</sup>. Accumulation of the HP1 isoforms was not affected in ATR mutant cells following local UV irradiation (Figure 3F). This demonstrates that HP1 recruitment to sites of DNA damage does not require DNA damage-induced signalling mediated by the ATR kinase.

---

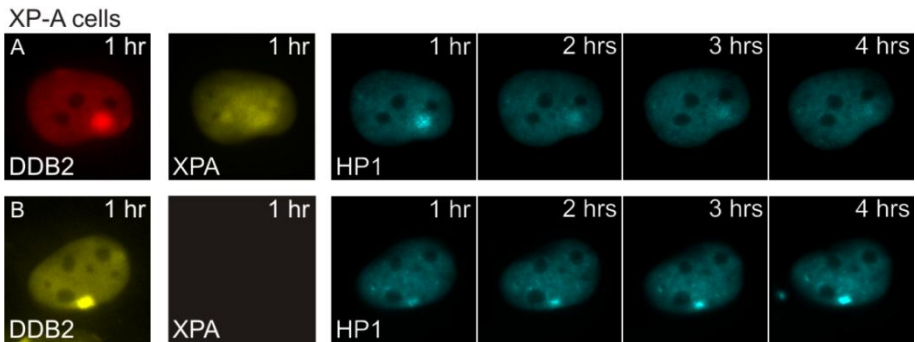


**Fig 4.** Long-term accumulation of HP1 $\beta$  in repair-proficient and repair-deficient cells. (A) XP-A cells were transfected with mVenus-XPA (to complement the repair-deficient phenotype), DDB2-mCherry and SCFP3a-HP1 $\beta$ . Cells were irradiated at 100 J.m<sup>-2</sup> and accumulation of HP1 $\beta$  was monitored for 4 hrs following UV irradiation. (B) XP-A cells were transfected with DDB2-mVenus and SCFP3a-HP1 $\beta$ . Cells were irradiated at 100 J.m<sup>-2</sup> and accumulation of HP1 $\beta$  was monitored for 4 hrs following UV irradiation. The accumulation of DDB2-mVenus or DDB2-mCherry indicates the site of local damage. Accumulation of mVenus-XPA is observed at the site of DNA damage and in nucleoli.

### HP1 is recruited to double-stranded breaks

To investigate whether the recruitment of HP1 is restricted to UV-induced DNA damage or if it is a more general response to different types of lesions, we tested HP1 recruitment upon producing double strand DNA breaks (DSBs). Cells were irradiated with  $\alpha$ -particles from a radioactive Americium (Am-241) source thereby producing linear tracks of DSBs in cell nuclei<sup>58-60</sup>. Human U2OS and mouse NIH/3T3 cells were irradiated with  $\alpha$ -particles and clear linear tracks of  $\gamma$ H2A.X were observed by immunolabelling. Accumulation of EGFP-HP1 $\beta$  in mouse cells and endogenous HP1 $\beta$  in human U2OS cells co-localized with the linear  $\gamma$ H2A.X pattern. (Figure 5A,B). In addition, accumulation of GFP-HP1 $\alpha$  and GFP-HP1 $\gamma$  was observed in MRC5 cells upon  $\alpha$ -particle irradiation, showing that all HP1 isoforms are recruited to DSBs (Figure 5; data not shown). Strikingly, complete co-localization of HP1 $\beta$  and  $\gamma$ H2A.X was observed near DSBs (Figure 5), which is different from the observed localization of many DSB repair proteins (e.g. Rad51 or DNA-PK) that are usually found only in a small area within larger  $\gamma$ H2A.X domains<sup>59,61</sup>. This suggests that HP1 associates with a chromatin area larger than the damaged DNA region. Mammalian cells utilize homologous recombination (HR; which is only operational in S and G2) or non-homologous end-joining (NHEJ) to remove DSBs from the genome<sup>62</sup>. The latter pathway is initiated by the KU70/80 dimer<sup>63</sup>, which was shown to interact with HP1 $\alpha$ <sup>64</sup>. To test whether HP1 accumulation at DSBs depends on NHEJ or KU70 in particular, we irradiated wild-type and KU80-deficient CHO cells with  $\alpha$ -particles. Clear recruitment of endogenous HP1 $\beta$  was observed in both cell types at all  $\gamma$ H2A.X tracks, showing that HP1 association is independent of NHEJ (Figure 5C). Co-localization of HP1 with

$\gamma$ H2A.X tracks was detected in all cells, indicating that HP1 binding is independent of the cell cycle stage. This argues against recruitment by homologous recombination (HR). Thus, similar to the NER-independent recruitment to UV-lesions, we provide evidence that HP1 associates with DSBs independent of NHEJ and possibly independent of HR.

### **Several HP1-interacting proteins are recruited to UV-lesions**

Having established that HP1 proteins are recruited to UV-induced DNA damage through the CSD, we next investigated whether proteins that interact with this domain also accumulate at sites of DNA damage. DNA methyltransferase 1 (Dnmt1) directly interacts with the CSD of HP1 and has previously been shown to accumulate at damaged DNA sites<sup>65</sup>. Indeed, EGFP-Dnmt1 accumulated upon UV irradiation (Figure 6A). If Dnmt1 methylates DNA at the locally irradiated site, this may trigger the binding of MeCP2, which is a protein that binds methylated DNA<sup>66</sup>. Also, EGFP-tagged MeCP2 did not accumulate after localized UV irradiation (data not shown). We also tested accumulation of EYFP-tagged H3K9 methyltransferase Suv39H1<sup>67</sup> at sites of UV-lesions. Local UV irradiation did not result in recruitment of EYFP-Suv39H1 (data not shown). This demonstrates that H3K9Me3 is not involved in HP1 recruitment to DNA damage, consistent with the findings that HP1 is recruited in cells deficient for Suv39h and that the CD is not required for HP1 binding (data not shown, Figure 2). Interestingly, the H4K20 methyl-transferase EGFP-Suv4-20h1<sup>53,68</sup> did accumulate following UV irradiation (Figure 6F). Previous studies showed that H4K20me3 depends on Suv3-9 and direct interactions between HP1 and Suv4-20<sup>53</sup>. It appears that after UV damage HP1 recruits Suv4-20 independently of Suv3-9 at damaged sites.

Previous *in vitro* experiments have suggested a role for ATP-dependent chromatin remodelling factors like SWI/SNF and ACF1 during DNA repair<sup>12,15</sup>. Interestingly, ACF1 and the SNF2-like BRG1 protein directly interact with the CSD of HP1 and we tested whether these factors are recruited to sites of damage *in vivo*<sup>44,45</sup>. Upon UV irradiation of HeLa cells, we observed accumulation of EYFP-BRG1 and ACF1-EGFP, which can form a heterodimer with ISWI, showing that ATP-dependent remodelling factors are recruited to sites of UV-induced DNA damage (Figure 6B, data not shown). Similar to HP1, accumulation of EGFP-Dnmt1, EYFP-BRG1 and ACF1-EGFP was also detected in NER-deficient cells (Figure 6C, D, data not shown), suggesting that HP1, Dnmt1, ACF1 and BRG1 may be involved in a DNA damage response pathway other than DNA repair. To investigate if the accumulation of HP1 depends on Dnmt1, we expressed SCFP3a-HP1 $\beta$  in Dnmt1 knock-out cells<sup>69</sup>. Results show that HP1 $\beta$  accumulates upon UV irradiation in the absence of Dnmt1 (Figure 6E), suggesting that HP1 is not recruited to DNA lesions by this protein.

### **Loss of HP1 renders *C.elegans* highly sensitive to UV irradiation**

---

Because knockout of HP1 in mammalian cells is lethal<sup>53,70</sup>, we used the nematode *C. elegans* to test whether HP1 is functionally required for the DNA damage response. Two HP1 homologues (HPL-1 and HPL-2) are present in *C. elegans* and loss of both HP1 proteins is also lethal in worms<sup>71,72</sup>. To circumvent this problem, we employed animals lacking HPL-1 and carrying a temperature-sensitive allele of HPL-2, which is expressed at 20°C but not at 25°C<sup>72</sup>. To test whether loss of HPL-1 and HPL-2 results in sensitivity to UV, we exposed eggs of single and double mutant animals (grown at 25°C) carrying null alleles of *hpl-1* and *hpl-2* to UV-B radiation (80 J.m<sup>-2</sup>). Wild-type and NER-deficient *xpa-1* null eggs<sup>73</sup> were also irradiated at 80 J.m<sup>-2</sup>. The survival of irradiated eggs was subsequently determined compared to non-irradiated eggs (Figure 7). Wild-type and *hpl-1* or *hpl-2*

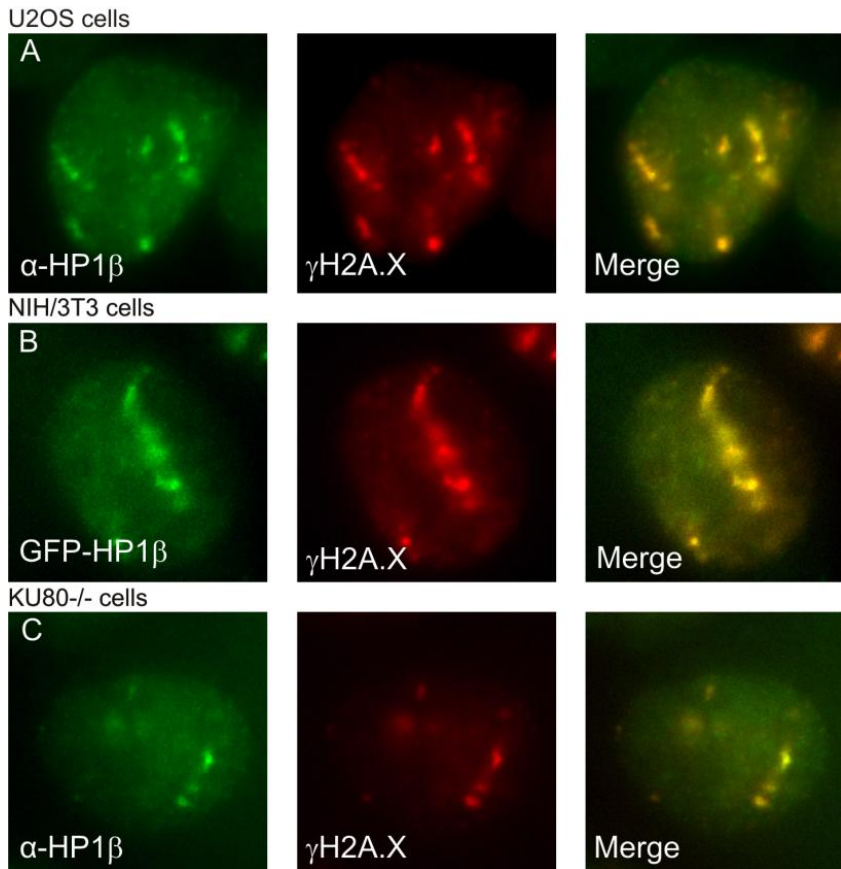


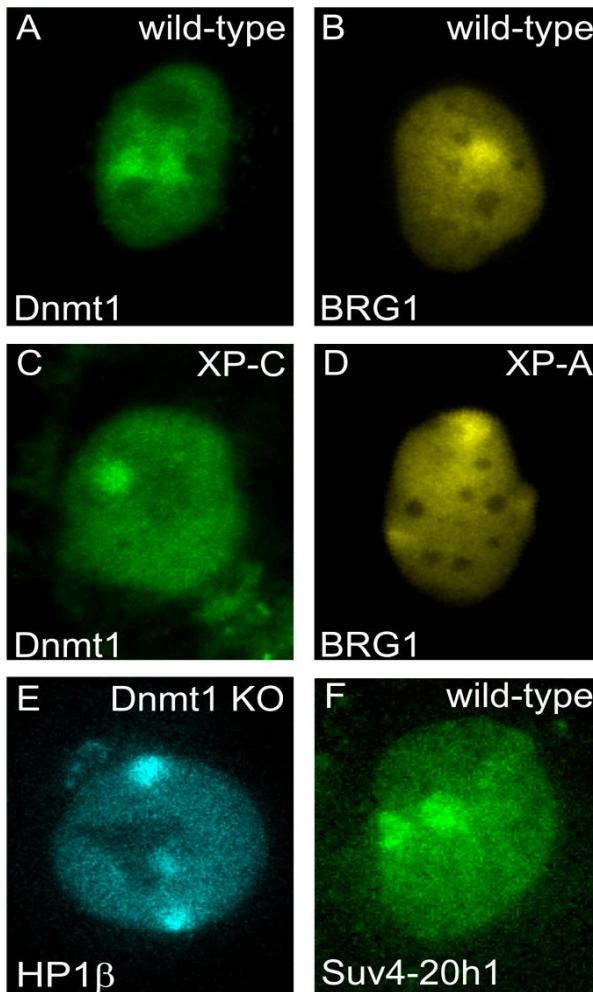
**Fig 5.** Recruitment of HP1 $\beta$  to DSBs. (A) Wild-type U2OS cells were irradiated with  $\alpha$ -particles and subsequently labeled for endogenous HP1 $\beta$  (green) and  $\gamma$ H2A.X (red). (B) Mouse cells expressing EGFP-HP1b (green) were irradiated with  $\alpha$ -particles and subsequently labeled for  $\gamma$ H2A.X (red). (C) Hamster cells deficient in Ku80 were irradiated with  $\alpha$ -particles and subsequently labeled for endogenous HP1 $\beta$  (green) and  $\gamma$ H2A.X (red). A merged image of HP1 and  $\gamma$ H2A.X is shown.



single mutant worms did not exhibit increased sensitivity to UV-B. Strikingly, UV-B irradiation caused an immediate growth arrest in *hpl-2/hpl-1* double mutant worms comparable to NER-deficient *xpa-1* mutant worms. Similar results were obtained when juvenile *hpl-2/hpl-1* worms were irradiated instead of eggs (data not shown). This indicates that either HPL-1 or HPL-2 is sufficient for a normal response to DNA damage, but that loss of both HP1 proteins renders *C. elegans* highly sensitive to UV irradiation. These results reveal an essential role for the HP1 proteins in the DNA damage response in *C. elegans*. The association of HP1 proteins with several types of DNA lesions in mammalian cells suggests that this DNA damage response mechanism is conserved between *C. elegans* and humans.

### Discussion

In this study, we provide evidence for a novel function of the HP1 proteins in



the DNA damage response. We show that all three isoforms of human HP1 ( $\alpha$ ,  $\beta$  and  $\gamma$ ) are recruited to sites of UV-induced DNA damage (Figure 1) and to areas of DSBs (Figure 5; data not shown). Moreover, HP1 is also recruited to DNA lesions repaired by base excision repair (Zarebski and Dobrucki, unpublished results). This indicates that HP1

**Fig 6.** Recruitment of HP1-binding proteins to UV-damage. (A) Accumulation of Dnmt1-EGFP and (B) EYFP-BRG1 in living HeLa cells or MRC5-Sv cells locally irradiated at  $100 \text{ J.m}^{-2}$  through  $5 \mu\text{m}$  pores or irradiated using a UV-C laser. (C) Accumulation of Dnmt1-EGFP, and (D) EYFP-BRG1 in living XP-A or XP-C cells locally irradiated at  $100 \text{ J.m}^{-2}$  through  $5 \mu\text{m}$  pores or irradiated using a UV-C laser. (E) Accumulation of SCFP3a-HP1 $\beta$  in Dnmt1 knock-out cells and (F) Accumulation of EGFP-Suv4-20h1 in locally irradiated MRC5-SV cells.



is involved in a variety of DNA repair systems in mammalian cells. Our finding that *C. elegans* without HP1 is highly UV sensitive, suggests that HP1 is an essential component of the DNA damage response. Unexpectedly, recruitment of HP1 to DNA damage is independent of any of the known damage recognition proteins, such as XPC and DDB2 in NER and KU70/80 in DSB repair. Moreover, HP1 binding is independent of DNA-damage induced signalling by ATR kinase (Figure 3). We show that HP1 binding does not require active NER. However, loss of DNA damage-induced HP1 binding sites occurs only in cells that are proficient in NER. HP1 remains bound under conditions that the NER system is inactive (Fig. 4). This shows that the NER system and the HP1 system communicate with

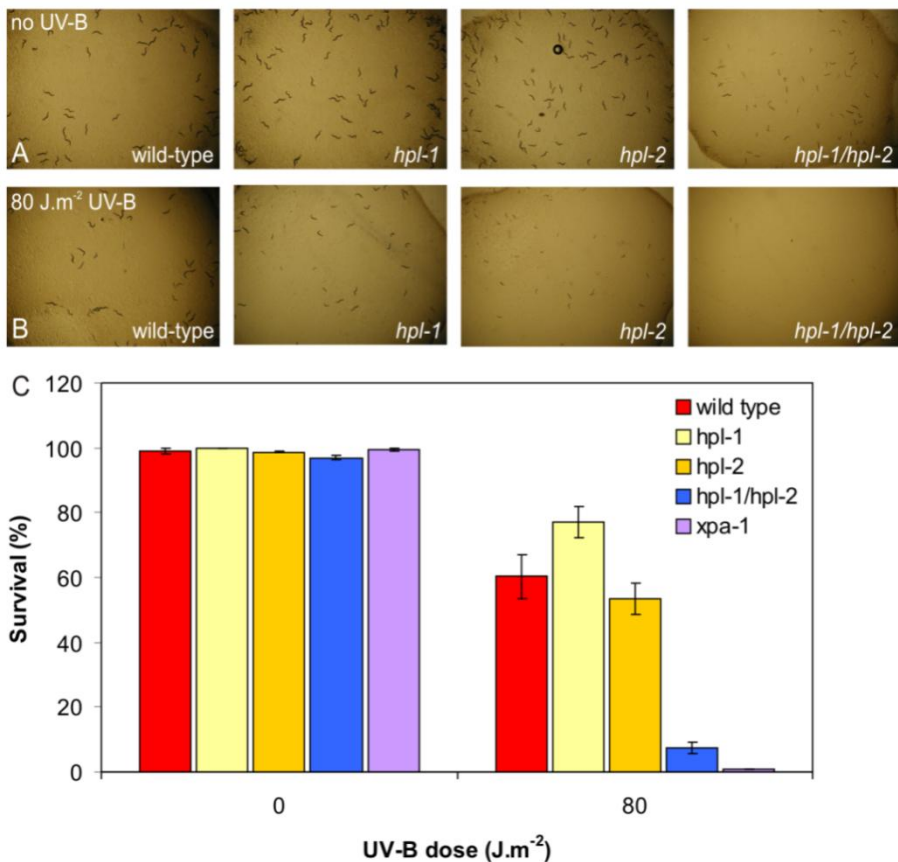


**Fig 7.** Survival of *C. elegans* HP1 knock-out worms upon UV irradiation. (A) Hatching of wild-type, *hpl-1*, *hpl-2* and *hpl-2/hpl-1* mutant eggs 8 hours following collection. (B) Hatching of wild-type, *hpl-1*, *hpl-2* and *hpl-2/hpl-1* mutant eggs 8 hours following collection and subsequently irradiated with UV-B at 80 J.m<sup>-2</sup>. (C) Quantification of hatching and non-hatching eggs following UV-irradiation relative to non-irradiated eggs. In addition to wild-type (red bars), *hpl-1* (light-yellow bars), *hpl-2* (dark-yellow bars) and *hpl-2/hpl-1* (blue bars) mutant eggs, the survival of *xpa* mutant eggs was also quantified (purple bars).

each other. In conjunction, these results indicate that the HP1 proteins are involved in NER via a novel mechanism that acts in parallel to the well-studied NER repair pathway. HP1 is likely involved in a process that modifies and/or re-establishes the correct chromatin structure at the sites of DNA damage and that serves various repair systems.

Recently, Ayoub et al.<sup>74</sup> presented evidence that suggested that HP1 $\beta$  is mobilized from DNA breaks, seemingly in contrast with results presented here. This may be due to the fact these authors use an exceedingly harsh method to inflict DNA damage in living cells: 200 iterations of 100% power from a 405 nm diode laser under conditions that the DNA is photo-sensitized with Hoechst and BrdU. Very likely, under these conditions severe and diverse types of photodamage are induced in the DNA<sup>49,58</sup>. Therefore, the data of Ayoub et al.<sup>74</sup> cannot easily be compared to our conditions, which have been chosen so that either the NER or the DSB repair system is activated.

Recruitment of HP1 to UV-lesions is strictly dependent on the C-terminal chromoshadow domain (CSD) and does not require the N-terminal chromodomain (CD) or hinge region (Figure 2). Therefore is unlikely that interaction with methylated H3K9 plays a major role. The CSD of HP1 is known to interact with many nuclear proteins, including chromatin remodelling factors ACF1 and BRG1, maintenance DNA methyltransferase Dnmt1 and histone chaperone CAF-1<sup>44-47</sup>. We have shown that, similar to HP1 recruitment, Dnmt1 is recruited to UV-damaged areas in the nucleus independently of the activity of pre-incision NER proteins (Figure 6). However, recruitment of HP1 did not depend on Dnmt1, showing that HP1 does not bind to DNA lesions via this protein. Alternatively, HP1 may serve as a loading platform for various epigenetic regulators that are involved in DNA damage response mechanisms and are uncoupled from NER. In this scenario, HP1 would recruit proteins such as Dnmt1, Suv4-20, BRG1 and ACF1 to damage. Previous studies have demonstrated that, in contrast to HP1, recruitment of CAF-1 depends on dual incision<sup>28</sup> and it is not clear if HP1 and CAF-1 interact at sites of DNA damage.

What is the molecular mechanism and the function of HP1 in DNA damage response? Evidently, binding of HP1 at sites of DNA damage after UV damage does neither require any of the known damage response proteins (XPC, DDB2 or Ku80), nor DNA repair activity. Consistent with these results, HP1 is not required for NER on naked DNA in vitro<sup>75</sup>. Binding of HP1 fully depends on its chromoshadow domain, excluding a role of H3K9 methylation. Accordingly, Suv39H1 does not accumulate on damaged DNA and HP1 $\beta$  still accumulates in cells deficient for Suv39H1. Moreover, HP1 binding does not depend on the presence of the DNA methyltransferase Dnmt1, which interacts with the chromoshadow domain. In contrast, the H4K20 methyl-transferase Suv4-20h1 did accumulate, possibly cooperating

---

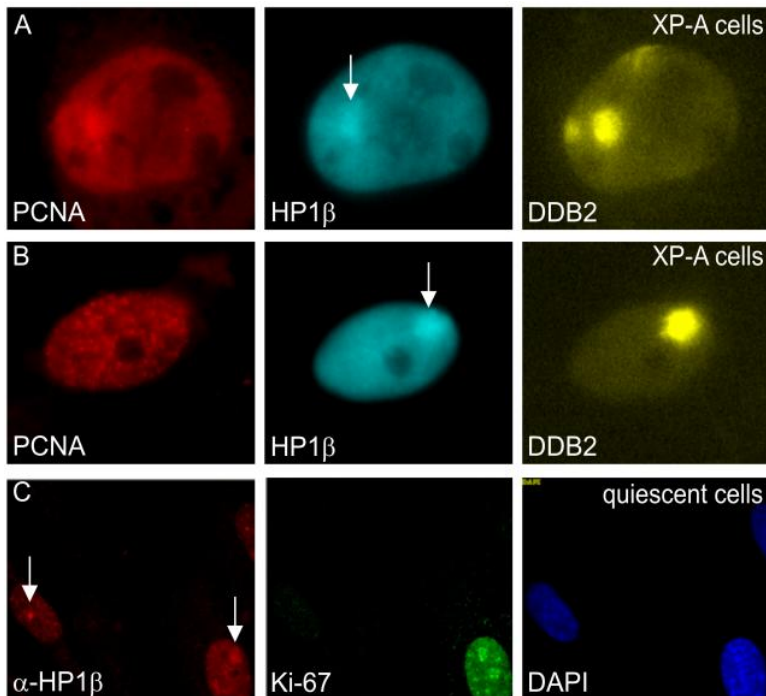
with HP1 in modifying chromatin structure. Our studies unveil an unexpected, intriguing and apparently ubiquitous link between DNA repair systems and chromatin modifiers. It is tempting to speculate that HP1 is involved in re-establishing the correct chromatin state after DNA repair. HP1 $\beta$  was recently shown to associate with inactive RNA pol II resulting in gene repression, while HP1 $\gamma$  binds to elongating RNA pol II, linking the HP1 proteins directly to regulation of transcription<sup>76,77</sup>. It is attractive to speculate that HP1 proteins play a role in regulation of transcription in chromatin containing UV lesions or DNA breaks, since DNA damage inhibits transcription independently of DNA repair<sup>78,79</sup>. This process involves a yet unknown damage detection system in addition to the known detection pathways.

### Materials and Methods

**Cell lines.** Cell lines used in this study were HeLa, U2OS, CHOK1, NIH/3T3, NIH/3T3 EGFP-HP1 $\beta$ <sup>35</sup>, VH10 hTERT immortalised normal human fibroblasts, ATR-deficient GM18366-hTERT Seckel cells<sup>55</sup>, Dnmt1-deficient HCT116 cells<sup>69</sup>, Suv3-9h double knockout MEFs<sup>52,53</sup> and KU80-deficient XR-V15B CHO cells<sup>63</sup>. The NER-deficient SV40-immortalized cell lines were XP4PA (XP-C), XP20S (XP-A), XP12RO (XP-A), XP23PV (XP-E), MEFs XPC-/- and CS1AN (CS-B). All cell lines were cultured in a 1:1 mixture of DMEM/Ham's F10 medium. All media contained glutamine (Gibco, Breda, the Netherlands) supplemented with antibiotics and 10% FCS and all cells were cultured at 37°C in an atmosphere of 5% CO<sub>2</sub>. For immunolocalisation experiments of endogenous HP1 $\beta$  hTERT immortalised human fibroblasts were grown to confluency for approximately 10 days. Subsequently, cells were synchronised in G0 phase by keeping them for a minimum of 5 days in medium supplemented with 0.2% FCS (serum starved cells).

**DNA constructs.** HP1 $\alpha$  and HP1 $\beta$  cDNA were ligated in frame with mRFP and super cyan fluorescent protein 3a (SCFP3a) resulting in mRFP-HP1 $\alpha$  and SCFP3a-HP1 $\beta$ , respectively. EGFP-HP1 $\beta$  and EGFP-HP1 $\gamma$  were a gift from Dr. P. Hemmerich<sup>36</sup>. All constructs were transiently transfected in various cell lines cells using Lipofectamine 2000. EGFP-HP1 $\beta$  was stably expressed in mouse NIH-3T3 cells as described previously<sup>35</sup>. HP1 $\beta$  ( $\Delta$ CD) was tagged with mCherry as described elsewhere<sup>35</sup> and EGFP-HP1 $\beta$  ( $\Delta$ CSD) and EGFP-HP1 $\beta$  ( $\Delta$ hinge) were kindly provided by Dr. T. Misteli<sup>54</sup>. EYFP-tagged CSD was provided by Dr. Y. Hirako<sup>80</sup>. The genes encoding NER proteins XPC, DDB2 and XPA were fused to the yellow fluorescent protein variant, monomeric Venus (mVenus), resulting in XPC-mVenus, DDB2-mVenus and mVenus-XPA. In addition, DDB2 was fused to mCherry<sup>50</sup>. MeCP2 cDNA (kind gift from M.C. Cardoso) was fused to EGFP and EGFP-Dnmt1 was provided by Dr. H. Leonardt<sup>65</sup>. EYFP-BRG1 was provided by Dr. T. Misteli<sup>81</sup> and ACF1-EGFP by Dr. P.D. Varga-Weisz<sup>82</sup>. EYFP-Suv3-9H1 was provided by Dr. R.W. Dirks and EGFP-Suv4-20H1 and H2 by Dr. T. Jenuwein. The cDNAs for SCFP3a and mVenus were provided by Dr. J. Goedhart<sup>83</sup> and mCherry and mRFP cDNA by Dr. R.Y. Tsien<sup>84,85</sup>.

---



**Supplemental figure S1.** HP1 $\beta$  accumulation is independent of cell cycle. Representative images of human XP-A cells expressing mCherry-PCNA (red), SCFP3a-HP1 $\beta$  (cyan) and DDB2-mVenus (yellow) following local irradiation at 100 J.m<sup>-2</sup> through 5  $\mu$ m pores. (A) Accumulation of HP1 $\beta$  is observed outside S-phase when PCNA is homogeneously distributed in the cell nucleus and (B) in S-phase cells (indicated by the typical S-phase pattern of PCNA). (C) Immunolocalisation of endogenous HP1 $\beta$  in locally UV-irradiated (3  $\mu$ m pores, 100 J.m<sup>-2</sup>) in quiescent human fibroblasts as visualised by Ki67 negative staining and in cycling cells as visualised by Ki67 positive staining.

**UV-C irradiation.** Lamp-induced UV damage was inflicted using a UV source containing four UV lamps (Philips TUV 9W PL-S) above the microscope stage. The UV dose rate was measured to be 3 W.m<sup>-2</sup> at 254 nm. For induction of global UV-damage, cells were rinsed with medium and irradiated for 9 seconds (25 J.m<sup>-2</sup>). For induction of local UV-damage, cells were UV irradiated through a polycarbonate mask (Millipore Billerica, Massachusetts, USA) with pores of 3 or 5  $\mu$ m for 39 or 11.7 seconds (100 or 30 J.m<sup>-2</sup>)<sup>50</sup>. Laser-induced UV damage was inflicted by using a 2 mW pulsed (7.8 kHz) diode pumped solid state laser emitting at 266 nm (Rapp OptoElectronic, Hamburg GmbH). The laser was connected to a Zeiss LSM 510 confocal microscope with an Axiovert 200 M housing adapted for UV by all-quartz optics. A special adaptor (ZSI-A200, Rapp OptoElectronic) to fit in the aperture slider position of an Axiovert 200 microscope was developed by Rapp OptoElectronic to focus the laser on a sample. For local UV-C irradiation experiments, cells were grown on 25 mm diameter quartz coverslips (010191T-AB, SPI supplies)<sup>49</sup>.

**$\alpha$ -particle irradiation.** Cells were plated in custom-made culture dishes containing an ultra-thin Mylar bottom.<sup>59,60</sup> The Mylar membrane was coated with carbon to improve attachment of cells. Cells were incubated for 24 hours at 37 °C and subsequently irradiated using an americium (Am-241) source with an activity of 140 kBq. The americium source was placed underneath the dish, just touching the Mylar membrane. The source was placed at an angle of 30° with the

horizontal plane to obtain long linear arrays of DSBs. Cells were irradiated at room temperature for 0.5 min and subsequently fixed using paraformaldehyde (final concentration 2%).

**Immunofluorescence.** Fixed cells were immunostained as described previously<sup>59,60</sup>. The following primary antibodies were used: mouse monoclonal antibody against  $\gamma$ H2A.X (clone JBW301, Upstate Biotechnology, Waltham, MA, USA), mouse monoclonal antibody against XPA (clone 12F5, Abcam) and rat monoclonal antibody against HP1 $\beta$  (1:250; a kind gift from Dr. Prim Singh<sup>86</sup>). Secondary antibodies: goat anti-mouse Cy3 and goat anti-rat FITC (both from Jackson ImmunoResearch Laboratories, West Grove, Pennsylvania, USA). All antibodies were diluted in PBS containing 0.1% Triton-X 100 and 1% Foetal Calf Serum. Fluorescence microscopy images were acquired using a Leica DM RA HC microscope (Leica Microsystems, Wetzlar, Germany) equipped with a PLAN APO 100x / 1.40 oil objective and a cooled CCD camera (KX1400, Apogee Instruments, CA, USA).

**Microscopic analysis.** Cells were imaged on a Zeiss LSM 510 confocal microscope, equipped with a 63x Ultrafluar (1.2 NA) glycerol immersion lens (Zeiss, Oberkochen, Germany) and a 30 mW Argon laser (488 and 514 nm), or on a Zeiss Axiovert 200M wide field fluorescence microscope, equipped with a 100x Plan-Apochromat (1.4 NA) oil immersion lens (Zeiss, Oberkochen, Germany) and a Cairn Xenon Arc lamp with monochromator (Cairn research, Kent, U.K.). Images were recorded with a cooled CCD camera (Coolsnap HQ, Roper Scientific, USA). Both microscopes were equipped with an objective heater and cells were examined in microscopy medium (137 mM NaCl, 5.4 mM KCl, 1,8 mM CaCl<sub>2</sub>, 0.8 mM MgSO<sub>4</sub>, 20 mM D-glucose and 20 mM HEPES) at 37°C.

**Combined FLIP and FRAP.** FRAP analysis was used to measure the immobilization of EGFP-HP1 $\beta$  after global UV irradiation as described by Houtsmuller and co-workers<sup>87,88</sup>. Briefly, ~50% of the nuclei of NIH/3T3 cells expressing EGFP-HP1 $\beta$  were bleached using 100% power of a 488 and 514 laser line. The loss of fluorescence from the non-bleached half (FLIP) and the gain of fluorescence in the bleached half (FRAP) were determined. The data was corrected for background values and normalized to pre-bleach intensity.

**C. elegans UV-B survival assay.** *C. elegans* strains used were Bristol N2 (wild type), *hpl-1(tm1624)*, *hpl-2(tm1489)*, *hpl-2(tm1489); hpl-1(tm1624)* (constructed using PCR to confirm deletions) and *xpa-1(ok698)*. The *hpl-1(tm1624)* and *xpa-1(ok698)* are likely null alleles<sup>71,73</sup>, whereas *hpl-2(tm1489)* is a null allele that causes severe growth delay and sterility only at 25°C but not at 20°C<sup>72</sup>. Thus, it was possible to test UV-sensitivity by growing animals at 20°C and transferring them to 25°C directly following UV-irradiation. To test UV-sensitivity, eggs were collected from gravid adult animals by ClNaO/NaOH treatment and placed on culture plates seeded with HT115 bacteria at 20°C. Eight hours following egg collection, eggs were irradiated using two FS20 erythematous UV-B lamps (Phillips, Eindhoven, the Netherlands), after which survival rate was determined by counting the amount of hatching eggs (surviving animals) and non-hatching, dead eggs. Additional details are available upon request.

### Acknowledgements

This work was supported by ZonMW, the Netherlands (grant 912-03-012). The authors thank Drs. P. Hemmerich, T. Misteli, R.W. Dirks, R.Y. Tsien, J. Goedhart, H. Leonardt, M.C. Cardoso, P.D. Varga-Weisz, K.E. Schuebel and T. Jenuwein for kindly providing constructs and cells and Dr. P. Singh for providing HP1 antibodies. The authors are grateful to the *Caenorhabditis* Genetics Center and the Japanese National Bioresource Project for *hpl-1*, *hpl-2* and *xpa-1* strains. The authors thank Drs. E.M.M. Manders and T.W.J. Gadella (Center for advanced microscopy (CAM)/UvA) for support.

### References

1. Bartek, J. & Lukas, J. DNA damage checkpoints: from initiation to recovery or adaptation. *Curr Opin Cell Biol* **19**, 238-45 (2007).
-

2. Shimada, M. et al. Chk1 is a histone H3 threonine 11 kinase that regulates DNA damage-induced transcriptional repression. *Cell* **132**, 221-32 (2008).
  3. Huen, M.S. & Chen, J. The DNA damage response pathways: at the crossroad of protein modifications. *Cell Res* **18**, 8-16 (2008).
  4. Hoeijmakers, J.H. Genome maintenance mechanisms for preventing cancer. *Nature* **411**, 366-74 (2001).
  5. de Laat, W.L., Jaspers, N.G. & Hoeijmakers, J.H. Molecular mechanism of nucleotide excision repair. *Genes Dev* **13**, 768-85 (1999).
  6. Fousteri, M. & Mullenders, L.H. Transcription-coupled nucleotide excision repair in mammalian cells: molecular mechanisms and biological effects. *Cell Res* **18**, 73-84 (2008).
  7. Friedberg, E.C. How nucleotide excision repair protects against cancer. *Nat Rev Cancer* **1**, 22-33 (2001).
  8. Kanaar, R., Wyman, C. & Rothstein, R. Quality control of DNA break metabolism: in the 'end', it's a good thing. *Embo J* **27**, 581-8 (2008).
  9. Jenuwein, T. & Allis, C.D. Translating the histone code. *Science* **293**, 1074-80 (2001).
  10. Turner, B.M. Cellular memory and the histone code. *Cell* **111**, 285-91 (2002).
  11. Henikoff, S., Furuyama, T. & Ahmad, K. Histone variants, nucleosome assembly and epigenetic inheritance. *Trends Genet* **20**, 320-6 (2004).
  12. Ura, K. et al. ATP-dependent chromatin remodeling facilitates nucleotide excision repair of UV-induced DNA lesions in synthetic dinucleosomes. *Embo J* **20**, 2004-14 (2001).
  13. Hara, R., Mo, J. & Sancar, A. DNA damage in the nucleosome core is refractory to repair by human excision nuclease. *Mol Cell Biol* **20**, 9173-81 (2000).
  14. Wang, Z.G., Wu, X.H. & Friedberg, E.C. Nucleotide excision repair of DNA by human cell extracts is suppressed in reconstituted nucleosomes. *J Biol Chem* **266**, 22472-8 (1991).
  15. Hara, R. & Sancar, A. The SWI/SNF chromatin-remodeling factor stimulates repair by human excision nuclease in the mononucleosome core particle. *Mol Cell Biol* **22**, 6779-87 (2002).
  16. Kapetanaki, M.G. et al. The DDB1-CUL4ADDB2 ubiquitin ligase is deficient in xeroderma pigmentosum group E and targets histone H2A at UV-damaged DNA sites. *Proc Natl Acad Sci U S A* (2006).
  17. Wang, H. et al. Histone H3 and H4 Ubiquitylation by the CUL4-DDB-ROC1 Ubiquitin Ligase Facilitates Cellular Response to DNA Damage. *Mol Cell* **22**, 383-394 (2006).
  18. Fousteri, M., Vermeulen, W., van Zeeland, A.A. & Mullenders, L.H. Cockayne syndrome A and B proteins differentially regulate recruitment of chromatin remodeling and repair factors to stalled RNA polymerase II in vivo. *Mol Cell* **23**, 471-82 (2006).
  19. Brand, M. et al. UV-damaged DNA-binding protein in the TFIIIC complex links DNA damage recognition to nucleosome acetylation. *Embo J* **20**, 3187-96 (2001).
  20. Martinez, E. et al. Human STAGA complex is a chromatin-acetylating transcription coactivator that interacts with pre-mRNA splicing and DNA damage-binding factors in vivo. *Mol Cell Biol* **21**, 6782-95 (2001).
  21. Carrier, F. et al. Gadd45, a p53-responsive stress protein, modifies DNA accessibility on damaged chromatin. *Mol Cell Biol* **19**, 1673-85 (1999).
  22. Smith, M.L. et al. Antisense GADD45 expression results in decreased DNA repair and sensitizes cells to u.v.-irradiation or cisplatin. *Oncogene* **13**, 2255-63 (1996).
  23. Smith, M.L. et al. p53-mediated DNA repair responses to UV radiation: studies of mouse cells lacking p53, p21, and/or gadd45 genes. *Mol Cell Biol* **20**, 3705-14 (2000).
  24. Kuo, W.H., Wang, Y., Wong, R.P., Campos, E.I. & Li, G. The ING1b tumor suppressor facilitates nucleotide excision repair by promoting chromatin accessibility to XPA. *Exp Cell Res* **313**, 1628-38 (2007).
  25. Wang, J., Chin, M.Y. & Li, G. The novel tumor suppressor p33ING2 enhances nucleotide excision repair via inducement of histone H4 acetylation and chromatin relaxation. *Cancer Res* **66**, 1906-11 (2006).
  26. Cheung, K.J., Jr., Mitchell, D., Lin, P. & Li, G. The tumor suppressor candidate p33(ING1) mediates repair of UV-damaged DNA. *Cancer Res* **61**, 4974-7 (2001).
-

- 
27. Groth, A., Rocha, W., Verreault, A. & Almouzni, G. Chromatin challenges during DNA replication and repair. *Cell* **128**, 721-33 (2007).
  28. Green, C.M. & Almouzni, G. Local action of the chromatin assembly factor CAF-1 at sites of nucleotide excision repair in vivo. *Embo J* **22**, 5163-74 (2003).
  29. Polo, S.E., Roche, D. & Almouzni, G. New Histone Incorporation Marks Sites of UV Repair in Human Cells. *Cell* **127**, 481-93 (2006).
  30. Green, C.M. & Almouzni, G. When repair meets chromatin. First in series on chromatin dynamics. *EMBO Rep* **3**, 28-33 (2002).
  31. Smerdon, M.J. DNA repair and the role of chromatin structure. *Curr Opin Cell Biol* **3**, 422-8 (1991).
  32. Lomberk, G., Wallrath, L. & Urrutia, R. The Heterochromatin Protein 1 family. *Genome Biol* **7**, 228 (2006).
  33. Maison, C. & Almouzni, G. HP1 and the dynamics of heterochromatin maintenance. *Nat Rev Mol Cell Biol* **5**, 296-304 (2004).
  34. Cowieson, N.P., Partridge, J.F., Allshire, R.C. & McLaughlin, P.J. Dimerisation of a chromo shadow domain and distinctions from the chromodomain as revealed by structural analysis. *Curr Biol* **10**, 517-25 (2000).
  35. Mateos-Langerak, J. et al. Pericentromeric heterochromatin domains are maintained without accumulation of HP1. *Mol Biol Cell* **18**, 1464-71 (2007).
  36. Schmiedeberg, L., Weisshart, K., Diekmann, S., Meyer Zu Hoerste, G. & Hemmerich, P. High- and low-mobility populations of HP1 in heterochromatin of mammalian cells. *Mol Biol Cell* **15**, 2819-33 (2004).
  37. Ayyanathan, K. et al. Regulated recruitment of HP1 to a euchromatic gene induces mitotically heritable, epigenetic gene silencing: a mammalian cell culture model of gene variegation. *Genes Dev* **17**, 1855-69 (2003).
  38. van der Vlag, J., den Blaauwen, J.L., Sewalt, R.G., van Driel, R. & Otte, A.P. Transcriptional repression mediated by polycomb group proteins and other chromatin-associated repressors is selectively blocked by insulators. *J Biol Chem* **275**, 697-704 (2000).
  39. Verschure, P.J. et al. In vivo HP1 targeting causes large-scale chromatin condensation and enhanced histone lysine methylation. *Mol Cell Biol* **25**, 4552-64 (2005).
  40. de Wit, E., Greil, F. & van Steensel, B. High-resolution mapping reveals links of HP1 with active and inactive chromatin components. *PLoS Genet* **3**, e38 (2007).
  41. Minc, E., Courvalin, J.C. & Buendia, B. HP1gamma associates with euchromatin and heterochromatin in mammalian nuclei and chromosomes. *Cytogenet Cell Genet* **90**, 279-84 (2000).
  42. Vakoc, C.R., Mandat, S.A., Olenchock, B.A. & Blobel, G.A. Histone H3 lysine 9 methylation and HP1gamma are associated with transcription elongation through mammalian chromatin. *Mol Cell* **19**, 381-91 (2005).
  43. Jacobs, S.A. & Khorasanizadeh, S. Structure of HP1 chromodomain bound to a lysine 9-methylated histone H3 tail. *Science* **295**, 2080-3 (2002).
  44. Eskeland, R., Eberharter, A. & Imhof, A. HP1 binding to chromatin methylated at H3K9 is enhanced by auxiliary factors. *Mol Cell Biol* **27**, 453-65 (2007).
  45. Nielsen, A.L. et al. Selective interaction between the chromatin-remodeling factor BRG1 and the heterochromatin-associated protein HP1alpha. *Embo J* **21**, 5797-806 (2002).
  46. Fuks, F., Hurd, P.J., Deplus, R. & Kouzarides, T. The DNA methyltransferases associate with HP1 and the SUV39H1 histone methyltransferase. *Nucleic Acids Res* **31**, 2305-12 (2003).
  47. Murzina, N., Verreault, A., Laue, E. & Stillman, B. Heterochromatin dynamics in mouse cells: interaction between chromatin assembly factor 1 and HP1 proteins. *Mol Cell* **4**, 529-40 (1999).
  48. Thiru, A. et al. Structural basis of HP1/PXVXL motif peptide interactions and HP1 localisation to heterochromatin. *Embo J* **23**, 489-99 (2004).
  49. Dinant, C. et al. Activation of multiple DNA repair pathways by sub-nuclear damage induction methods. *J Cell Sci* **120**, 2731-40 (2007).
-

50. Luijsterburg, M.S. et al. Dynamic in vivo interaction of DDB2 E3 ubiquitin ligase with UV-damaged DNA is independent of damage-recognition protein XPC. *J Cell Sci* **120**, 2706-16 (2007).
  51. Moné, M.J. et al. In vivo dynamics of chromatin-associated complex formation in mammalian nucleotide excision repair. *Proc Natl Acad Sci U S A* **101**, 15933-7 (2004).
  52. Peters, A.H. et al. Loss of the Suv39h histone methyltransferases impairs mammalian heterochromatin and genome stability. *Cell* **107**, 323-37 (2001).
  53. Schotta, G. et al. A silencing pathway to induce H3-K9 and H4-K20 trimethylation at constitutive heterochromatin. *Genes Dev* **18**, 1251-62 (2004).
  54. Cheutin, T. et al. Maintenance of stable heterochromatin domains by dynamic HP1 binding. *Science* **299**, 721-5 (2003).
  55. Bergink, S. et al. DNA damage triggers nucleotide excision repair-dependent monoubiquitylation of histone H2A. *Genes Dev* **20**, 1343-52 (2006).
  56. Choi, J.H., Lindsey-Boltz, L.A. & Sancar, A. Reconstitution of a human ATR-mediated checkpoint response to damaged DNA. *Proc Natl Acad Sci U S A* **104**, 13301-6 (2007).
  57. O'Driscoll, M., Ruiz-Perez, V.L., Woods, C.G., Jeggo, P.A. & Goodship, J.A. A splicing mutation affecting expression of ataxia-telangiectasia and Rad3-related protein (ATR) results in Seckel syndrome. *Nat Genet* **33**, 497-501 (2003).
  58. Williams, E.S. et al. DNA double-strand breaks are not sufficient to initiate recruitment of TRF2. *Nat Genet* **39**, 696-8; author reply 698-9 (2007).
  59. Aten, J.A. et al. Dynamics of DNA double-strand breaks revealed by clustering of damaged chromosome domains. *Science* **303**, 92-5 (2004).
  60. Stap, J. et al. Induction of linear tracks of DNA double-strand breaks by alpha-particle irradiation of cells. *Nat Methods* **5**, 261-6 (2008).
  61. Bekker-Jensen, S. et al. Spatial organization of the mammalian genome surveillance machinery in response to DNA strand breaks. *J Cell Biol* **173**, 195-206 (2006).
  62. Wyman, C. & Kanaar, R. DNA double-strand break repair: all's well that ends well. *Annu Rev Genet* **40**, 363-83 (2006).
  63. Mari, P.O. et al. Dynamic assembly of end-joining complexes requires interaction between Ku70/80 and XRCC4. *Proc Natl Acad Sci U S A* **103**, 18597-602 (2006).
  64. Song, K., Jung, Y., Jung, D. & Lee, I. Human Ku70 interacts with heterochromatin protein 1alpha. *J Biol Chem* **276**, 8321-7 (2001).
  65. Mortusewicz, O., Schermelleh, L., Walter, J., Cardoso, M.C. & Leonhardt, H. Recruitment of DNA methyltransferase 1 to DNA repair sites. *Proc Natl Acad Sci U S A* **102**, 8905-9 (2005).
  66. Ho, K.L. et al. MeCP2 binding to DNA depends upon hydration at methyl-CpG. *Mol Cell* **29**, 525-31 (2008).
  67. Krouwels, I.M. et al. A glue for heterochromatin maintenance: stable SUV39H1 binding to heterochromatin is reinforced by the SET domain. *J Cell Biol* **170**, 537-49 (2005).
  68. Yang, H. et al. Preferential dimethylation of histone H4-lysine 20 by Suv4-20. *J Biol Chem* (2008).
  69. Rhee, I. et al. CpG methylation is maintained in human cancer cells lacking DNMT1. *Nature* **404**, 1003-7 (2000).
  70. Filesi, I. et al. Loss of heterochromatin protein 1 (HP1) chromodomain function in mammalian cells by intracellular antibodies causes cell death. *J Cell Sci* **115**, 1803-13 (2002).
  71. Schott, S., Coustham, V., Simonet, T., Bedet, C. & Palladino, F. Unique and redundant functions of *C. elegans* HP1 proteins in post-embryonic development. *Dev Biol* **298**, 176-87 (2006).
  72. Coustham, V. et al. The *C. elegans* HP1 homologue HPL-2 and the LIN-13 zinc finger protein form a complex implicated in vulval development. *Dev Biol* **297**, 308-22 (2006).
  73. Stergiou, L., Doukometzidis, K., Sendoel, A. & Hengartner, M.O. The nucleotide excision repair pathway is required for UV-C-induced apoptosis in *Caenorhabditis elegans*. *Cell Death Differ* **14**, 1129-38 (2007).
-



74. Ayoub, N., Jeyasekharan, A.D., Bernal, J.A. & Venkitaraman, A.R. HP1-beta mobilization promotes chromatin changes that initiate the DNA damage response. *Nature* (2008).
  75. Aboussekhra, A. et al. Mammalian DNA nucleotide excision repair reconstituted with purified protein components. *Cell* **80**, 859-68 (1995).
  76. Mateescu, B., Bourachot, B., Rachez, C., Ogryzko, V. & Muchardt, C. Regulation of an inducible promoter by an HP1beta-HP1gamma switch. *EMBO Rep* (2008).
  77. Smallwood, A., Black, J.C., Tanese, N., Pradhan, S. & Carey, M. HP1-mediated silencing targets Pol II coactivator complexes. *Nat Struct Mol Biol* (2008).
  78. Moné, M.J. et al. Local UV-induced DNA damage in cell nuclei results in local transcription inhibition. *EMBO Rep* **2**, 1013-7 (2001).
  79. Solovjeva, L.V., Svetlova, M.P., Chagin, V.O. & Tomilin, N.V. Inhibition of transcription at radiation-induced nuclear foci of phosphorylated histone H2AX in mammalian cells. *Chromosome Res* **15**, 787-97 (2007).
  80. Hayakawa, T., Haraguchi, T., Masumoto, H. & Hiraoka, Y. Cell cycle behavior of human HP1 subtypes: distinct molecular domains of HP1 are required for their centromeric localization during interphase and metaphase. *J Cell Sci* **116**, 3327-38 (2003).
  81. Phair, R.D. et al. Global nature of dynamic protein-chromatin interactions in vivo: three-dimensional genome scanning and dynamic interaction networks of chromatin proteins. *Mol Cell Biol* **24**, 6393-402 (2004).
  82. Collins, N. et al. An ACF1-ISWI chromatin-remodeling complex is required for DNA replication through heterochromatin. *Nat Genet* **32**, 627-32 (2002).
  83. Kremers, G.J., Goedhart, J., van Munster, E.B. & Gadella, T.W., Jr. Cyan and yellow super fluorescent proteins with improved brightness, protein folding, and FRET Forster radius. *Biochemistry* **45**, 6570-80 (2006).
  84. Campbell, R.E. et al. A monomeric red fluorescent protein. *Proc Natl Acad Sci U S A* **99**, 7877-82 (2002).
  85. Shaner, N.C. et al. Improved monomeric red, orange and yellow fluorescent proteins derived from *Discosoma* sp. red fluorescent protein. *Nat Biotechnol* **22**, 1567-72 (2004).
  86. Wreggett, K.A. et al. A mammalian homologue of *Drosophila* heterochromatin protein 1 (HP1) is a component of constitutive heterochromatin. *Cytogenet Cell Genet* **66**, 99-103 (1994).
  87. Hoogstraten, D. et al. Rapid switching of TFIIH between RNA polymerase I and II transcription and DNA repair in vivo. *Mol Cell* **10**, 1163-74 (2002).
  88. Zotter, A. et al. Recruitment of the nucleotide excision repair endonuclease XPG to sites of UV-induced dna damage depends on functional TFIIH. *Mol Cell Biol* **26**, 8868-79 (2006).
-



## Chapter 7

### minireview: Assembly of Multi-Protein Complexes that Control Genome Function

Christoffel Dinant, Martijn S. Lijsterburg, Wim  
Vermeulen, Adriaan B. Houtsmuller and Roel van Driel

## Introduction

The nucleus is the information repository of the cell. In this 200-500  $\mu\text{m}^3$  container, mammalian cells store the genetic material. The 3-6 billion base-pairs of the human genome associate with histone proteins to form a chain of basic units of chromatin: the nucleosomes. Functioning of the genome; i.e. replication required for cellular duplication, transcription to read the genetic code and repair to restore genomic insults requires modification of the dense chromatin structure to provide access for the multiple enzymes that regulate these processes to target sites in the DNA (origins of replication, promoters and lesions, respectively). Each of these processes is controlled by a large number of proteins that have to cooperate in space and time in a coordinated fashion. Classical biochemical analysis and histological examination using high-resolution microscopy have provided a wealth of information on these genome-controlling pathways. However, these procedures do not provide information on dynamic interactions. Recent developments in live cell imaging and improvements in quantitative fluorescence microscopy have provided unprecedented insight into dynamic protein interaction in living cells. *In vivo* studies have revealed that many proteins that control genome function rapidly diffuse inside the mammalian nucleus (31, 53) with apparent diffusion rates ranging between  $\sim 0,1$  and  $15 \mu\text{m}^2/\text{s}$  depending on the shape and size of the molecule but also on transient interactions with immobile elements in the nucleus. If such a diffusing protein encounters a site for which it has affinity, it binds for a certain time depending on its dissociation rate. Many nuclear proteins exchange fast between the bound and freely diffusing state at the scale of seconds or minutes (29, 43, 55). Due to the short binding time of individual chromatin-binding proteins, the formation of a multi-protein complex consisting of tens of protein molecules is a low probability event. Although the binding kinetics of many individual proteins has been measured, little is known about how proteins assemble into functional multi-protein complexes that are involved in controlling genome function in living cells. In this perspective, we focus on the general mechanism and kinetics of the assembly of multi-protein complexes involved in controlling genome functions, studied using live-cell imaging. We discuss how proteins find their target site on the genome, and give an overview of the binding kinetics of proteins involved in genome controlling processes, such as transcription of rRNA and mRNA genes, replication of the genome and DNA repair. Finally, we discuss how live-cell studies aided by mathematical modelling have unveiled characteristic properties of assembly of multi-protein complexes on the chromatin fibre, which appears to be similar for different genome controlling processes. We argue that complex data sets from kinetic studies are difficult to interpret intuitively and require mathematical modelling to gain comprehensive insight into the dynamic organization and functioning of multi-protein complexes that control genome function.

## How do site-specific proteins find target site on chromatin?

---

Essentially all processes that control genome function are carried out by complexes that contain multiple proteins that assemble on specific genomic sites to exert their function. Assembly of such multi-protein complexes at specific sites is often initiated by proteins with affinity for such specific target site, e.g. DNA lesions, promoters or origins of replication. Several mechanisms have evolved to ensure that site-specific proteins bind their target sites with sufficient rates. Proteins often bind to specific and non-specific sites with similar on-rates. Differences in affinity are often determined by a slower rate of dissociation (30, 57). Site-specific proteins diffuse through the nucleus until they transiently interact with chromatin by chance. Since non-specific (i.e. low affinity) sites are usually present in large excess over specific sites, it is more likely that a protein binds a non-specific site (50). Typically, a protein transiently interacts with a low affinity site on chromatin and then dissociates, diffuses and binds again until it encounters a specific site (i.e. high affinity) from which it dissociates more slowly (18, 49). Some proteins associate *in vitro* with their target sites several orders of magnitude faster than can be accounted for by mere diffusional collisions between proteins and DNA ( $\sim 10^8 \text{ M}^{-1}\text{s}^{-1}$ ) (2, 7, 17, 33, 38, 59). This rapid association can be explained by movement of a protein from its initial non-specific site to its target site by one-dimensional (1D) diffusion along the DNA by a sliding mechanism, which involves electrostatic DNA-protein interactions (2, 9, 24, 61). Many DNA-binding proteins are able to move along a DNA strand without dissociating from it, including restriction enzymes, transcription factors and DNA repair proteins (3, 5, 20-22, 26, 61). However, at physiological ionic strength, proteins only diffuse along the DNA over distances of about 50 bp, suggesting that 1D diffusion is not the main mode of translocation of site-specific proteins (21).

Several examples indicate that also in eukaryotes site-specific proteins have affinity for non-specific DNA sites. For instance, repair factor XPC continuously associates with and dissociates from chromatin and occasionally encounters a lesion that it binds to with higher affinity. More precisely, at each moment 55% of the XPC molecules are bound to DNA for on average 300 ms in undamaged cells (28). These 300 ms possibly represent the time that XPC diffuses along the DNA until it dissociates or encounters a DNA lesion. Other damage recognition proteins, Rad51, Ogg1 and mismatch repair protein MutS, were shown by single molecule techniques to diffuse along double stranded DNA and bind with higher affinity upon encountering a lesion (3, 16, 22, 67). Similarly, proteins involved in transcription initiation were found to move along DNA by 1D diffusion and bind more tightly once encountering promoter regions or other regulatory elements (9, 26). Structural studies support a model in which target binding is coupled to a conformational change in the protein. Such a scenario would reconcile fast 1D diffusion with strong specific interaction of proteins with target sites (10, 17, 35). In eukaryotes, sliding is likely restricted to the linker regions that have no histones bound (20). In agreement, promoter binding by RNA polymerase is equally efficient for promoters in

---

the linker DNA of chromatin in living cells as for promoters in naked DNA (25). Moreover, the C-terminus of p53 was shown to mediate 1D-diffusion along DNA and a p53 mutant lacking this domain was unable to bind specific promoters in vivo (46), suggesting that 1D-diffusion is also important for locating target sites in a chromatin context. Since sliding is mainly due to electrostatic interactions, the sliding properties will be determined by the distribution of (mainly positively) charged residues on the protein surface that interact with DNA. A protein that displays 1D diffusion is often envisioned to track the major groove of DNA, thus spiralling around the helix as it diffuses along the DNA. Another possibility is that proteins diffuse freely on the DNA surface (termed 2D-diffusion). Experiments revealed that such a mechanism is indeed employed by bacterial proteins and modelling showed that 2D diffusion would allow a protein to bypass obstacles such as nucleosomes (36). Therefore, 2D diffusion of proteins might be more relevant in a chromatin context.

Mere 3D diffusion is not sufficient to explain the high rates at which some proteins appear to associate with target sites (24). A mechanism that can increase the rate of binding is 3D diffusion alternated with diffusion along the DNA (either tracking the major groove or by diffusing freely on the cylindrical DNA surface) for short stretches. Clearly, the contribution of 3D and 1D diffusion to finding a target site depends on the biophysical properties of the protein, the number and nature of the binding sites and the concentration of the binding protein.

### **Assembly of multi-protein complexes that control genome function**

Finding a target site by a recognition-protein is only the starting point for genome controlling processes. Upon recognition of an origin of replication, DNA lesion or promoters by a recognition protein, multi-protein complexes are assembled that subsequently carry out replication, DNA repair or transcription. Here, we give an overview of live-cell imaging studies on proteins that form such multi-protein complexes during DNA repair, transcription and replication. First, we discuss the mechanism of protein complex assembly during DNA repair by the nucleotide excision repair system. This process has been studied extensively and may therefore serve as a paradigm for other chromatin-associated processes.

### **Assembly of DNA repair complexes**

To protect the integrity of the genome, multiple DNA repair mechanisms have evolved to deal with specific DNA injuries (13, 27). For example, nucleotide excision repair (NER) removes helix-distorting injuries that affect one of the DNA strands, whereas homologous recombination (HR) and non-homologous end-joining (NHEJ) repair double strand breaks (DSBs) (27). Particularly the kinetics of proteins involved in NER has been well studied. NER involves the assembly of repair complexes that contain tens of polypeptides, which cooperate in space and time. Damage-recognition protein XPC was recently shown to continuously associate and dissociate

---

with chromatin for on average 300 ms per binding event (28). At any moment, about half of the XPC molecules is freely mobile and half immobile, most likely bound to chromatin. It is possible that the chromatin-bound fraction of XPC diffuses along the DNA during this short period, similar to 1D diffusion reported for some restriction enzymes and the lac repressor (9). In the absence of damage, other NER proteins XPA, XPG, and ERCC1/XPF diffuse rapidly through the nucleus with rates that correspond to their molecular size (31, 43, 58, 70). Upon DNA damage induction by for example UV-C light, XPC occasionally encounters a helix-distorting lesion to which it binds more stably ( $t_{1/2} = 25\text{s}$ ) (28). Lesion detection by XPC subsequently triggers assembly of NER complexes at the site of damage from freely diffusing constituents. NER proteins XPG, TFIIH and ERCC1/XPF rapidly exchange ( $t_{1/2} \approx 1\text{ min}$ ) with emerging repair complexes, while XPA exchanges somewhat slower ( $\sim 2\text{ min}$ ) and, as mentioned above, XPC exchanges is somewhat faster ( $t_{1/2} = 25\text{s}$ ) (31, 43, 58, 70). Fast exchange of proteins between the diffusing and bound state may ensure a high free concentration of these factors allowing a dynamic competition for binding sites, which may facilitate cross talk between different processes that control genome function (32). However, this fast exchange also makes the formation of functional multi-protein repair complexes a time-consuming process, since binding of all proteins at the same site at the same time has a very low probability. This means that the binding of individual proteins is not unlikely, but their simultaneous binding at the same site to form a multi-protein complex is. Thus, there will be an ensemble of mostly incomplete assembled repair complexes.

In this scenario, only a few complexes will be functional, having all the necessary repair proteins bound at the same time (Luijsterburg and van Driel, unpublished). This does not exclude that repair complexes containing all the individual components are formed with a relatively high rate. However, the reaction is inefficient in terms of the number of binding events for each individual component required to assembly complete repair complexes. This does not appear specific for DNA repair complexes, since assembly of complexes containing multiple proteins was also shown to be time-consuming during other genome-controlling processes (see below and (6, 8)). Indeed, mathematical modelling suggests that most of the repair time is spent on assembly of functional complexes, which is an inherent property of large multi-protein complexes (Luijsterburg and van Driel, unpublished). NER involves some of the same enzymatic reactions (e.g. helix unwinding and DNA synthesis) that are carried out during transcription and replication, which are performed by proteins that are shared between these different processes, such as TFIIH, RPA and PCNA (29, 41, 65, 66). The nucleoplasmic pool of TFIIH is in a continuous equilibrium between non-bound molecules and molecules engaged/bound in RNA pol I, RNA pol II transcription and NER (if DNA damage is present) (29). Live-cell imaging showed that TFIIH binds to transcription initiation complexes in the order of

---

seconds whereas binding times at DNA damage were in the order of minutes ( $t_{1/2} \sim 50$  s) (29). Similarly, PCNA and RPA are shared factors between replication and several repair pathways including NER (12, 62). PCNA is bound for about 3 minutes during replication, while its exchange rate at sites of DNA damage is almost twice as long ( $t_{1/2} \sim 300$ s). RPA is also more stably associated with repair sites than with replication (62). Thus, it appears that TFIIH, RPA and PCNA have higher affinities for DNA repair intermediates than for sites of transcription and replication, respectively.

Repair of DSBs by homologous recombination involves assembly of a protein complex that is initiated by the formation of a Rad51 nucleo-protein filament and subsequent binding of additional repair proteins such as Rad54, Rad52 and RPA (27, 69). Live cell imaging revealed that Rad51 filaments are highly stable and the binding time of Rad51 proteins is in the order of hours. Exchange rates of Rad52 ( $\sim 1$ min) and Rad54 ( $\sim 10$  s) are much faster (11). Thus, it seems that Rad51 is a structural component during HR, possibly serving as a binding platform for several other repair proteins that exchange rapidly between the bound and free diffusing state. Such a mechanism is reminiscent of replication in which PCNA is bound relatively long.

Besides HR, DSBs can be repaired by NHEJ if a sister chromatid is not present (e.g. in G1), which involves, among others, the ring-shaped Ku70/80 dimer and the kinase DNA-PKcs. Current models suggest that multiple Ku70/80 dimers encircle the broken DNA ends and become trapped there. After ligation of the broken ends, it has been suggested that Ku70/80 could be permanently trapped (44). However, live-cell imaging challenged this model and revealed that binding of Ku70/80 to broken DNA ends is reversible and that exchange between bound and soluble pools occurs within 40s. Similar to Ku70, DNA-PKcs was shown to exchange between soluble and DNA bound pools within 1 min. Nevertheless, when DNA-PKcs cannot be phosphorylated or perform its kinase activity, a much larger fraction of the DNA-PKcs pool is bound for longer times (44, 68). These studies highlight the importance of post-translational modification of repair proteins and show that, in case of DNA-PKcs, phosphorylation decreases the residence times of repair intermediates at the DNA lesion.

Collectively these FRAP studies are in agreement with a model in which repair factors assemble at sites of DNA damage from freely diffusing components and form short-lived complexes on damaged chromatin (11, 29, 31, 44, 58, 70). Affinity differences between specific and non-specific sites (both for protein-protein and for protein-DNA interactions) appear to be small. Likely, the affinity of repair proteins is precisely tuned such that transient binding is sufficient to assemble complexes at specific (in this case damaged) sites with an acceptable rate, while at the same time the low affinity ensures that complete complex assembly at non-specific sites is not very likely. Indeed, a recent study showed that tethering of DSB repair proteins Mre11, Rad50 or Nbs1 to chromatin, thus artificially increasing their

---



affinity for DNA, elicits a DNA damage response that includes activation of Chk1/Chk2 and cell cycle arrest (64). This suggests that binding of a single repair protein with high affinity to non-specific sites is sufficient to trigger a cellular DNA damage response.

### **Assembly of transcription initiation and elongation complexes**

Transcription involves assembly of a multi-protein transcription initiation complex on the chromatin fibre. Various live-cell imaging studies in combination with kinetic modelling have unveiled that, like DNA repair proteins, transcription factors, co-activators and RNA polymerases (RNA pol) bind rapidly and reversibly to target-sites (promoters) in a stochastic fashion (1, 23). Occasionally, these factors assemble in a way that leads to onset of transcription and the production of RNA (6). Several transcription factors and co-activators (e.g. GR, GRIP-1, p53, TFIIB and TFIIH) diffuse rapidly through the nucleus and at any given time about 15% - 25% of these proteins is bound for 3-5 s to chromatin (4, 29, 52). Although short residence times (i.e. several seconds) are common for transcription factors, some have binding times in the order of 1 min (e.g. AR and TBP) (4, 14). The majority (~85%) of RNA pol II in living cells rapidly exchanges within on average 6 s, reflecting reversible binding to promoters or to non-specific sites with low affinity (6). The remaining 15% of RNA pol II molecules binds for on average about 1 min, reflecting transcription initiation attempts at the promoter. About half of these 1 min binding events leads to elongation with ~70 nt/s during which RNA pol II exchanges slowly from transcribed genes (~10 min) (6, 39). These live-cell studies combined with mathematical modelling reveal that only 1% of the RNA pol II binding events at promoters lead to a complete RNA molecule, showing that the majority of RNA pol II-promoter interactions are not productive (6). This at first sight inefficient onset of transcription may indicate that there is only a low probability of forming an active transcription initiation complex at promoters, similar to complex assembly during DNA repair. Recently, the steady-state level of a bound transcription factor to a natural promoter was found to oscillate *in vivo* on a time-scale of 20-40 min after transcription initiation by stimulation with a hormone, while the exchange rate of this transcription factor with chromatin was in the order of 1 min. These slow oscillations in steady-state levels of bound transcription components have also been detected by CHIP (48) and it was suggested that these slow cycles reflect stable interactions of activators with promoters leading to mRNA production, while fast cycles reflect transient interactions of activators that do not result in mRNA production (48). On the other hand, live-cell imaging suggested that rapid exchange (within 1 min) of transcription factors reflects active transcription, whereas slow cycles reflect gradual changes in accessibility of binding sites at promoters (resulting in 20-40 min oscillations) (37). In agreement, the occupancy of histones at promoters was also found to oscillate and to inversely mirror the slow cycle of a transcriptional activator. However, it is currently not clear, why the

---

number of accessible binding sites of transcription factors gradually changes in time and whether this is functionally important for transcription regulation.

In addition to RNA pol II, transcription of rRNA genes by the RNA pol I system is also highly dynamic (8). The majority of pre-initiation factors (UBF1 and 2), transcription factors (TAF<sub>48</sub>) as well as individual subunits of RNA pol I rapidly exchanges within 5 s at rRNA genes, while TFIIF exchange in nucleoli is considerably slower (~25s) (29). Similar to RNA pol II transcription, only 1-3% of the RNA pol I binding events result in elongation, which is inefficient in terms of association/dissociation steps needed to initiate transcription. However, because there are several hundred transcription factors binding events per second, such an 'inefficient' mechanism still results in a relatively fast rate of rRNA production in time. Interestingly, RNA pol I subunits exchange on rRNA promoters about 4 times slower in S-phase, during which the rRNA transcriptional output is much higher than in G1, suggesting that longer binding times of individual RNA pol I subunits to promoters results in more efficient assembly of functional RNA pol I complexes able to produce an rRNA (19). Thus, modulation of RNA pol I assembly kinetics is a mechanism to control the transcriptional output of rRNA genes. In conclusion, these studies show that the assembly of active transcription initiation complexes is inefficient compared to the number of binding events of the individual components, similar to the formation of repair complexes. It is not likely that multiple proteins bind at the same site at the same time. The onset of transcription therefore takes multiple association/dissociation events. Additionally, the 'inefficiency' of complex assembly during transcription serves as a regulatory mechanism that reduces the incorporation of wrong (i.e. non-specific binding) proteins in the complex, a process named kinetic proofreading (see below).

### **Assembly of replication complexes**

Faithful duplication of the genome is essential to maintain genome integrity and cellular identity. Besides DNA polymerases  $\delta$  and  $\epsilon$ , many proteins are involved in replication, including the sliding clamp PCNA, endonuclease Fen1, ssDNA-binding protein RPA and DNA ligase 1 (Lig 1)(19, 42, 45). The leading strand is synthesized continuously during replication, while lagging strand synthesis requires the discontinuous synthesis and joining of Okazaki fragments. Fen1, RPA and Lig 1 (and probably DNA polymerase  $\delta$ ), are specifically required for synthesis of the lagging strand (45). Initiation of replication involves origin recognition complex (ORC) proteins, which bind chromatin and exchange rapidly with soluble pools within 2 min (47). Replication of DNA occurs in discrete areas in the nucleus termed replication foci or factories, which appear at the onset of S phase and disappear as soon as replication is finished (41). These microscopically visible replication foci represent clusters of replication forks and associated replication machineries and are often several MDa in size. Although replication foci appear to be static structures, the proteins that make up these structures exchange rapidly between the bound and freely diffusing pool (40, 49).

---

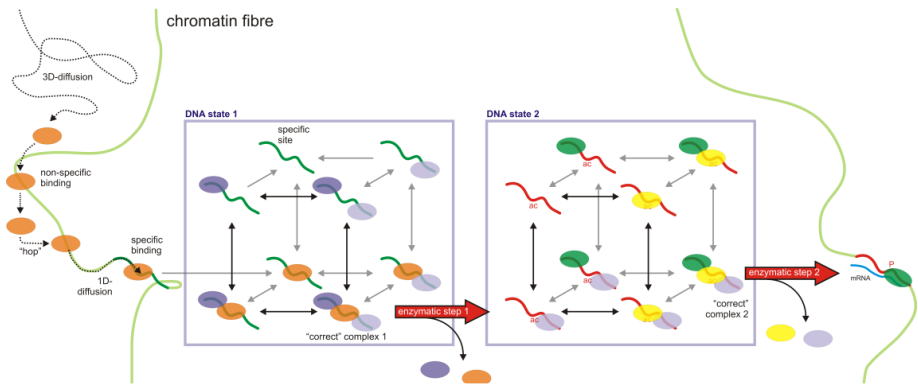


**Fig 1.** Model for binding of a site-specific protein to a target site and subsequent assembly of a multi-protein complex on that site. A site-specific protein (orange oval) diffuses rapidly inside the nucleus and binds non-specifically to chromatin (represented by the light-green line), dissociates and re-binds close to the site it dissociated from (so-called “hopping”). Finally, it moves along chromatin by 1-dimensional diffusion and encounters a specific site (dark-green) to which the protein binds more stably. The orange protein mediates the assembly of a complex consisting of two additional proteins (light-purple and dark-purple). Binding of all these proteins is stochastic and 8 different assembly states can be formed on the specific site consisting of one or a combination of the 3 proteins or the site can be devoid of any protein. Once the “correct” complex containing all 3 proteins is formed, the specific site is modified (for example acetylated shown in red) resulting in dissociation of the orange and dark-purple protein while the light-purple protein remains bound (since it has affinity for the altered state while the other proteins do not). The red arrow reflects an enzymatic step (in this case acetylation, which is in principal irreversible). This altered state is the substrate for a new set of proteins (the green and yellow protein and the light-purple protein from the last box) to bind to. Complex assembly is again stochastic and 8 different assembly states can be formed. Assembly of the “correct” complex containing all three proteins in the second box results in an enzymatic step that produces mRNA, resulting in dissociation of the yellow and light-purple protein. The probability of the overall reaction (i.e. binding of 5 different proteins to the same site) is increased by splitting the reactions in assembly of complex 1 and complex 2 separated by an irreversible enzymatic reaction. The irreversible step drives the reaction forward. Completion of processes involving more proteins can be kinetically driven by multiple irreversible reactions.

Live-cell imaging has shown that there is a remarkable difference in exchange kinetics between different replication proteins to replication foci. For example, exchange of PCNA at replication foci takes about 10 min ( $t_{1/2} \sim 100$  s) (12, 63, 66), while proteins involved in lagging strand synthesis exchange much faster compared to PCNA. For instance, Fen 1 and DNA lig 1 exchange at replication foci takes about 1s (63, 65). Similarly, RPA exchanges within several seconds (66). The exchange rates of these proteins are in the same range as the time it takes to synthesize one Okazaki fragment (estimated at 6 s), which is roughly 180 bp in size (34, 63, 65), suggesting that these proteins bind during the synthesis of one Okazaki fragment and dissociate upon completion of such a fragment. Fen1 and DNA ligase 1 are indeed required for Okazaki fragment maturation, performing removal of the RNA-DNA primer and sealing of the remaining nick, respectively (42). This favours a scenario in which proteins such as RPA,

Fen 1 and DNA lig 1 exchange after each Okazaki fragment has been synthesized, whereas PCNA remains bound for the synthesis of multiple Okazaki fragments (65). This, together with interaction studies, suggests that PCNA serves as a binding platform for many proteins that are transiently involved in replication, including proteins involved in epigenetic maintenance such as Dnmt1, which methylates the newly synthesized DNA during replication (51, 60). The use of a binding platform for transiently interacting proteins is conceptually similar to transcription elongation, during which RNA pol II exchanges very slowly, while other proteins, such as TFIIB or TFIIH, can transiently interact with the active transcription machinery (6). Whether DNA polymerases act similarly to RNA pol II with respect to chromatin interaction kinetics has not been studied so far.

### **Understanding assembly and functioning of genome- controlling complexes**

The live cell study of GFP-tagged proteins involved in chromatin-associated processes generates large and complex sets of data that generally are difficult to interpret intuitively without the aid of deterministic models (i.e. using differential equations) or simulation-based approaches (such as Monte Carlo simulations) (54). Kinetic modelling of quantitative *in vivo* data is a powerful tool in obtaining mechanistic insight into genome-controlling processes. It allows estimation of biophysical properties of proteins such as diffusion rates and association/dissociation rate constants that cannot be determined directly *in vivo*. Moreover, modelling of the kinetic properties of chromatin-associated systems provides detailed insight into their behaviour (6, 8, 56)(Luijsterburg and van Driel, unpublished results). FRAP studies combined with mathematical modelling revealed that proteins only occasionally form a complete protein complex on chromatin. For example, components of the RNA pol I machinery frequently associate with ribosomal genes with a rate of several hundred molecules per second, but only occasionally (1-10% of the binding events) form the correct complex that is capable of transcription (8). Likewise, *in vivo* studies and modelling revealed that only 1% of the RNA pol II-promoter interactions results in completion of an mRNA (6), suggesting the formation of the complete protein complex is a low probability event. Recent modelling of the kinetics of NER in terms of the collective action of eight repair proteins and six enzymatic steps, revealed that protein complex assembly during NER is remarkably slow compared to the enzymatic processes involved in the actual repair steps. More than 99% of the time is spent on the assembly of catalytically active complexes, whereas enzymatic reactions during repair (such as unwinding of DNA and dual incision) take only a small fraction of the total repair time (Luijsterburg and van Driel, unpublished). Although the term inefficient has been used for these processes, it should be noted that if several hundred molecules bind per second and even only 1% of the binding events results in assembly of a

---

functional complex, this still results in complex formation on specific sites at sufficient high rates. In conclusion, a low probability to assemble the correct protein complex appears a shared characteristic of different genome controlling processes. In this scenario, most proteins do not bind in a fixed order, but rather an ensemble of protein complexes with different subunit composition is formed. The correct protein complex, capable of performing a specific function (repair, transcription, replication), is formed with a low probability compared to the number of incomplete complexes that are assembled. This “chaotic” view on complex assembly is radically different from the often-held view that complex assembly on chromatin occurs through an ordered and stepwise mechanism in which each protein is incorporated in a long-lived chromatin-bound complex (13, 15, 56). This stochastic mechanism of complex assembly is schematically depicted in figure 1.

Completion of a process in which assembly of large protein complexes is a low probability event can be kinetically driven by irreversible (often-enzymatic) reactions, which split up the process in smaller sub-processes that are executed sequentially. Such a mechanism, known as kinetic proofreading, increases the specificity of molecular processes above the level of difference in free energy between correct and incorrect substrates (30). This creates a system that rejects 'wrong' proteins, despite the similar on-rates of specific and non-specific interactions. This allows a system to deal with the binding of non-specific proteins to multi-protein complexes. Many genome-controlling processes involve enzymatic reactions including ATP-hydrolysis, DNA unwinding, cleavage of DNA, DNA synthesis and ligation, which due to their often irreversible nature can drive genome controlling processes to completion (see fig 1). Moreover, these irreversible reactions increase the specificity at which multi-protein complexes are assembled to a degree that is not present at the level of individual proteins. Concluding, live-cell analyses combined with mathematical modelling are essential tools for understanding the robust mechanisms to assemble multi-protein complexes at specific sites on the chromatin fibre. This combined approach is expected to provide deep insight into the behaviour of systems that control the genome in years to come.

#### References

1. **Becker, M., C. Baumann, S. John, D. A. Walker, M. Vigneron, J. G. McNally, and G. L. Hager.** 2002. Dynamic behavior of transcription factors on a natural promoter in living cells. *EMBO Rep* **3**:1188-94.
2. **Berg, O. G., R. B. Winter, and P. H. von Hippel.** 1981. Diffusion-driven mechanisms of protein translocation on nucleic acids. 1. Models and theory. *Biochemistry* **20**:6929-48.
3. **Blainey, P. C., A. M. van Oijen, A. Banerjee, G. L. Verdine, and X. S. Xie.** 2006. A base-excision DNA-repair protein finds intrahelical lesion bases by fast sliding in contact with DNA. *Proc Natl Acad Sci U S A* **103**:5752-7.
4. **Chen, D., C. S. Hinkley, R. W. Henry, and S. Huang.** 2002. TBP dynamics in living human cells: constitutive association of TBP with mitotic chromosomes. *Mol Biol Cell* **13**:276-84.

5. **Coppey, M., O. Benichou, R. Voituriez, and M. Moreau.** 2004. Kinetics of target site localization of a protein on DNA: a stochastic approach. *Biophys J* **87**:1640-9.
6. **Darzacq, X., Y. Shav-Tal, V. de Turris, Y. Brody, S. M. Shenoy, R. D. Phair, and R. H. Singer.** 2007. In vivo dynamics of RNA polymerase II transcription. *Nat Struct Mol Biol* **14**:796-806.
7. **Dhavan, G. M., D. M. Crothers, M. R. Chance, and M. Brenowitz.** 2002. Concerted binding and bending of DNA by *Escherichia coli* integration host factor. *J Mol Biol* **315**:1027-37.
8. **Dundr, M., U. Hoffmann-Rohrer, Q. Hu, I. Grummt, L. I. Rothblum, R. D. Phair, and T. Misteli.** 2002. A kinetic framework for a mammalian RNA polymerase in vivo. *Science* **298**:1623-6.
9. **Elf, J., G. W. Li, and X. S. Xie.** 2007. Probing transcription factor dynamics at the single-molecule level in a living cell. *Science* **316**:1191-4.
10. **Erie, D. A., G. Yang, H. C. Schultz, and C. Bustamante.** 1994. DNA bending by Cro protein in specific and nonspecific complexes: implications for protein site recognition and specificity. *Science* **266**:1562-6.
11. **Essers, J., A. B. Houtsmuller, L. van Veelen, C. Paulusma, A. L. Nigg, A. Pastink, W. Vermeulen, J. H. Hoeijmakers, and R. Kanaar.** 2002. Nuclear dynamics of RAD52 group homologous recombination proteins in response to DNA damage. *Embo J* **21**:2030-7.
12. **Essers, J., A. F. Theil, C. Baldeyron, W. A. van Cappellen, A. B. Houtsmuller, R. Kanaar, and W. Vermeulen.** 2005. Nuclear dynamics of PCNA in DNA replication and repair. *Mol Cell Biol* **25**:9350-9.
13. **Essers, J., W. Vermeulen, and A. B. Houtsmuller.** 2006. DNA damage repair: anytime, anywhere? *Curr Opin Cell Biol* **18**:240-6.
14. **Farla, P., R. Hersmus, B. Geverts, P. O. Mari, A. L. Nigg, H. J. Dubbink, J. Trapman, and A. B. Houtsmuller.** 2004. The androgen receptor ligand-binding domain stabilizes DNA binding in living cells. *J Struct Biol* **147**:50-61.
15. **Feuerhahn, S., and J. M. Egly.** 2008. Tools to study DNA repair: what's in the box? *Trends Genet.*
16. **Gorman, J., A. Chowdhury, J. A. Surtees, J. Shimada, D. R. Reichman, E. Alani, and E. C. Greene.** 2007. Dynamic basis for one-dimensional DNA scanning by the mismatch repair complex Msh2-Msh6. *Mol Cell* **28**:359-70.
17. **Gorman, J., and E. C. Greene.** 2008. Visualizing one-dimensional diffusion of proteins along DNA. *Nat Struct Mol Biol* **15**:768-74.
18. **Gorski, S. A., M. Dundr, and T. Misteli.** 2006. The road much traveled: trafficking in the cell nucleus. *Curr Opin Cell Biol* **18**:284-90.
19. **Gorski, S. A., S. K. Snyder, S. John, I. Grummt, and T. Misteli.** 2008. Modulation of RNA polymerase assembly dynamics in transcriptional regulation. *Mol Cell* **30**:486-97.
20. **Gowers, D. M., and S. E. Halford.** 2003. Protein motion from non-specific to specific DNA by three-dimensional routes aided by supercoiling. *Embo J* **22**:1410-8.
21. **Gowers, D. M., G. G. Wilson, and S. E. Halford.** 2005. Measurement of the contributions of 1D and 3D pathways to the translocation of a protein along DNA. *Proc Natl Acad Sci U S A* **102**:15883-8.
22. **Graneli, A., C. C. Yeykal, R. B. Robertson, and E. C. Greene.** 2006. Long-distance lateral diffusion of human Rad51 on double-stranded DNA. *Proc Natl Acad Sci U S A* **103**:1221-6.
23. **Hager, G. L., C. Elbi, T. A. Johnson, T. Voss, A. K. Nagaich, R. L. Schiltz, Y. Qiu, and S. John.** 2006. Chromatin dynamics and the evolution of alternate promoter states. *Chromosome Res* **14**:107-16.
24. **Halford, S. E., and J. F. Marko.** 2004. How do site-specific DNA-binding proteins find their targets? *Nucleic Acids Res* **32**:3040-52.
25. **Hannon, R., E. G. Richards, and H. J. Gould.** 1986. Facilitated diffusion of a DNA binding protein on chromatin. *Embo J* **5**:3313-9.
26. **Harada, Y., T. Funatsu, K. Murakami, Y. Nonoyama, A. Ishihama, and T. Yanagida.** 1999. Single-molecule imaging of RNA polymerase-DNA interactions in real time. *Biophys J* **76**:709-15.

- 
27. **Hoeijmakers, J. H.** 2001. Genome maintenance mechanisms for preventing cancer. *Nature* **411**:366-74.
  28. **Hoogstraten, D., S. Bergink, V. H. M. Verbiest, M. S. Luijsterburg, B. Geverts, A. Raams, C. Dinant, J. H. J. Hoeijmakers, W. Vermeulen, and A. B. Houtsmuller.** 2008. Versatile DNA damage detection by the global genome nucleotide excision repair protein XPC. *J Cell Sci*;jcs.031708.
  29. **Hoogstraten, D., A. L. Nigg, H. Heath, L. H. Mullenders, R. van Driel, J. H. Hoeijmakers, W. Vermeulen, and A. B. Houtsmuller.** 2002. Rapid switching of TFIIH between RNA polymerase I and II transcription and DNA repair in vivo. *Mol Cell* **10**:1163-74.
  30. **Hopfield, J. J.** 1974. Kinetic proofreading: a new mechanism for reducing errors in biosynthetic processes requiring high specificity. *Proc Natl Acad Sci U S A* **71**:4135-9.
  31. **Houtsmuller, A. B., S. Rademakers, A. L. Nigg, D. Hoogstraten, J. H. Hoeijmakers, and W. Vermeulen.** 1999. Action of DNA repair endonuclease ERCC1/XPF in living cells. *Science* **284**:958-61.
  32. **Houtsmuller, A. B., and W. Vermeulen.** 2001. Macromolecular dynamics in living cell nuclei revealed by fluorescence redistribution after photobleaching. *Histochem Cell Biol* **115**:13-21.
  33. **Hsieh, M., and M. Brenowitz.** 1997. Comparison of the DNA association kinetics of the Lac repressor tetramer, its dimeric mutant Lacladi, and the native dimeric Gal repressor. *J Biol Chem* **272**:22092-6.
  34. **Jackson, D. A., and A. Pombo.** 1998. Replicon clusters are stable units of chromosome structure: evidence that nuclear organization contributes to the efficient activation and propagation of S phase in human cells. *J Cell Biol* **140**:1285-95.
  35. **Kalodimos, C. G., N. Biris, A. M. Bonvin, M. M. Levandoski, M. Guenneugues, R. Boelens, and R. Kaptein.** 2004. Structure and flexibility adaptation in nonspecific and specific protein-DNA complexes. *Science* **305**:386-9.
  36. **Kampmann, M.** 2004. Obstacle bypass in protein motion along DNA by two-dimensional rather than one-dimensional sliding. *J Biol Chem* **279**:38715-20.
  37. **Karpova, T. S., M. J. Kim, C. Spriet, K. Nalley, T. J. Stasevich, Z. Kherrouche, L. Heliot, and J. G. McNally.** 2008. Concurrent fast and slow cycling of a transcriptional activator at an endogenous promoter. *Science* **319**:466-9.
  38. **Kim, J. G., Y. Takeda, B. W. Matthews, and W. F. Anderson.** 1987. Kinetic studies on Cro repressor-operator DNA interaction. *J Mol Biol* **196**:149-58.
  39. **Kimura, H., K. Sugaya, and P. R. Cook.** 2002. The transcription cycle of RNA polymerase II in living cells. *J Cell Biol* **159**:777-82.
  40. **Kitamura, E., J. J. Blow, and T. U. Tanaka.** 2006. Live-cell imaging reveals replication of individual replicons in eukaryotic replication factories. *Cell* **125**:1297-308.
  41. **Leonhardt, H., H. P. Rahn, P. Weinzierl, A. Sporbert, T. Cremer, D. Zink, and M. C. Cardoso.** 2000. Dynamics of DNA replication factories in living cells. *J Cell Biol* **149**:271-80.
  42. **Liu, Y., H. I. Kao, and R. A. Bambara.** 2004. Flap endonuclease 1: a central component of DNA metabolism. *Annu Rev Biochem* **73**:589-615.
  43. **Luijsterburg, M. S., J. Goedhart, J. Moser, H. Kool, B. Geverts, A. B. Houtsmuller, L. H. Mullenders, W. Vermeulen, and R. van Driel.** 2007. Dynamic in vivo interaction of DDB2 E3 ubiquitin ligase with UV-damaged DNA is independent of damage-recognition protein XPC. *J Cell Sci* **120**:2706-16.
  44. **Mari, P. O., B. I. Florea, S. P. Persengiev, N. S. Verkaik, H. T. Bruggenwirth, M. Modesti, G. Giglia-Mari, K. Bezstarosti, J. A. Demmers, T. M. Luider, A. B. Houtsmuller, and D. C. van Gent.** 2006. Dynamic assembly of end-joining complexes requires interaction between Ku70/80 and XRCC4. *Proc Natl Acad Sci U S A* **103**:18597-602.
  45. **McCulloch, S. D., and T. A. Kunkel.** 2008. The fidelity of DNA synthesis by eukaryotic replicative and translesion synthesis polymerases. *Cell Res* **18**:148-61.
  46. **McKinney, K., M. Mattia, V. Gottifredi, and C. Prives.** 2004. p53 linear diffusion along DNA requires its C terminus. *Mol Cell* **16**:413-24.
-

47. **McNairn, A. J., Y. Okuno, T. Misteli, and D. M. Gilbert.** 2005. Chinese hamster ORC subunits dynamically associate with chromatin throughout the cell-cycle. *Exp Cell Res* **308**:345-56.
  48. **Metivier, R., G. Reid, and F. Gannon.** 2006. Transcription in four dimensions: nuclear receptor-directed initiation of gene expression. *EMBO Rep* **7**:161-7.
  49. **Misteli, T.** 2007. Beyond the sequence: cellular organization of genome function. *Cell* **128**:787-800.
  50. **Misteli, T.** 2008. Physiological importance of RNA and protein mobility in the cell nucleus. *Histochem Cell Biol* **129**:5-11.
  51. **Moldovan, G. L., B. Pfander, and S. Jentsch.** 2007. PCNA, the maestro of the replication fork. *Cell* **129**:665-79.
  52. **Mueller, F., P. Wach, and J. G. McNally.** 2008. Evidence for a common mode of transcription factor interaction with chromatin as revealed by improved quantitative fluorescence recovery after photobleaching. *Biophys J* **94**:3323-39.
  53. **Phair, R. D., and T. Misteli.** 2000. High mobility of proteins in the mammalian cell nucleus. *Nature* **404**:604-9.
  54. **Phair, R. D., and T. Misteli.** 2001. Kinetic modelling approaches to in vivo imaging. *Nat Rev Mol Cell Biol* **2**:898-907.
  55. **Phair, R. D., P. Scaffidi, C. Elbi, J. Vecerova, A. Dey, K. Ozato, D. T. Brown, G. Hager, M. Bustin, and T. Misteli.** 2004. Global nature of dynamic protein-chromatin interactions in vivo: three-dimensional genome scanning and dynamic interaction networks of chromatin proteins. *Mol Cell Biol* **24**:6393-402.
  56. **Politi, A., M. J. Moné, A. B. Houtsmuller, D. Hoogstraten, W. Vermeulen, R. Heinrich, and R. van Driel.** 2005. Mathematical Modeling of Nucleotide Excision Repair Reveals Efficiency of Sequential Assembly Strategies. *Mol Cell* **19**:679-690.
  57. **Qian, H.** 2008. Cooperativity and specificity in enzyme kinetics: a single-molecule time-based perspective. *Biophys J* **95**:10-7.
  58. **Rademakers, S., M. Volker, D. Hoogstraten, A. L. Nigg, M. J. Moné, A. A. Van Zeeland, J. H. Hoeijmakers, A. B. Houtsmuller, and W. Vermeulen.** 2003. Xeroderma pigmentosum group A protein loads as a separate factor onto DNA lesions. *Mol Cell Biol* **23**:5755-67.
  59. **Riggs, A. D., S. Bourgeois, and M. Cohn.** 1970. The lac repressor-operator interaction. 3. Kinetic studies. *J Mol Biol* **53**:401-17.
  60. **Schermelleh, L., A. Haemmer, F. Spada, N. Rosing, D. Meilinger, U. Rothbauer, M. C. Cardoso, and H. Leonhardt.** 2007. Dynamics of Dnmt1 interaction with the replication machinery and its role in postreplicative maintenance of DNA methylation. *Nucleic Acids Res* **35**:4301-12.
  61. **Shimamoto, N.** 1999. One-dimensional diffusion of proteins along DNA. Its biological and chemical significance revealed by single-molecule measurements. *J Biol Chem* **274**:15293-6.
  62. **Solomon, D. A., M. C. Cardoso, and E. S. Knudsen.** 2004. Dynamic targeting of the replication machinery to sites of DNA damage. *J Cell Biol* **166**:455-63.
  63. **Solovjeva, L., M. Svetlova, L. Sasina, K. Tanaka, M. Saijo, I. Nazarov, M. Bradbury, and N. Tomilin.** 2005. High Mobility of Flap Endonuclease 1 and DNA Polymerase {eta} Associated with Replication Foci in Mammalian S-Phase Nucleus. *Mol Biol Cell* **16**:2518-28.
  64. **Soutoglou, E., and T. Misteli.** 2008. Activation of the cellular DNA damage response in the absence of DNA lesions. *Science* **320**:1507-10.
  65. **Sporbert, A., P. Domaing, H. Leonhardt, and M. C. Cardoso.** 2005. PCNA acts as a stationary loading platform for transiently interacting Okazaki fragment maturation proteins. *Nucleic Acids Res* **33**:3521-8.
  66. **Sporbert, A., A. Gahl, R. Ankerhold, H. Leonhardt, and M. C. Cardoso.** 2002. DNA polymerase clamp shows little turnover at established replication sites but sequential de novo assembly at adjacent origin clusters. *Mol Cell* **10**:1355-65.
  67. **Tafvizi, A., F. Huang, J. S. Leith, A. R. Fersht, L. A. Mirny, and A. M. van Oijen.** 2008. Tumor suppressor p53 slides on DNA with low friction and high stability. *Biophys J* **95**:L01-3.
-



68. **Uematsu, N., E. Weterings, K. Yano, K. Morotomi-Yano, B. Jakob, G. Taucher-Scholz, P. O. Mari, D. C. van Gent, B. P. Chen, and D. J. Chen.** 2007. Autophosphorylation of DNA-PKCS regulates its dynamics at DNA double-strand breaks. *J Cell Biol* **177**:219-29.
69. **Wyman, C., and R. Kanaar.** 2006. DNA double-strand break repair: all's well that ends well. *Annu Rev Genet* **40**:363-83.
70. **Zotter, A., M. S. Luijsterburg, D. O. Warmerdam, S. Ibrahim, A. Nigg, W. A. van Cappellen, J. H. Hoeijmakers, R. van Driel, W. Vermeulen, and A. B. Houtsmuller.** 2006. Recruitment of the nucleotide excision repair endonuclease XPG to sites of UV-induced dna damage depends on functional TFIIH. *Mol Cell Biol* **26**:8868-79.



## Summary

### Summary

Genetic information is stored in DNA. Cells use this information to make mRNA, which is translated into proteins. Because errors in protein production can lead to cancer, aging and other defects, the integrity of the DNA is ultimately important for life. Many different sources, both exogenous and endogenous, can challenge the integrity of DNA by causing many different types of lesions. Several DNA repair mechanisms have evolved that deal with these lesions. In eukaryotic cells, DNA is bound by many structural and regulatory proteins together referred to as chromatin. The most important and abundant chromatin proteins are histones. Four pairs of histones come together to form a nucleosome, around which approximately 146 basepairs of DNA are wrapped. Chromatin forms a barrier for many proteins involved in for example transcription and DNA repair. Therefore, in order to allow these processes to efficiently proceed, the structure of chromatin has to be locally adapted when access of these processes is required. In **chapter 1** the process of chromatin remodeling, mainly with respect to one repair pathway, nucleotide excision repair (NER), is discussed in light of what is known about chromatin remodeling during transcription. As expected, many of the chromatin remodeling activities that are essential to allow access of transcription proteins to DNA, are also active during DNA repair. However, some remodeling factors that are present at sites of DNA damage are known to inhibit transcription rather than activate it. These factors might either be involved in restoration of the chromatin after repair has taken place, or in inhibition of transcription after DNA damage induction, which is known to occur during NER.

**Chapter 2** gives an introduction to the main tool used in the experimental chapters 3-6: fluorescence microscopy. Mainly emphasized are confocal laser scanning microscopy and techniques that can be applied to living cells, such as FRAP, FRET and DNA damage induction by lasers. A revolutionary discovery that made it possible to study proteins in living cells with fluorescence microscopy is that of the green fluorescent protein (GFP). DNA coding for GFP can be linked to DNA coding for almost any protein of interest and expression of this gene fusion in cells allows monitoring of the localization and behavior of this protein by fluorescently visualizing its GFP tag. Many variants of GFP, with enhanced characteristics and different colors, are available allowing simultaneous detection of multiple proteins in almost any type of cell. When two fluorescent molecules come in close proximity to each other (<10 nm), energy transfer can occur if the emission wavelength of the energy donor overlaps with the excitation wavelength of the acceptor. This process is called fluorescence resonance energy transfer (FRET) and it is used to study protein-protein interactions of proteins tagged with variants of GFP. Higher overlap between the donor emission wavelength and the acceptor excitation wavelength results in higher FRET efficiencies, but two fluorescent proteins that overlap too much are difficult to separately visualize on a microscope. In **chapter 3** a technique is described

---

that uses GFP and YFP (yellow) as FRET donor and acceptor, which have a too high overlap between emission and excitation wavelengths for conventional detection. We used spectral imaging and linear unmixing to separately visualize GFP and YFP and found that this couple has a very high FRET efficiency and, by using two DNA repair proteins ERCC1 and XPF, that it can be used to study protein-protein interactions in living cells.

A very important tool in the study of the DNA damage response (DDR) is induction of DNA damage at small regions within a living cell nucleus. The recruitment of many proteins involved in the DDR to such areas of DNA damage can be visualized in living cells by tagging them with GFP (or a color variant). In **chapter 4** we analyze and discuss three methods of laser-assisted local DNA damage induction, some of which we developed ourselves. It is concluded that irradiation with lasers will in general activate multiple repair pathways, with the exception of low doses of UV-C, which seems to activate NER specifically. In this chapter we also describe the direct connection of a UV-C laser to a confocal microscope that has been equipped with quartz optics (glass absorbs UV-C) to induce NER-repaired lesions in small areas in living cell nuclei and immediately monitor the response in real time.

**Chapter 5** deals with the involvement of heterochromatin protein 1 (HP1) in the DNA damage response. HP1 is known to be involved in the stabilization of heterochromatin, the dense form of chromatin which is thought to be non-permissive for transcription. We found that HP1 is recruited to areas of local UV-C-induced DNA damage and that it does not require expression of NER proteins for this recruitment. Furthermore we determined that the domain of HP1 that is responsible for this recruitment is different from the domain involved in heterochromatin stabilization and that its absence in a nematode worm renders it highly sensitive to UV irradiation. These results show that HP1 is involved in a novel DDR pathway.

One type of chromatin remodeling taking place during transcription and replication is the dissociation and re-association of histone proteins to the DNA. In **chapter 6** we describe experiments that show that histones H2A and H2B rapidly exchange from chromatin at areas of local UV-C damage. This faster exchange is not dependent on the expression of NER proteins but requires the histone chaperone protein FACT. Another H2A/H2B chaperone, NAP1L1, is not involved in this accelerated exchange.

In the final chapter, **chapter 7**, we review the process of target-site identification and complex formation on chromatin by DNA repair, transcription and replication proteins. We discuss how a combination of 3D and 1D diffusion along the DNA helix allows rapid target-site identification and we explain how the process of kinetic proofreading allows formation of specific complexes by inserting irreversible reactions in the assembly mechanism. We argue that computer modeling is required to accurately interpret the massive data sets acquired in protein kinetics studies.

This thesis represents a research period that focused on both the development of new microscopy techniques and the application of these

---

## Summary

---

techniques to study basic questions with regard to the cellular DDR. This work resulted in new insights in the response to DNA damage besides the known pathways of DNA repair. Furthermore, regarding two topics that are often overlooked, the first and last chapters give an essential overview on chromatin remodeling during the DDR and mechanistic insight into protein complex formation, respectively.

## Samenvatting

Genetische informatie is opgeslagen op het DNA. Deze informatie wordt door cellen gebruikt om mRNA mee te maken, wat vervolgens wordt vertaald in eiwitten. Een fout in de productie van een eiwit kan leiden tot kankervorming of andere afwijkingen en daarom is de stabiliteit van de informatie op het DNA buitengewoon belangrijk voor leven. Vele verschillende soorten schades worden voortdurend aan DNA gevormd en een aantal DNA schade herstel mechanismen zijn in de loop van de tijd geëvolueerd om de meesten van deze schades weer te verwijderen. In eukaryotische cellen is DNA gebonden aan een hoop eiwitten, waaronder histonen. De stabiele structuur die DNA samen met histonen maakt, heet chromatine. Vier paar histon eiwitten samen met 146 baseparen eromheengewikkeld DNA vormen een nucleosoom, het herhalende element van chromatine. De compacte structuur van chromatine is een obstakel voor eiwitten die toegang nodig hebben tot DNA, om bijvoorbeeld transcriptie of DNA herstel uit te voeren. Om deze processen efficiënt uit te kunnen voeren, moet chromatine eerst worden ge'remodeled'. In **hoofdstuk 1** wordt chromatine remodeling besproken voornamelijk met betrekking tot één specifiek DNA herstel mechanism, NER (nucleotide excision repair), in vergelijking met wat bekend is over chromatine remodeling tijdens transcriptie. Zoals verwacht zijn veel van de chromatine remodeling activiteiten die noodzakelijk zijn voor transcriptie, ook actief tijdens NER. Nochtans zijn er ook remodeling eiwitten aanwezig op beschadigd DNA die een inhiberende, in plaats van een activerende invloed op transcriptie hebben. Mogelijk zijn deze eiwitten nodig om het chromatine, nadat NER is afgerond, weer te herstellen, of om transcriptie te remmen na DNA schade inductie.

**Hoofdstuk 2** geeft een introductie in de voornaamste techniek die in hoofdstukken 3-6 wordt gebruikt: microscopie. Nadruk wordt gelegd op confocale microscopie en methodes die kunnen worden toegepast op levende cellen, zoals, FRAP, FLIP en DNA schade inductie met behulp van lasers. Waarschijnlijk een van de belangrijkste ontdekking voor de celbiologie is die van GFP (groen fluorescerend eiwit). DNA dat codeert voor GFP kan worden gefuseerd met DNA dat codeert voor bijna elk eiwit en na expressie van dit fusie-eiwit in cellen kan de lokalisatie en het gedrag van dit eiwit worden bestudeerd door middel van visualisatie van GFP. Vele varianten van GFP zijn inmiddels beschikbaar met andere kleuren en verbeterde eigenschappen waardoor gelijktijdige visualisatie van verschillende eiwitten in bijna elk celttype mogelijk is.

Wanneer twee fluorescente moleculen dichter dan 10 nanometer bij elkaar in de buurt komen kan energie overdracht plaatsvinden als het emissie spectrum van de energie donor overlapt met het excitatie spectrum van de acceptor. Dit proces heet fluorescence resonance energy transfer (FRET) en het wordt gebruikt om eiwit-eiwit interacties te bestuderen van eiwitten die zijn gefuseerd met GFP varianten. Hoe groter de overlap tussen het donor

---

emissie spectrum en het acceptor excitatie spectrum hoe hoger de energie overdracht, maar twee fluorescente moleculen met een te grote overlap zijn moeilijk van elkaar te scheiden op een microscoop. In **hoofdstuk 3** wordt een methode beschreven waar twee fluorescente moleculen met een grote spectrale overlap, GFP en YFP (yellow fluorescent protein), worden gebruikt als donor en acceptor voor FRET. Door middel van spectral imaging en lineair ontmengen konden GFP en YFP gescheiden van elkaar gedetecteerd worden. We toonden aan dat dit FRET koppel een hoge FRET efficiëntie heeft en door de NER eiwitten ERCC1 en XPF met GFP en YFP, respectievelijk, te fuseren dat de methode geschikt is voor het bestuderen van eiwit-eiwit interacties in levende cellen.

Een belangrijke techniek voor het bestuderen van de DNA schade respons (DDR) is het beschadigen van DNA in klein gebiedje binnen de kern van een levende cel. De ophoping van veel DNA schade respons eiwitten is aangetoond door ze te fuseren met GFP of varianten van GFP. In **hoofdstuk 4** analyseren we drie technieken om lokaal DNA schade te induceren met lasers. Bestraling met lasers resulteert meestal in activatie van meer dan één schade herstel systeem, met uitzondering van UV-C bestraling, waardoor alleen NER geactiveerd wordt. In dit hoofdstuk wordt ook de installatie van een UV-C laser aan een met kwarts optica uitgeruste confocale microscoop beschreven (glas absorbeert UV-C), waarmee de directe NER respons op UV-C schade in levende cellen kan worden bestudeerd.

**Hoofdstuk 5** beschrijft de betrokkenheid van heterochromatine eiwit 1 (HP1) in de DNA schade respons. Van HP1 is bekend dat het een functie heeft in de stabilisatie van heterochromatine, een compacte vorm van chromatine waarin in het algemeen geen transcriptie kan plaatsvinden. Wij toonden aan dat HP1 ophoopt in DNA-beschadigde gebieden en dat deze ophoping onafhankelijk is van de aanwezigheid van reparatie eiwitten. Bovendien laten we zien dat het deel van HP1 dat verantwoordelijk is voor deze ophoping niet hetzelfde is als het deel dat betrokken is bij de heterochromatine-stabilisatie functie van HP1 en dat het weghalen van de twee HP1 homologen in *Caenorhabditis elegans* (een rondworm) resulteert in hypersensitiviteit voor UV bestraling. Deze resultaten laten zien dat HP1 essentieel is voor een tot nog toe onbekend DNA schade respons systeem.

Een manier van chromatine remodeling die plaatsvindt tijdens transcriptie en replicatie is de dissociatie en re-associatie van histon eiwitten aan DNA. In **hoofdstuk 6** beschrijven we experimenten die aantonen dat histonen H2A en H2B sneller uitgewisseld worden op gebieden in de celkern die DNA schade bevatten dan in de rest van de kern. Deze versnelde uitwisseling van H2A en H2B vereist niet de aanwezigheid van NER eiwitten, maar het is wel afhankelijk van histon chaperone eiwit FACT. Een ander histon chaperone eiwit, NAP1L1, is niet nodig voor deze versnelde uitwisseling.

Het laatste hoofdstuk, **hoofdstuk 7**, is een review van het proces van eiwit complex vorming op DNA door transcriptie, replicatie en schade herstel systemen. We bespreken hoe herkennings-eiwitten door middel van een

---



combinatie van 3D en 1D diffusie langs de DNA helix snel hun doel-sequentie of schade lokatie vinden en hoe 'kinetic proofreading' ervoor zorgt dat eiwitcomplexen met de juiste samenstelling kunnen worden gevormd door 'onomkeerbare' stappen in te voegen in het assemblage proces. Ook beargumenteren wij dat modelering met behulp van computers nodig is om de grote data sets die voortkomen uit eiwit dynamiek studies te kunnen analyseren.

Dit proefschrift kwam voort uit een onderzoeksperiode waarin ik mij richtte op zowel de ontwikkeling van nieuwe microscopie technieken als de toepassing van deze technieken in studies naar de DNA schade respons. Uit dit werk zijn nieuwe inzichten voortgekomen in de cellulaire respons op DNA schade buiten de bekende reparatie systemen. Bovendien geven het eerste en laatste hoofdstuk een overzicht van twee processen die vaak over het hoofd worden gezien, chromatine remodeling tijdens schade herstel en eiwit complex vorming van DNA-manipulerende systemen.

**Curriculum vitae**

Naam	Christoffel Dinant
Geboren	Amsterdam, 13-04-1979
2008	Post-doc in het lab van Dr. Jiri Lukas en Dr. Jiri Bartek, Dept. of Cell-Cycle and Cancer, Institute of Cancer Biology, Kopenhagen, Denemarken
2003-2008	Promotie onderzoek Erasmus MC Rotterdam, afdeling Celbiologie en Genetica en afdeling Pathologie  Promotor: Prof. Dr. J.H.J. Hoeijmakers Co-promotor: Dr. W. Vermeulen Co-promotor: Dr. A. B. Houtsmuller
1997-2003	Studie Biologie, Universiteit van Amsterdam
2002	Stage in het lab van Dean Jackson, UMIST, Manchester, UK
2001	Stage in het lab van Roel van riel, UvA, Amsterdam
1991-1997	VWO, Christelijk Gymnasium, Utrecht

---

**List of publications**

**Mone, M. J., Bernas, T., Dinant, C., Goedvree, F. A., Manders, E. M., Volker, M., Houtsmuller, A. B., Hoeijmakers, J. H., Vermeulen, W. and van Driel, R. (2004).** In vivo dynamics of chromatin-associated complex formation in mammalian nucleotide excision repair. *Proc Natl Acad Sci U S A* **101**, 15933-7.

**Giglia-Mari, G., Miquel, C., Theil, A. F., Mari, P. O., Hoogstraten, D., Ng, J. M., Dinant, C., Hoeijmakers, J. H. and Vermeulen, W. (2006).** Dynamic Interaction of TTDA with TFIIH Is Stabilized by Nucleotide Excision Repair in Living Cells. *PLoS Biol* **4**, e156.

**Dinant, C., de Jager, M., Essers, J., van Cappellen, W. A., Kanaar, R., Houtsmuller, A. B. and Vermeulen, W. (2007).** Activation of multiple DNA repair pathways by sub-nuclear damage induction methods. *J Cell Sci* **120**, 2731-40.

**Dinant, C., van Royen, M. E., Vermeulen, W. and Houtsmuller A. B. (2008).** Fluorescence Resonance Energy Transfer of GFP and YFP by Spectral Imaging and Quantitative Acceptor Photobleaching. *J Microsc* **231**(Pt 1): 97-104

**Hoogstraten, D., Bergink, S., Verbiest, V. H. M., Luijsterburg, M. S., Geverts, B., Raams, A., Dinant, C., Hoeijmakers, J. H. J., Vermeulen, W. and Houtsmuller, A. B. (2008).** Versatile DNA damage probing by the global genome nucleotide excision repair protein XPC. *J Cell Sci* **121**, 2850-9

**Dinant, C., Luijsterburg, M. S., Wiernasz, E., Lans, H., Stap, J., Fousteri, M. I., Warmerdam, D. O., Brink, M. C., Lagerwerf, S., Dobrucki, J. W., Jansen, W., Vermeulen, W., Mullenders, L. H. F., Houtsmuller, A. B., Verschure, P. J. and van Driel, R. (2008).** Heterochromatin Protein 1 is involved in the DNA damage response. *Submitted*

**Nishi, R., Alekseev, S., Dinant, C., Hoogstraten, D., Houtsmuller, A. B., Hoeijmakers, J. H. J., Vermeulen, W., Hanaoka, F. and Sugawara, K. (2008).** UV-DDB dependent regulation of nucleotide excision repair kinetics in living cells. *Submitted*

**Dinant, C., Luijsterburg, M. S., Vermeulen, W., Houtsmuller, A. B. and van Driel, R. (2008).** Assembly of multi-protein complexes that control genome function. *Submitted*

---

**Dinant, C., Houtsmuller, A. B. and Vermeulen, W. (2008).** Nucleotide excision repair in a chromatin context. *Submitted*

**Verbiest, V., Mari, P. O., Gourdin, A., Dinant, C., Sabioneda, S., Wijgers, N., Lehmann, A., Vermeulen, W. and Giglia-Mari, G. (2008).** New applications of the live-cell DNA marker Draq5 in spatio-temporal analysis of chromatin-associated processes. *Manuscript in preparation*

**Bergink, S., Dinant, C., Toussaint, W., Alekseev, S., Yousaf, H., Hoogstraten, D., Nishi, R., Geverts, B., Houtsmuller, A. B., Sugasawa, K., Hoeijmakers, J. H. J. and Vermeulen, W. (2008).** Rad23 facilitates XPC binding to damaged DNA and dissociates from the immobilized complex. *Manuscript in preparation*

## Dankwoord

Een promotie onderzoek doe je niet alleen. Daarom zal ik op deze laatste pagina alle personen die mij hebben gesteund en geholpen proberen de dank te geven die hen toekomt. Na de stellingen is dit deel van een proefschrift volgens mij het meestgelezen stuk, dus ik voel de druk om eerlijk en vooral aardig te blijven en er niet een 'ondankswoord' van te maken. So, here we go.

Adriaan, *ondanks* de ongeschiktheid van dit boekje als platform voor grappen, doe ik het hierbij toch. Nee, maar nu serieus. Jij bent zo iemand die je maar een paar keer in je leven tegenkomt. Jouw intelligentie en fascinatie voor zo veel verschillende dingen hebben mij de afgelopen (bijna) vijf jaar heel veel inspiratie gegeven. Ik zal vooral de openhartigheid waarmee jij de vele misstanden in onze samenleving weet aan te kaarten erg missen. Wim, ik heb onder jouw hoede heel veel vrijheid gekregen om mijn eigen richting op te gaan en voor mij interessante proeven te doen. Maar je was er tegelijkertijd ook om mijn resultaten in de juiste context te plaatsen, bedankt.

Jan, wij hebben elkaar gedurende mijn periode in jouw afdeling niet heel veel gesproken en daar spreekt denk ik jouw vertrouwen in mij uit. Ik hoop dat ik je vertrouwen niet heb beschaamd. Besprekingen met jou zijn altijd erg inspirerend omdat jij altijd de vinger op de zere plek weet te leggen. Daardoor heb ik heel veel van jou geleerd in de afgelopen vijf jaar.

Thanks to my promotion committee for critical reading and suggestions.

Dan celbiologie en genetica: Ambra and P.O., thanks for the support and the many interesting discussions we've had and the best of luck in la France! Ana, thanks for your beautiful smile. Talking with you always made me happy. Arjan, bedankt voor de altijd nuttige ondersteuning, je enthousiasme, je grappen, je zang en natuurlijk de FACS. Audrey, working with you was always interesting and fun. I very much appreciate how easy it is to talk with you about so many subjects. Nils, bedankt voor je technische ondersteuning, FACS en interessante gespreksonderwerpen naast wetenschap. Lise, good luck in Singapore! Jurgen, in iets meer dan een jaar heb je mij een voorbeeld gegeven hoe een beginnende post-doc in een nieuw lab te zijn. Hannes, heiden als ik ben vond ik het altijd erg fascinerend met jouw over religie te praten. Je muzieksmaak maakt alles meer dan goed! Marieke, bedankt voor de snowboardlessen en het vaak nuttige uitbalanceren van mijn traagheid met jouw snelheid. Eugin, Filippo, Erik, Sander, ik mis poker! Ons bungalowweekend was een hoogtepunt in vijf jaar Rotterdam. Blij dat we foto's (en een film!) hebben. Tiago, Debbie, Alireza, Harald, thanks for the great times outside the lab and of course at the Kleinwalsertal meetings! Laura, making music with you was always lots of fun! Frank, bedankt voor good times bij het wetenschapscafe en je openhartigheid in KWT. And thanks as well to Angelika, Astrid, Deborah, Catherine, Sergey, Sander, Gosia, Karl (good luck with your young family), Jaan Olle (I'm riding your old bike in Copenhagen, it's fantastic!), Sanja, Miyata (great bassplayer!) Daniel, Roland, Jeroen (vooral je

---

aanmoedigen om gewoon te onderzoeken wat me interesseert), Akiko en natuurlijk Jasperina en Marieke.

Het JNl: Martin, jouw grondigheid is een (weinig toegepast) voorbeeld voor mij geweest. Sonya, Bart and Shehu, thanks for the good company in the office. Petra, bedankt voor de goede samenwerking in het celfusieveld. Martijn, over muziek zullen we het niet altijd eens zijn, maar ik lees je recensies vaak met plezier.

Uit Leiden en Amsterdam wil ik bedanken: Leon, Roel (jammer dat jullie niet bij mijn verdediging kunnen zijn) en Martijn Moné (mister NER). Martijn Luijsterburg, onze nauwe, en vruchtbare, samenwerking de laatste twee (ofzo) jaar vanaf CSH heeft mij heel veel geleerd en plezier gebracht. Moge het in de toekomst nog vele vruchten afwerpen.

The last paragraph is reserved for the extra-special people. Vincent, Steven and Wendy. The former for being a magnificent drummer and terrific guy, and the latter two voor vriendschap en paranimfchap.